Regionalization of global climate change scenarios: An ensemble study of possible changes in the North Sea storm surge statistics

(Vom Fachbereich Geowissenschaften der Universität Hamburg als Dissertation angenommene Arbeit)

Authoress:
K. Woth

Regionalization of global climate change scenarios: An ensemble study of possible changes in the North Sea storm surge statistics

(Vom Fachbereich Geowissenschaften der Universität Hamburg als Dissertation angenommene Arbeit)

Authoress:

K. Woth

(Institute for Coastal Research)

GKSS 2006/13

Regionalization of global climate change scenarios: An ensemble study of possible changes in the North Sea storm surge statistics

(Vom Fachbereich Geowisssenschaften der Universität Hamburg als Dissertation angenommene Arbeit)

Katja Woth

104 pages, 32 figures and 2 tables

Abstract

Possible changes in North Sea storm-related water heights due to increasing atmospheric greenhouse gas concentrations have been studied. The main tool is a barotropic tide surge model, which is used to derive storm surge climate from atmospheric conditions. The analysis has been carried out by using several 30-year atmospheric regional simulations under present-day conditions and for possible future atmospheric greenhouse gas concentrations. In addition, a statistical transfer function between a grid box of the tide surge model and the tide gauge in St. Pauli (Hamburg, Germany) has been calculated. This downscaling model has been derived by statistically linking observed high water levels in St. Pauli with hindcasted tide levels of a coastal model grid box. With the help of this transfer function local climate change conditions have been deduced for St. Pauli.

The ensemble of surge projections comprises two groups of experiments, distinguished only by the atmospheric forcing:

- four projections that are based on atmospheric input from four different regional climate models driven by the same General Circulation Model. These projections are all based on the same emission scenario;

- four projections that are based on input from the same Regional Climate Model driven by simulations with two different General Circulation Models under two different emission scenarios.

The different projections provide a range of possible evolutions of surge extremes under changing climate conditions. The differences among these future projections are statistically not significant. The results suggest that under future climate conditions storm surge extremes along the North Sea coast may increase towards the end of the 21th century locally up to 30% (around 30 – 40 cm). Based on the variability of the storm surge reconstruction for the recent decades it is found that this increase is significant (at the 5% level) for most of the continental North Sea coast. The East coast of the UK shows only small and statistically not significant increases in high storm surges.

Regionalisierung von globalen Klimaänderungsszenarien: Eine Ensemble-Studie möglicher Änderungen in der Statistik sturmbedingter Wasserstände der Nordsee

Zusammenfassung

Mögliche Änderungen von hohen, windbedingten Wasserständen in der Nordsee infolge eines Anstiegs der atmosphärischen Treibhausgaskonzentrationen wurden untersucht. Dazu wurde ein barotropes Wasserstandsmodell genutzt, um das Klima der sturmbedingten Wasserstände (surge) von den atmosphärischen Bedingungen abzuleiten. Die Analysen basieren auf einer Reihe von 30 Jahre umfassenden regionalen Klimasimulationen für heutige Bedingungen sowie für mögliche zukünftige atmosphärische Treibhausgaskonzentrationen. Zusätzlich wurde eine statistische Transferfunktion zwischen einer Gitter-Box des Wasserstandsmodells und des Pegels Hamburg, St. Pauli (Deutschland) angepasst. Für dieses „Downscaling-Modell" wurde eine statistische Relation zwischen beobachteten Hochwasserdaten von St. Pauli und rekonstruierten Daten (sog. Hindcast) einer küstennahen Gitterbox erstellt. Mit Hilfe dieser Transferfunktion wurden Klimaänderungsszenarien für den lokalen Pegel St. Pauli abgeleitet.

Die Simulationen möglicher Klimaänderungen wurde in zwei Gruppen eingeteilt, die sich nur durch den atmosphärischen Antrieb unterscheiden:

- vier Projektionen basierend auf atmosphärischen Antrieben von vier unterschiedlichen regionalen Klimamodellen, die alle mit dem gleichen globalen Klimamodell sowie dem gleichen Emissionsszenario angetrieben wurden;

- vier Projektionen basierend auf atmosphärischen Antrieben mit dem gleichen regionalen Klimamodell, welches jedoch mit je zwei unterschiedlichen globalen Klimamodellen und Emissions-Szenarien angetrieben wurde.

Aus den unterschiedlichen Projektionen ergibt sich eine Bandbreite möglicher Veränderungen hoher, windbedingten Wasserstände unter veränderten Klimabedingungen. Die Unterschiede zwischen diesen zukünftigen Projektionen sind statistisch nicht signifikant. Die Ergebnisse lassen einen Anstieg der sehr hohen Wasserstände um lokal bis zu 30% (ca. 30 – 40 cm) bis zum Ende des 21. Jh. erwarten. Basierend auf Rekonstruktionen der Variabilität windbedingter Wasserstände der letzten Dekaden ist dieser Anstieg für den größten Teil der kontinentalen Nordseeküste statistisch signifikant (auf dem 5% Niveau). Die Ostküste Großbritanniens zeigt dagegen nur geringe, statistisch nicht signifikante Anstiege windbedingter hoher Wasserstände.

CONTENTS

List of publications

The thesis is based on the following journal publications:

Woth K, R Weisse and H von Storch (2005) Climate change and North Sea storm surge extremes: An ensemble study of storm surge extremes expected in a changed climate projected by four different Regional Climate Models. Ocean Dyn: 56, p 3-15, doi:10.1007/s10236-005-0024-3

Woth K (2005) Projections of North Sea storm surge extremes in a warmer climate: How important are the RCM driving GCM and the chosen scenario? Geophys Res Lett: 32, L22708, doi:10.1029/2005GL023762

Grossmann I, **K Woth** and H von Storch (2005) Localization of global climate change: Storm surge scenarios for Hamburg in 2030 and 2085. Submitted to 'Die Küste'

Chapter 1

Introduction

Storm surges are natural phenomena along the North Sea coasts. They present the most important risk in this area affected by natural forces. An area of about 40.000 km² along the North Sea coast encompasses coastal lowlands, home to more than 16 million people and major economic activities [*Hofstede*, 2005]. During extreme storm tides, large areas of flood-prone coastal lowlands can be, and have been, flooded [*Petersen and Rohde*, 1991], causing loss of life and property. In all, more than 2,400 people lost their lives in the storm floods of 1953, which affected mainly the Netherlands and the United Kingdom, and the storm flood of 1962, which affected the German Bight and its large river estuaries.

As a reaction to and consequence of these two disasters in particular, national governments undertook huge efforts to improve the safety standards. For instance, in Germany a completely revised plan for coastal defence was established in 1963. At this time important arrangements were formulated for coastal protection which to this point had been considered low priority. These efforts to introduce a new safety standard [e.g., *Hofstede*, 2004] helped to significantly reduce the risks of coastal flooding: subsequent storm floods, in particular the storm flood of 1976, with higher water levels than those in 1962 (e.g., water levels observed in Hamburg in 1976 were 0.8 meter higher than in 1962) were well-managed and did not lead to severe damage and losses. As the last storm flood with disastrous consequences dates back more than 40 years, people feel safe in coastal lowlands. But the risk of catastrophic floods still exists.

Today, we live in a period where increasing greenhouse gas (GHG) concentrations in the atmosphere are beginning to change the global climate. In 1988, the Intergovernmental Panel on Climatic Change (IPCC) was established with the aim to document the knowledge about such climate change, on both the global and the regional/local scale. In three assessment reports, vulnerable zones were identified and possible changes based on a range of different scenarios – implying possible future greenhouse gas

concentrations - were analysed. The North Sea coast area is one of the regions that might be adversely affected by changing climate conditions.

Within the EU funded project PRUDENCE (Prediction of Regional scenarios and Uncertainties for Defining EuropeaN Climate change risks and Effects) such future climate changes, conditional upon assumed projections of future GHG emissions ("Scenarios"), were simulated using a cascade of numerical climate models. Global climate models (GCMs) were used to simulate future climatic conditions globally. For computational feasibility a coarse grid with a mesh size of about 300 km × 400 km was used. Regional climate models (RCMs) were applied to "dynamically downscale" these coarse resolved global conditions to a finer grid, of about 50 km × 50 km mesh size, covering Western Europe including the North Sea area. These atmospheric simulations were used in this thesis to derive climate change scenarios of storm-related water levels of the North Sea. In Figure 1.1 the experimental set up is sketched, showing on the left hand side the results provided by PRUDENCE partners and on the right hand side those parts conducted in this thesis.
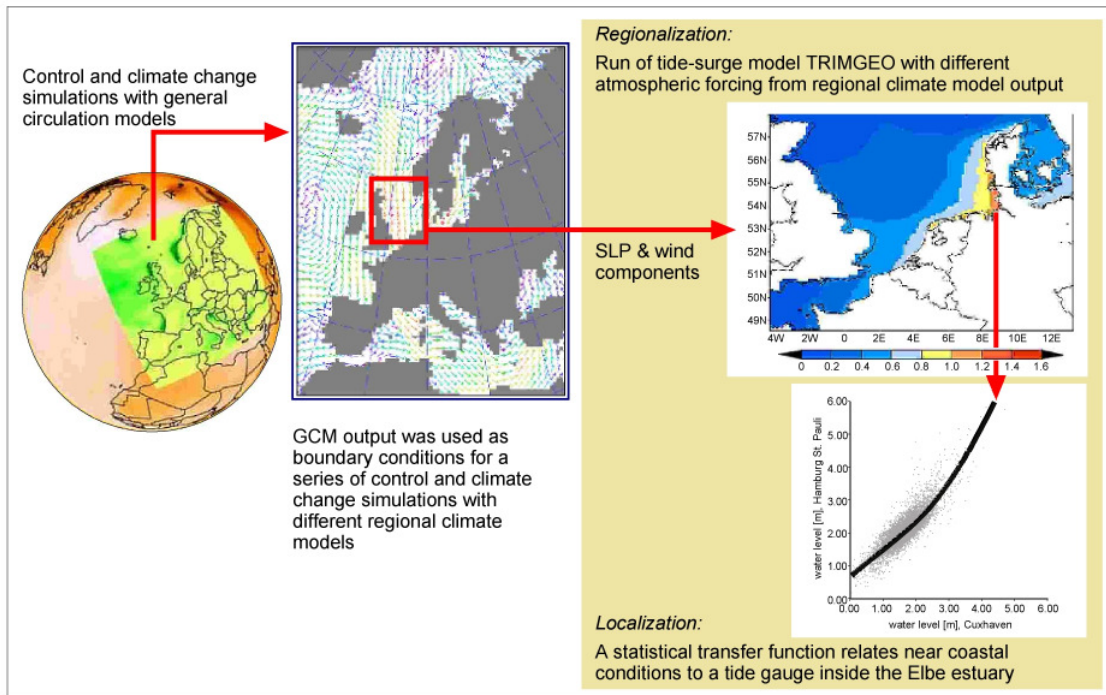

Figure 1.1: Methodology used to derive climate change information for regional (North Sea) and local (tide gauge St. Pauli: Hamburg, Germany) storm surge climate.

A hydrodynamic model covering the North Sea area is exposed to the downscaled wind and air pressure fields to produce consistent water levels and currents with a high resolution. This is done for present conditions (1961 to 1990) as well as under assumed future atmosphere GHG concentrations for the time horizon 2071 to 2100. Additionally, based on these scenarios of possible future storm-related water levels, a "localization step" was added to specify water levels at the tide gauge of Hamburg, St. Pauli (Germany), situated more than 100 km inside the Elbe estuary. This was conducted by creating a statistical transfer function, which relates high water levels in simulated grid boxes to the corresponding water levels at the tide gauge of Hamburg, St. Pauli. Such localization steps are needed to obtain results interpretable on a scale interesting for local decision makers. In contrast to previous work, this thesis allows for the systematic investigation of similarities and differences in possible future storm surge climate related to the use of different global and regional climate models, as well as to the use of different emission scenarios. In this way, a range of equally plausible scenarios of storm surge levels was deduced.

The thesis is based mainly on three publications: *Woth et al*. [2005], *Woth* [2005] and *Grossmann et al*. [2005] (see list of publications). The focus of the first publication [*Woth et al*., 2005] is on the response of high water levels when the North Sea model is exposed to wind and pressure conditions derived from four different RCM simulations each driven with the same GCM boundary conditions and the same emission scenario. This publication includes the required information concerning the hydrodynamic model, the model area and also the model validation. Additionally, the different atmospheric forcings produced by different RCMs are compared and the degree of realism of the control runs is examined. The second publication [*Woth*, 2005] deals with the response in storm surge heights, when using the meteorological forcing from one RCM driven with boundary conditions of two different global GCM integrations, both integrated for two different future emission scenarios. After having modeled and analyzed the regional water levels, an example of further downscaling or 'localization' of these regionalized climate change projections is given in the third publication [*Grossmann et al*., 2005]. Using a statistical model, the regional storm surge heights – as given in a grid box in the hydrodynamic simulation exposed to anthropogenically induced climate change conditions – are "localized" to a tide gauge located in the harbor of Hamburg, Germany. An estimation of the expected changes of yearly maximum water levels relative to today's statistics is given for two chosen time horizons: a closer one, around 2035 and a remote one, around 2085. The latter results from the data time slice 2071 - 2100, the closer time horizon is derived by an extrapolation from 2071 - 2100.

The remainder of this thesis is organized as follows: Section 2 gives an overview of key concepts used in this thesis. Among these are scenarios, which are used to provide assumptions and details of the expected climate change, and the phenomenon of North Sea storm surges and their causes. A review of relevant previous work is also provided, both in terms of methodology as well as knowledge about past, present and possible future storm surge climate. An extended summary is provided in section 3, which is complemented by an approach to deal with uncertainties, inherent in all climate change studies. The complete versions of the publications are reprinted as sections 4, 5 and 6. An outlook completes this thesis.

Chapter 2

Overview: Climate change and North Sea storm surge climate

This chapter is intended to give an introduction on studying climate change and the possible impacts on North Sea storm surges. First, the concept and usage of scenarios in climate change studies is explained. An introduction to the phenomenon 'storm surge' is followed by an overview of the conditions affecting local storm surge levels. Aspects of the expected rise in mean sea level and the natural variability of the North Sea storm surge climate are discussed. The last subsection provides information concerning the modeling of North Sea storm surges. Different methods and results are summarized.

A reader interested in a broader presentation should refer to a number of publications such as: *Gönnert et al*. [2001], who give a broad and detailed overview of storm surges, their causes and occurrence on a global basis. The monograph of *Petersen and Rohde* [1991] gives a general introduction and historic overview of storm floods of the North Sea and the Baltic Sea. There are many more articles on storm surges and storm floods, especially a large number of regional case studies, which are not explicitly referred to here. Also more general information about present North Sea research is given in a report by *Sündermann et al*. [2001], summarizing the endangering due to anthropogenic influences on the North Sea system and the need for future research.

2.1   Scenarios in climate change studies

In the late 1980s, when climate change moved into the focus of the socio-political discussion, the Intergovernmental Panel on Climate Change (IPCC) was founded. The IPCC in its early days introduced the concept of 'climate scenarios' [*Houghton et al*., 1990, 1992, 1995, 2001]. Employing scenarios requires the construction of a series of possible, mutually exclusive but internally consistent, futures, which describe different developments of the dynamics conditional upon a number of key assumptions. These futures are not equally probable but they are all possible, and should be plausible and

logical [*von Storch*, 2005]. When concerning climate change, these 'story-lines' are typically 'translated' into different amounts of climatically relevant greenhouse gas emissions (GHG) and aerosols until the end of the 21st century. Scenarios are an often used tool in planning exercises, dealing both with economic and political perspectives. An overview of the general concepts is provided by *James* [2002] and *Godet* [1987] among others.

With these scenarios it is possible to analyze the impacts of specific disturbances, decisions or actions. Also the leverage of options to avoid specific future developments can be assessed. Stakeholders and policymakers can analyze possible future changes and also the usefulness of taking, or not taking, action. Thus one aspect of climate change scenarios is to identify undesirable futures, and identify the necessary degree of reduction of greenhouse gases and aerosols. The other application is to plan for adaptations to future changes, to avoid adverse impacts by reducing the vulnerability of societies and ecosystems before such changes become a reality.

In this thesis only two different emission scenarios are used, namely SRES A2 and SRES B2, where SRES is the *IPCC Special Report on Emission Scenarios* [*Nakicenovic*, 2000]. These emission scenarios are widely used: the SRES A2-scenario specifies a tripling of atmospheric greenhouse gas concentrations by the end of the 21st century and the SRES B2-scenario leads to slightly more than a doubling of pre-industrial levels for the same time horizon. A2 is a 'medium-high' scenario and B2 is a 'medium-low' scenario (see also http://www.grida.no/climate/ipcc/emission). When considering the whole span of all IPCC SRES emission scenarios, A2 and B2 cover a range of approximately 60 % of the full span between the uppermost and the lowest IPCC emission scenarios. In the following the socio-economic conditions giving rise to the scenario A2 and B2 are presented.

SRES describes the A2-scenario as follows:

> "*... characterized by lower trade flows, relatively slow capital stock turnover, and slower technological change. The world ``consolidates'' into a series of economic regions. Self-reliance in terms of resources and less emphasis on economic, social, and cultural interactions between regions are characteristic for this future. Economic growth is uneven and the income gap between now-industrialized and developing parts of the world does not narrow. People, ideas, and capital are less mobile so that technology diffuses more slowly. International disparities in productivity, and hence income per capita, are largely maintained or increased in absolute terms. With the emphasis on family and community life, fertility rates decline relatively slowly, which makes the population the largest*

among the storylines (15 billion by 2100). Technological change is more hetero-geneous. Regions with abundant energy and mineral resources evolve more re-source-intensive economies, while those poor in resources place a very high pri-ority on minimizing import dependence through technological innovation to im-prove resource efficiency and make use of substitute inputs. Energy use per unit of GDP declines with a pace of 0.5 to 0.7% per year. Social and political struc-tures diversify; some regions move toward stronger welfare systems and reduced income inequality, while others move toward ``leaner'' government and more heterogeneous income distributions. With substantial food requirements, agri-cultural productivity is one of the main focus areas for innovation and research, development efforts, and environmental concerns. Global environmental con-cerns are relatively weak." [*Nakicenovic*, 2000; abbreviated version from *von Storch and Müller*, 2004, p. 145]

In B2, there is

"... increased concern for environmental and social sustainability. Increasingly, government policies and business strategies at the national and local levels are influenced by environmentally aware citizens, with a trend toward local self-re-liance and stronger communities. Human welfare, equality, and environmental protection all have high priority, and they are addressed through community-based social solutions in addition to technical solutions. Education and welfare programs are pursued widely, which reduces mortality and fertility. The popu-lation reaches about 10 billion people by 2100. Income per capita grows at an intermediate rate. The high educational levels promote both development and environmental protection. Environmental protection is one of the few truly inter-national common priorities. However, strategies to address global environ-mental challenges are not of a central priority and are thus less successful com-pared to local and regional environmental response strategies. The governments have difficulty designing and implementing agreements that combine global en-vironmental protection. Land-use management becomes better integrated at the local level. Urban and transport infrastructure is a particular focus of commu-nity innovation, and contributes to a low level of car dependence and less urban sprawl. An emphasis on food self-reliance contributes to a shift in dietary pat-terns toward local products, with relatively low meat consumption in countries with high population densities. Energy systems differ from region to region. The need to use energy and other resources more efficiently spurs the development of less carbon-intensive technology in some regions. Although globally the energy system remains predominantly hydrocarbon-based, a gradual transition occurs away from the current share of fossil resources in world energy supply." [*Nakicenovic*, 2000; abbreviated version from *von Storch and Müller*, 2004, p.146]

Based on these 'story-lines', expected emissions of greenhouse gases and aerosols into the atmosphere are derived. Figure 2.1a shows the expected SRES scenarios for carbon dioxide, that is a representative of greenhouse gases as well as for sulfate dioxide (Fig. 2.1c), which is a representative of anthropogenic aerosols. These emission scenarios are transformed into scenarios of atmospheric loadings of greenhouse gases (Fig. 2.1b) and aerosols. This is the first step in the cascade of several steps which eventually lead to scenarios of the impact of climate change (see below).
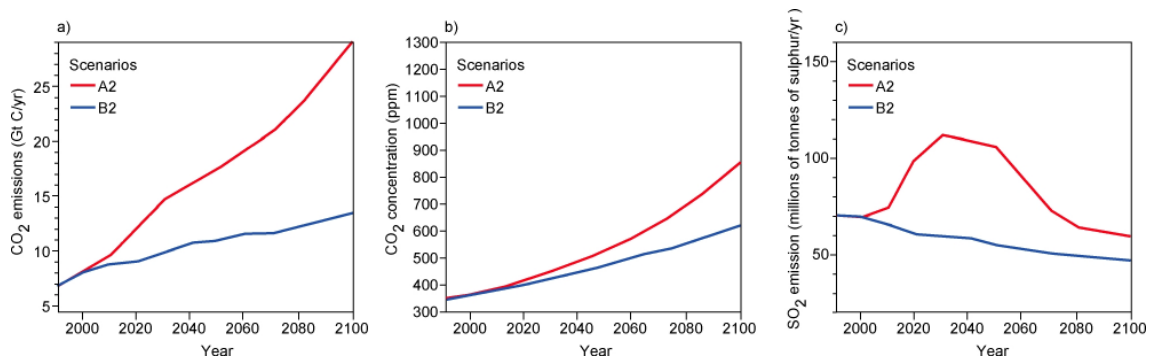

Fig: 2.1: SRES scenarios for the emissions of (a) carbon dioxide (in gigatons per year) and (c) sulfate dioxide (in megatons sulfur) and (b) the derived atmospheric concentrations of carbon dioxide [modified after *Houghton et al.*, 2001].

With the external specifications of greenhouse gas concentrations, global climate models compute several decades of weather, typically with a 6-hourly output interval. As global climate models show systematic errors in their simulations of the present climate, climate change simulations are not interpreted in absolute values but in terms of differences between future climate change conditions and the so-called 'control simulations'. These control simulations are forced with today's atmospheric loadings of greenhouse gases and aerosols. Assuming that these runs are producing the same biases as the climate change simulations, (statistically significant) differences in the statistics between both climate simulations are interpreted as the response to the applied emission scenario. To quantify the bias in the control simulations, re-analyses [e.g., *Kalnay et al.*, 1996] or observations can be used as a reference of today's conditions.

Climate change studies are generally intended to provide high resolution information, usable for stakeholders and policymakers, who are mostly concerned with expected damages and adaptation in limited regions. However the skillful-scale, i.e., that scale on which atmospheric features are described reasonably well, is larger than the actual grid

cell resolution of a climate model [*Pielke*, 1991; *von Storch*, 1995]. *Grotch and Mac-Cracken* [1991] specified this scale as likely four to eight times of the model grid cell size. Thus regional, or even local, atmospheric features which are smaller than a critical size of about typically 1000 km, are not well resolved using present state-oft-the-art GCMs. Therefore a follow-up treatment is usually conducted, transferring global climate conditions to a regional scale. For this purpose RCMs with a higher temporal and spatial resolution are integrated for a part of the GCM area [e.g., *Giorgi and Mearns*, 1991]. This downscaling allows for the computation of regional features inside the RCM model area influenced by, among other things, the regional orography, as e.g. the land-sea contrast, or small scale cyclones.

These temporally and spatially high resolved climate simulations can subsequently be used to derive climate change information for variables, which are not resolved or not described in global or regional climate models. This can be done by appending a numerical model simulation (e.g. a hydrodynamical model) or e.g. by applying a statistical transfer-function, linking the atmospheric output to a certain dependent variable.

2.2   North Sea storm surge

Given the configuration of the coastline and the bathymetry, the severity of the storm flood depends primarily on wind speed, wind direction and duration. In addition, the development of water levels, generated by persistent winds in the days before a strong surge event, modifies the threat for the coast [e.g., *Otto et al*. 1990]. Also the coincidence of the peak surge with the high tide or even a spring tide increases the severity of a storm flood. Changes in density caused by horizontal temperature and salinity gradients of the Shelf sea play only a minor role in this context and are not a concern in this study.

This study is dealing mainly with the storm-related part of the water level, the so-called 'surge'. In *Gönnert et al*. [2001, p.1] storm surges are defined as '….oscillations of the water level in a coastal or inland water body in the period of range of a few minutes to a few days, resulting from forcing from the atmospheric weather system'. The atmospheric induced surge is the difference of the water level, observed at a certain tide gauge, and of the astronomically conditioned water level (as illustrated in figure 2.2).
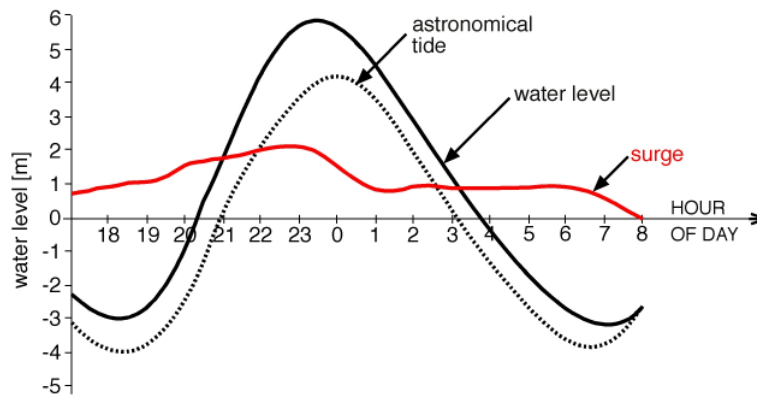
17

Fig. 2.2: Surge curve (red) and astronomical curve (dotted line) as parts of the overall water level (solid line). A time period over 11 hours is shown (modified after Heaps, 1983).

North Sea storm surges are mainly a result of local meteorological conditions over the Shelf sea area as will be seen in section 2.2.1. In some cases an additional portion of this storm-related sea level rise are observed which is externally generated. Under certain weather conditions an external surge can be generated in the North Atlantic, pushing additional water masses into the North Sea basin [*Gönnert et al.*, 2001]. The maximum of the storm flood from February 1962 had an additional portion of 90 cm for parts of the German Bight, coming as a long wave from the Atlantic [*Hensen*, 1966], resulting in that disastrous flood. A few authors, such as *Koopmann* [1962], *Schmitz et al.* [1988] and *Gönnert* [1999], have investigated this phenomenon for the southern North Sea under different conditions. For instance, *Gönnert* [1999; 2003] has shown that at Cuxhaven, a peak level of 10 cm to 108 cm can occur in addition to the local tide-surge water level. This study does not account for external surges. Most recent studies using GCMs project a strengthening of the North Atlantic storm track under increasing GHG conditions (see above). This would possibly lead to more frequent external surges in a future climate. Thus neglecting the effect of changing external surges may lead to an underestimation of storm surge extremes.

2.2.1 Conditions for North Sea storm surges and storm floods

Meteorological conditions

For the southern North Sea coast, mainly three different types of meteorological situations, which may lead potentially to high storm surges, can be distinguished [*Petersen and Rohde*, 1991]. These types, namely the Jutland type, the Scandinavian type and the Skagerrak type are depicted in figure 2.3. All shown storm tracks, observed at dates as specified, led to strong storm surge events.
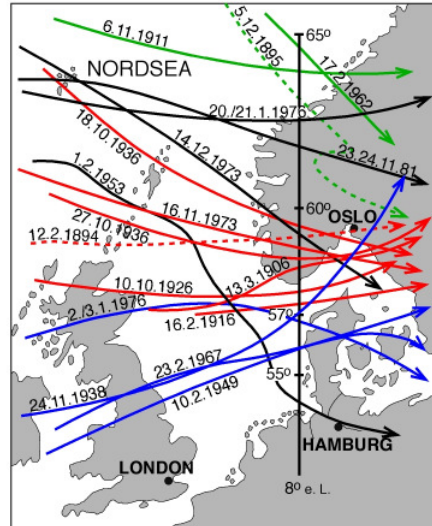
Figure 2.3: Storm depression tracks, which cause strong storm surges at the North Sea Coast [modified after *Petersen and Rohde*, 1991]. Types of depression systems as colored: Blue: Jutland type, red: Skagerrak type, green: Scandinavian type, black: mixed types.

In the following, the three types of meteorological situations leading to strong storm surge events are summarized:

- The Jutland-Type, developed over Newfoundland, traveling mostly very fast in easterly direction from England over the North Sea to Jutland. Jutland type storms result, at first, in strong southwesterly winds, shifting to westerly, and finally to northwest winds. The very heavy storm flood from the 2nd to 5th January 1976 was caused by this type, showing a very steep storm surge curve.

- The Scandinavia-type is a slow-moving depression system forming over Greenland and Iceland and traveling towards the southeast, crossing Scandinavia between the 60th and the 65th degree of latitude. Deep pressure systems from the Scandinavia type cause long, persistent storms with winds from northwesterly directions over the North Sea. Usually, the highest wind speeds are not as strong as those from the Jutland Type but the storm surge curve, derived from tide gauge observations, includes more than one high tide. The storm flood from 16th and 17th February 1962 is categorized as this type.

- The track of the third type, the Skagerrak-Type, is located between the other two types, traveling usually from WNW to ESE. It crosses the 8th degree of longitude, which lies just in front of the western coast of Schleswig-Holstein, between the tip of Denmark and the 60th degree of latitude. The very strong onshore winds at all parts of the German North Sea coast lead to high, over more than one tidal cycle persistent, storm surge curves.

For the end of the 21st century most state-of-the-art climate models point towards an increase in high wind speeds over Northwest Europe under the assumption of increasing greenhouse gases [e.g. *WASA group*, 1998; *STOWASUS group*, 2001; *Rauthe et al.*, 2004; *Rockel and Woth,* 2005; *Leckebusch et al.* 2005]. A systematic analysis of statistical significant changes in storm climate over North West Europe is difficult. One problem is the use of different parameterizations for the 10 m wind in the RCMs and also inconsistent storage of these variables (e.g. instantaneous values in different temporal resolution). This can lead to data sets for high wind speeds from different regional climate models with different informational content.

The analysis of storm tracks in future scenarios deduced from the Hadley Centre GCM, point to a southward displacement of the average NW European winter storm track. For instance, *McDonald* [2002] has shown that the number of low pressure storm systems with a minimum pressure below 1000 mb that cross the UK during winter, is predicted to increase from the average of five in present day simulation to about eight under climate change conditions. This result is somewhat different to storm track studies done in the STOWASUS project, derived from the ECHAM global climate model, where a north-western displacement was found [*STOWASUS group*, 2001].

Mean sea level heights

The absolute level of a storm flood also depends on the mean sea level height. As this study analyzes changes in near coastal water levels under future climate conditions, estimates of changes in mean sea level heights for the same future emission scenarios are of interest. Unfortunately, regionally disaggregated scenarios of future mean sea level are not yet available. However, estimates for the globally averaged mean sea level rise have been provided by the IPCC [*Houghton et al.*, 2001]. According to these scenarios, the global averaged mean sea level is expected to increase - depending on the emission scenario - between 30 and 50 cm (for the model average all SRES envelope) by the end of the 21st century but this estimate is associated with a large range of uncertainty (Figure 2.4). The colored lines inside the figure display estimations for the different emission scenarios averaged across a number of models, the colored lines outside the figure indicate the overall range resulting by the use of different models.
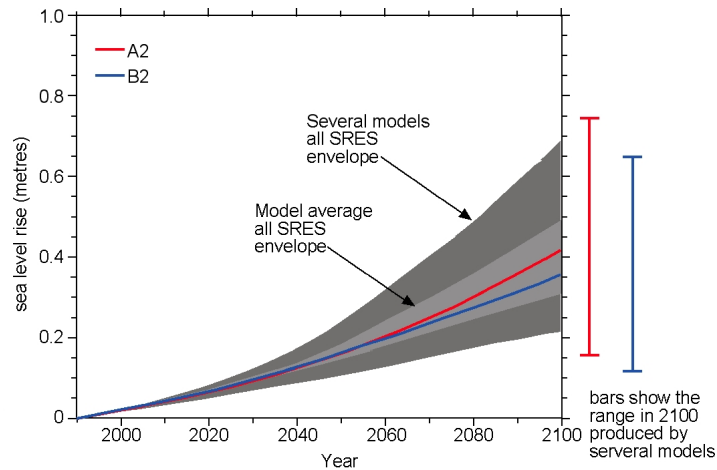
Figure 2.4: Projected sea level responses as an average of a series of AOGCMs by IPCC from 1990 to 2100 for the A2 and B2 SRES scenarios of greenhouse gas and other human-related emissions as shown in figure 2.1.
The light shading shows the range of the average of AOGCMs for all 35 SRES scenarios. The dark shading shows the range of all AOGCMs (all 35 scenarios). The bars show the range deduced from all AOGCMs in 2100 for the A2 and B2 scenario [modified after *Houghton et al.*, 2001].

This sea level rise compared to the ongoing secular mean sea level increase (i.e., past non-anthropogenic increase per 100 years) would lead to a more rapid rise as a result of anthropogenic climate change. For the German Bight, this secular increase of mean sea level due to e.g. geological and thermal effect, amounts in the last centuries to about 10 to 20 cm [*Niemeyer and Kaiser*, 1999]. Between 1993 and 2000, satellite altimeter measurements indicate a sea level rise of approximately 2.5 mm yr^{-1} [*Cabanes et al.*, 2001]. If this increase is not a result of inter-decadal variability, it may indicate a recent acceleration of a long-term trend, possibly as a result of anthropogenic climate change.

A relevant question in the context of (future) storm surge modeling is whether the storm surge heights are sensitive to changes in mean sea level. It could be that the increase in time-averaged sea level has, in addition to the direct effect of increasing surge height, significant indirect effects by changing the surge height and propagation. This problem was studied in detail by *Kauker* [1998] and *Lowe et al.* [2001] in coarse resolution models, who found no significant differences in simulations with or without elevated mean sea level. *Lowe and Gregory* [2005] confirmed these findings for the North Sea area.

2.2.2 Storm surge climate of the past

Truly observed time series of storm surge heights are not available for large areas and long time periods. Selectively it is possible to derive the storm-related variations from tide gauge measurements by subtracting the tides as estimated by harmonic analysis

21

from these observations. However this approach requires observations once an hour or more frequently. Unfortunately, with respect to storm surge information, the data base of water level along the North Sea coast is of limited utility as mostly only two measurements are made, the highest water level and the lowest water level within a tidal cycle. A severe limitation of the time series is their frequent in-homogeneity [e.g., *Karl et al.*, 1993; *WASA*, 1998] related to e.g. changing of the location or the environment of a tide gauge. Also construction work or natural and other anthropogenic changes in the surrounding of the station and the sea bed influence the observed time series.

One possibility for obtaining a homogeneous data-set is to perform a so-called hindcast. A hindcast of water level heights consist of 2 steps: first a regional re-analysis of atmospheric conditions is prepared [e.g., *Feser et al.*, 2001]; second, these "analysed" wind and air-pressure fields are fed into a tide surge model. *Weisse and Plüß*, [2005] have shown, based on such a hindcast data set for the North Sea area, that most positive trends found in the mean high water level derived from tide gauge observations are influenced by additional factors and can hardly be related to changes in the atmospheric conditions.

Several such multi-decadal hindcasts were successfully performed in the last years by several authors for the second half of the 20th century up to the present. They provide high resolution multi-decadal data sets of water level variations in the North Sea area [*Flather et al.*, 1998; *Langenberg et al.*,1999; *Weisse and Plüß*, 2005; *Kauker*, 1998; *Woth et al.*, 2005]. The quality of such hindcasts depends on the accuracy of the atmospheric wind and pressure fields as provided by operational analyses or 're-analysis' (see above) of atmospheric conditions.

For time horizons further back into the past than with hindcasts can be prepared, so-called 'proxy' data are usually used to estimate the variability of storm surge climate. As the variability of North Sea storm surge climate is determined by the variability of the storm climate and the mean circulation [*Wakelin et al.*, 2003], atmospheric pressure distributions can be used as a 'proxy' for storm related water level variations [e.g., *von Storch and Reichardt*, 1997; *Pfizenmaier*, 1997]. Statistics from wind-speed observations are usually not suitable in this context because of in-homogeneities related to changes in the environment or instrumentation of the weather station. Instead air pressure readings are used. The air pressure-indicators are usually derived from yearly distributions of e.g., daily air pressure at a certain station, 12-hourly air-pressure changes at a station or daily, spatial differences in air pressure between two or more stations [*Schmidt and von Storch*, 1993, *Alexandersson et al.* 1998 and 2000; *Kaas et al.* 1998,

Bärring and von Storch, 2004]. Then, yearly percentiles can be derived or a simple count, how often a certain threshold has been exceeded, e.g., how often a drop of 16 hPa in 12 hours has taken place [*WASA*, 1998] can be calculated. It was shown that the storm activity decreased from the outgoing 19th century to the middle of the 20th century. From 1960 to 1995 an increase in storm activity was found, leading to a storm activity in the 1990th comparable to that in the beginning of the 20th century. After 1995 the storm activity was found to decrease again (fig. 2.5).
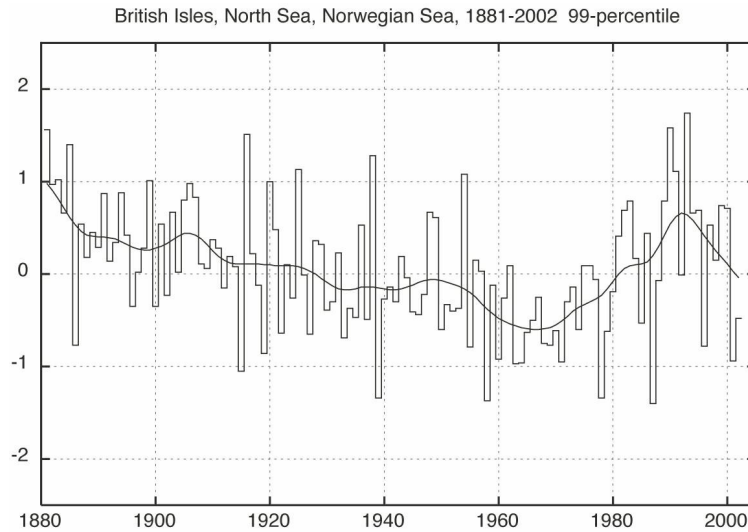

Figure 2.5: Average of standardized 99 percentile of geostrophic wind speeds (derived from 3 observations per day) calculated from triangles of station pressure data [*Alexandersson et al.*, 2000]

2.2.3 Modeling of North Sea water levels

For the modeling of storm surge climate, there are two different approaches. Statistical modeling exploits large scale variables with a direct or indirect link to surge statistics, such as the spatial distribution of monthly sea level pressure. The second approache, numerical model integrations [*Langenberg et al.*, 1999], has the advantage of being able to generate information also for locations without observations. Another advantage of model integrations is the high temporal sampling rate, every hour or even more frequently, while observations are often only available for tidal maxima and minima. The advantage of the statistical downscaling method is its simplicity and its low computational costs.

Since the early 1960s hydrodynamic-numerical models have become an established tool for the study of tidal phenomena. A detailed review, which emphasizes the first developments in hydrodynamic-numerical model studies since the advent of modern

computers can be found in *Heaps* [1967 and 1983] and *Jelesnianki* [1978]. In addition to studies of hydrodynamic modeling of tidal circulation and residual circulation, the influence from meteorology on water heights can also be modeled. Therefore, atmospheric forcing as wind stress and sea level pressure fields are prescribed as additional external force at the interface between water and air.

Many studies dealing with dynamical modeling of tide-surges exist. More recent examples include *Dolata et al.* [1982], *Heaps* [1983], *Flather et al.* [1998], *Kauker* [1998], *Langenberg et al.* [1999], *Kauker and Langenberg* [2000], *Wakelin et al.* [2003] or *Weisse and Plüß* [2005] among others. They have shown that, provided that the meteorological forcing has sufficient accuracy, storm surges and their statistics can be satisfactorily modeled with hydrodynamic models. Thus, in addition to these process studies, long term simulations or single event analysis, hydrodynamical models are also used for operational surge forecasts [e.g., *Plüß*, 2004].

In recent years storm surge models have also been used to assess the potential effects of anthropogenic global climate change on the North Sea storm surge climate. For instance, two large EU-funded projects dealt with North Sea storm and wave climate under climate change conditions. In the WASA project [Waves and Storms in the North Atlantic, *WASA-Group*, 1998; *Langenberg et al.*, 1999; *Flather and Smith*, 1998] the wind and pressure data originated from two global high-resolution (T106) 5-year simulations. These earlier climate change studies suffer from the lack of sufficient long time-slice simulations (shorter than one decade) and the lack of available high resolution atmospheric climate change scenarios (see above). Nevertheless these early regional climate change simulations pointed also to an increase of westerly wind speeds and thus an increase in storm related water levels. However, due to the short time-slice simulation, a statistically significance in the differences in storms and storm surge parameters could not been stated.

30-year time slice T106 simulations were used in the STOWASUS-2100 project [Regional storm, wave and surge Scenarios for the 2100 century, *STOWASUS-Group*, 2001]. Results have shown that under enhanced greenhouse gas conditions an increase of up to 10% in extreme wind speeds in the North Sea and the Norwegian Sea may take place, when atmospheric CO_2 concentrations are doubled. These changes suggest an increase in surge height extremes of the same proportion. *Lowe et al.* [2001] were the first, who applied a two-step procedure of a dynamical downscaling of coarse grid general circulation model (GCM) data via a regional climate model, followed by an integration of a hydrodynamic model. Their results indicate a statistically significant

increase in surge extremes at the continental coast and also an increase along a sizable fraction of the UK coastline under assumed future climate conditions.

In addition to these studies based on hydrodynamic numerical modeling, there are also a numbers of statistical downscaling studies dealing with North Sea storm surge climate in the past and under possible climate change conditions. For instance *von Storch* and *Reichardt* [1997] or *Pfizenmaier* [1997] used canonical correlation analyses and redundancy analysis, respectively [*von Storch* and *Zwiers*, 1999]. In this case, a downscaling model is linked to monthly large scale atmospheric pressure anomalies with small scale anomalies in percentiles in seasonal water level distributions. In *Langenberg* et al. [1999] these statistical downscaling methods were compared with dynamical downscaling for the North Sea region. The simpler statistical downscaling method provide results of comparable skill as the dynamical approach – but is limited to locations with good observational coverage.

CHAPTER 3

Extended summary

In the following, a brief overview is given of the model area, the hydrodynamic model used, the atmospheric forcing used to drive the model, and the resulting experiments that this thesis is based on. Methods and key results are then summarized first for the regionalization experiments, which generate a series of future atmospheric conditions for the North Sea area, and, secondly, for a localization via a simple statistical downscaling model of these rather coarsely resolved surge projections onto one local tide gauge, located in the harbor of Hamburg, Germany. The latter local analysis of changes in storm related water levels also consider a contribution from the increase in mean sea level, which has been projected by the IPCC for the considered time horizons.

3.1 The North Sea area

The Greater North Sea, a marginal sea of the Atlantic, is situated on the continental shelf of northwest Europe. It opens into the Atlantic Ocean in the North, via the English Channel to the southwest, and into the Baltic Sea to the East (Fig. 3.1). The bottom topography is important in relation to its effects on water circulation and vertical mixing. Despite the Norwegian Trench with depths of up to 700 m, the southern, the central and the northern North Sea are relatively shallow areas, with average depths of about 40, 80 and 150 m, respectively [*Otto et al.* 1990]. As northwest Europe is influenced strongly by westerly winds, a counterclockwise mean circulation in the North Sea is typical for most of the time [e.g., *Kauker and von Storch*, 2001].
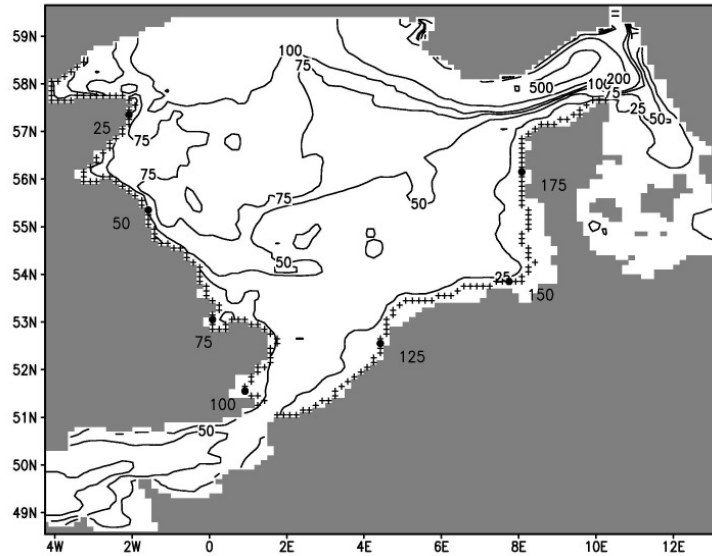
Figure 3.1: Model domain of the tide surge model TRIMGEO: the bathymetry (isolines) and the 196 near-coastal grid cells (crosses) located on the 10 m bathymetry line along the North Sea coast beginning with 1 in Scotland and ending with 196 in Denmark.

Superimposed on this mean North Sea circulation, a number of tides, with the semi-diurnal M2 being the dominant tide, propagate from the Atlantic via north of Scotland into the North Sea basin. The tidal range varies between 1.50 m (Den Helder) and 7.20 m (Immingham) [*Gönnert et al*., 2001]. Owing to strong tidal currents and the additional mixture during the storm season, most areas of the North Sea outside the Norwegian Trench, the Skagerrak and the Kattegat are vertically well mixed in winter, while the shallow North Sea waters are vertically well mixed throughout the year [*OSPAR Commission*, 2001]. Thus, comparing simulations with a 3-dimensional baroclinic model [*Kauker*, 1998] and a vertically integrated barotropic model, *Kauker and Langenberg* [2000] found that one-layer models are sufficient for a reasonable description of storm-related water level variations along the North Sea coast. For further information about the North Sea circulation refer for instance to *Backhaus* [1983].

3.2 The hydrodynamic model

The barotropic TRIMGEO model (Tidal Residual and Intertidal Mudflat) [*Casulli and Catani,* 1994] is used for modeling water levels as the response to 6-hourly North Sea meteorological forcing. This forcing, pressure at mean sea level and the horizontal wind components at 10 m height were simulated by different climate models.

28

The model domain covers the North Sea (Fig. 3.1) and is gridded with a mesh size of 6'
x 10' in latitude and longitude, which corresponds to a grid cell size of about 10×10
km^2. At the model boundary across the northern North Sea and across the English
Channel in the West, boundary conditions in terms of sea level anomalies are given by
17 partial tides. A net influx of freshwater is prescribed from the Baltic Sea [*OSPAR
Commission*, 2000] and from the largest rivers, specified from climatology.

3.3 The atmospheric forcing

The atmospheric forcing data sets used to drive the tide surge model in this study are
listed in table 1. The first four were obtained from the EU project PRUDENCE [*Chris-
tensen et al.* 2002].

Global boundary conditions

Boundary conditions from Global General Circulation Models (GCMs) are needed to
force the Regional Circulation Models (RCMs) in the lateral sponge zones. In chapter 4,
different RCMs were forced with output from the Hadley Center General Circulation
Model HadAM3H (high-resolution global atmosphere model) [*Hudson and Jones*,
2002; *Hulme et al.*, 2002], forced with recent and future atmospheric loadings of green-
house gases and aerosols but also with recent and future sea surface temperature and sea
ice conditions which, in turn, were obtained from a transient experiment with the
HadCM3 coupled Atmosphere Ocean General Circulation model (AOGCM). In chapter
5, one RCM was forced with boundary conditions derived from the coupled AOGCM
ECHAM4/OPYC3 [*Roeckner et al.*, 1999] in addition to HadAM3H. In the following
the abbreviation 'E' is used for the global forcing coming from ECHAM4/OPYC3 and
'H' for the HadAM3H global forcing.

Regional atmospheric forcing

Near-surface winds and sea level pressure as simulated by four RCMs are used. All four
RCMs are set up on a rotated grid with a mesh size between 0.44º and 0.5º, corre-
sponding to a resolution of about 50 km x 50 km over the North West European Shelf
Sea. Table 1 gives an overview of the RCMs and the publication describing their
physics and dynamics.

Institute	Model	Reference
SMHI	RCAO	Döscher et al. 2002
DMI	HIRHAM	Christensen et al. 1996
GKSS	CLM	Steppeler et al. 2003 Doms et al. 2005
MPI-HH	REMO	Jacob, 2001 Majewski, 1991
GKSS	SN-REMO	von Storch et al. 2000

Table 1: Regional model simulations used in this thesis

HIRHAM, REMO and CLM are stand-alone regional atmosphere models, RCAO [*Döscher et al.*, 2002] is a coupled atmosphere-ocean model, which incorporates the Rossby Center regional atmosphere model RCA [*Rummukainen et al.*, 2001, *Jones et al.*, 2004] and their ocean model RCO [*Meier et al.*, 2003].

3.4   The experiments

All hydrodynamic simulations were prepared for 30-year time slices, projecting present-day (1961-1990) control and assumed future greenhouse gas concentrations (2071-2100). For the validation of the hydrodynamic model setup, a hindcast simulation was performed with SN-REMO, driven with dynamically downscaled atmospheric NCEP re-analyses (cf. Feser et al., 2001) for the last four decades (see section 4.2.1). The hindcast simulation describes the actual weather throughout 1958-2000, in contrast to the control simulations which describe a random sequence of weather events, which share with the hindcast only the same statistics but not details at any time.

This hindcast was compared with observations and other available data and gave satisfying results (see section 4.2.1). However, a comparison of this hindcast with simulated control[1] conditions show some deviations, thus the scenario projections are interpreted not in absolute values but as relative changes to the present-day control simulations. By doing so, we assume that the systematic errors in both the control and the scenario

---

[1]   i.e., a hydrodynamic simulation with the winds and air pressure from a climate simulation using 1960-1990 sea surface temperature and sea ice conditions as well as 1960-1990 GHG and aerosol loadings – in contrast to the 'real' weather of the years 1960-1990.

simulations are the same to first order approximation. This assumption is inherent in all climate change studies based on time slice experiments and represents the best possible option so far.

Table 2 lists the different GCM and RCM forcing setups used to drive the tide surge model experiments. A first series of experiments comprises four control and four climate change experiments with atmospheric conditions taken from the HIRHAM, RCAO, CLM and REMO RCMs. In this case, the boundary conditions for all RCMs were computed with the Hadley Center GCM HadAM3H and based on the IPCC A2 SRES emission scenario [*Houghton et al.*, 2001]. The second series of experiments includes two control and four future climate simulations, using meteorological forcing generated only by the regional climate model RCAO [*Räisänen et al.*, 2004], that was this time forced with boundary conditions from different GCMs and for different emission scenarios. Two global climate models were used, the HadAM3H and the ECHAM4/OPYC3 In this set of experiments, two SRES emission scenarios (A2 and B2) were applied to estimate future atmospheric GHG conditions.

Regional Climate Model	HadAM3H	ECHAM4/OPYC3
RCAO	CTL, A2, B2	CTL, A2, B2
HIRHAM	CTL, A2	
CLM	CTL, A2	
REMO	CTL, A2	

Table 2: List of tide-surge model runs and their atmospheric forcing

3.5 Methods and results

By performing a dynamical downscaling of possible future atmospheric conditions on regional water level heights, the experimental design results in a series of 30-year long datasets of projected future North Sea water level heights under such meteorological conditions. To separate the surge residuum from the total of the water level variation, a tide-only run was performed without any meteorological forcing. The resulting water heights, representing the astronomical tide, were subtracted from the climate response simulations.

Quantitative information about possible changes in surge heights under increasing greenhouse gas conditions are deduced and their statistically significance to today's

conditions are investigated. Beside this a further questions is considered: Are there statistically significant differences among the storm surge projections using the different (future) atmospheric forcings? Results are summarized in sub-section 3.5.1. In subsection 3.5.2 a method is sketched of how to transfer the regional projection on a local scale in order to respond to coastal engineers' requirements. To do so, a nonlinear statistical transfer function is constructed to condition local water heights of the river Elbe at St. Pauli in the harbor of Hamburg, Germany, on water levels in a 10 km x 10 km grid box at the mouth of the Elbe estuary.

3.5.1 Climate change North Sea storm surge projections

Storm surge residuals are analyzed along the North Sea coastline where the most severe damages from elevated water elevations are expected. To avoid inconsistencies due to near-shore shallow water effects, which are not resolved in TRIMGEO, the analyses shown here are carried out for grid boxes following the 10-m depth line in the model bathymetry ranging from the North of Scotland along the southern North Sea coast to the northeastern tip of Denmark near Skagen (see Figure 3.1, crosses along the coast). All statistical analyses are limited to the winter months December, January and February (DJF), as most severe storm surges are generally expected during the winter season. Thus, 29 seasons are obtained for each of the 30-year time slice experiments. Thus the inter-annual means are derived from 29 seasonal values.

The natural year-to-year variability of the storm surge climate is inferred from a hindcast simulation with SN-REMO from the years 1961 to 1990, using the same setup of the hydrodynamic model (see section 4.2.1). Based on these variations, simple t-test statistics are applied to determine if the simulated future changes in storm surge climate are lying inside the range of natural variability. If this null hypothesis is rejected, i.e., when the changes fall outside this range, then the changes can be considered as being caused by the effect of human input of greenhouse gases into the atmosphere.

Generally the 99.5[th] percentile of water levels is chosen for the analyses of storm surge heights. Thus, when considering 90-day winter seasons (DJF) based on 30-minute model output data, we get 90×48 cases (time-steps) and the 99.5[th] percentile is exceeded about 22 times in one season. As the results in *Woth* [2005] (chapter 5) are based on 99th percentiles, these results are recalculated here to the same thresholds and statistics used in *Woth et al.* [2005], in order to make them comparable. The key results are summarized in the following.

The statistics derived from the different control climate experiments show a range up to 45 cm in the long-term mean of the annual 99.5[th] percentile of water level/surge (Figure 3.2). Compared to the hindcast, performed for the same 30-year period (black line), the magnitude is generally too weak (with the exception of CLM forced simulation) leading to an underestimation of the storm surge 99.5[th] percentile. This is a finding consistent with *Flather and Smith's* [1998] results. However, the spatial structure is well reproduced by all ensemble model runs with highest storm surge levels in the German Bight (up to 1.40 m) and decreasing levels along the Danish coast as well as on the East and West Frisian Islands. The UK coast shows relatively small values with an increase from Scotland (0.20 m) to South England (up to 0.80 m). The reason for the underestimation can be found by analyzing the driving wind fields (see sec. 4.3.1.1). High near surface wind speeds are generally underestimated by most of the atmospheric models in the control simulations compared to e.g. re-analyses.
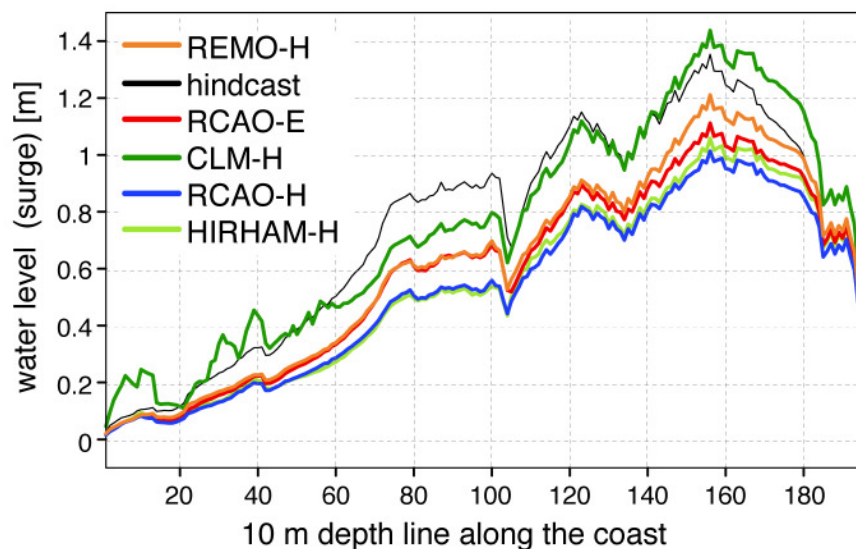

Figure 3.2: Long-term mean of the annual 99.5[th] percentile of water level/surge for the control period 1961-1990 (DJF) for all control climate simulations and the hindcast. Shown are values for the grid cells located along the 10-m depth line along the North Sea coast (x-axis; for the numbering of locations, refer to Figure 3.1).

Changes in storm surge statistics between a series of future climate change projections and the corresponding control simulations of today's climate conditions are shown in Figure 3.3. The upper panel displays changes as simulated in the first experiment series (different RCMs, all forced with the same GCM and the same emission scenario). The bottom panel shows simulated changes derived from the second experiment series (same RCM, but two different GCMs and two emission scenarios). All climate change projections show an increase in the magnitude of high storm surge events, although to a

different extent. The shift is statistically significant (at the 5% level) and as such attributable to the increased GHG concentrations, when the curve of differences lays outside the grey band. This band indicates the confidence limits based on student-t distribution and was derived from the hindcast variability. A statistical significant increase in the 99.5[th] percentile surge is found for most of the curves from the Belgian Coast northeastwards, up to Denmark. The highest increase is found at coastal grid points around the German Bight (up to 0.30 m). The inter-model spread of the 99.5[th] percentile in the ensemble reaches up to 15 cm (see section 3.6).
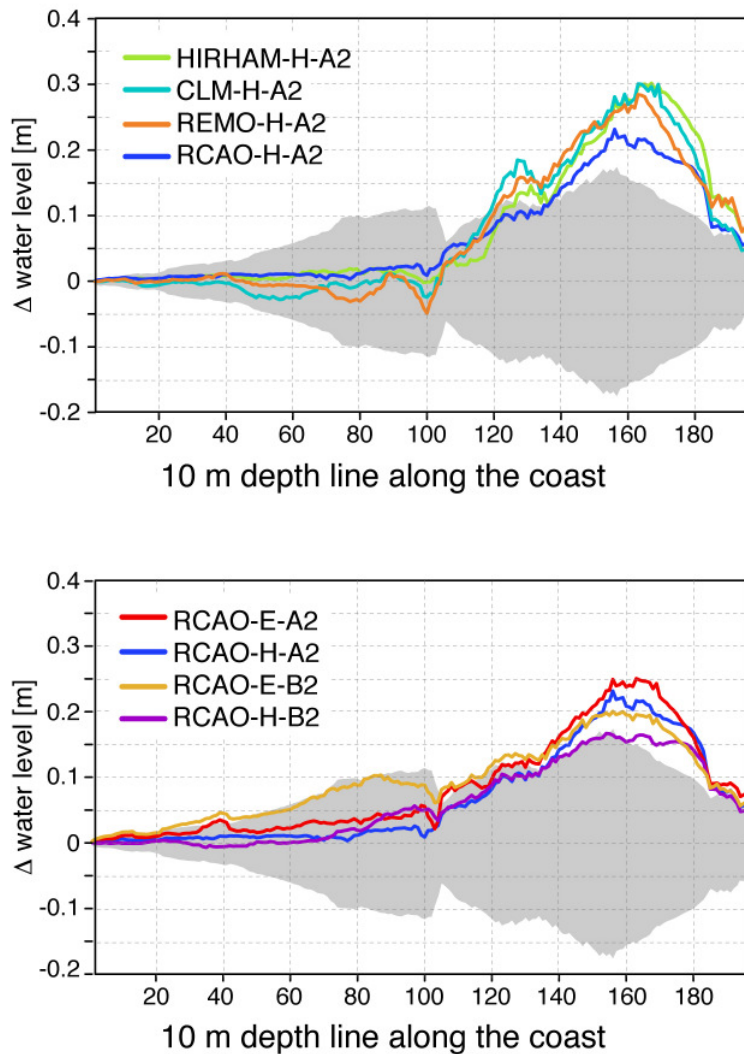

Figure 3.3: Differences "Scenario – CTL" in long-term mean of the annual 99.5th percentile of water level/surge (DJF) for all four ensemble members of the first series of experiments (top) and for all ensemble members of the second series of experiments (bottom). The shading indicates the 95% confidence interval based on hindcast variability. Depicted are grid cells located on the 10-m depth contour line along the North Sea coast (x-axis; for the numbering of locations, refer to Figure 3.1)

In the western part of the continental coast, the increase is primarily a result of more frequent extremes while in the eastern part, between the German Bight and Denmark, changes in the duration and the intensity of storm-related water level anomalies become more important (see section 4). These differences would have different implications for coastal protection. An increase in the frequency of extreme events alone would be less relevant for many coastal facilities whereas an increase in duration and magnitude of extreme events could stretch their security limits.

This increase in high storm-related water levels are due to changes in the local wind and pressure conditions. An increase of wind speeds of westerly winds of 6 to 8 % (depending on the simulation used) is found for strong winds over the southern part of the North Sea. Refer to chapter 4 for a more detailed discussion of the meteorological conditions.

The differences among the different members of each experiment series regarding the shift between today's and future storm surge extremes are not statistically distinguishable. That means the null hypothesis 'the shift in storm related water level from today's to future climate conditions is equal when using different RCMs (given the same global forcing and the same emission scenario)' is not rejected. Figure 3.4.a shows the confidence interval (grey band) and the differences in the climate change shift when all simulations in the first series of experiments (same GCM and same emission scenario) are compared against each other. It can be seen that these differences between the experiments are not significant. The same is true when comparing the climate change shift found in the simulations with one RCM forced with different GCMs as well as with different emission scenarios (fig 3.4.b), with the exception of a spatially very limited difference for the ECHAM4/OPYC3 forcings under the A2 and B2 scenarios.
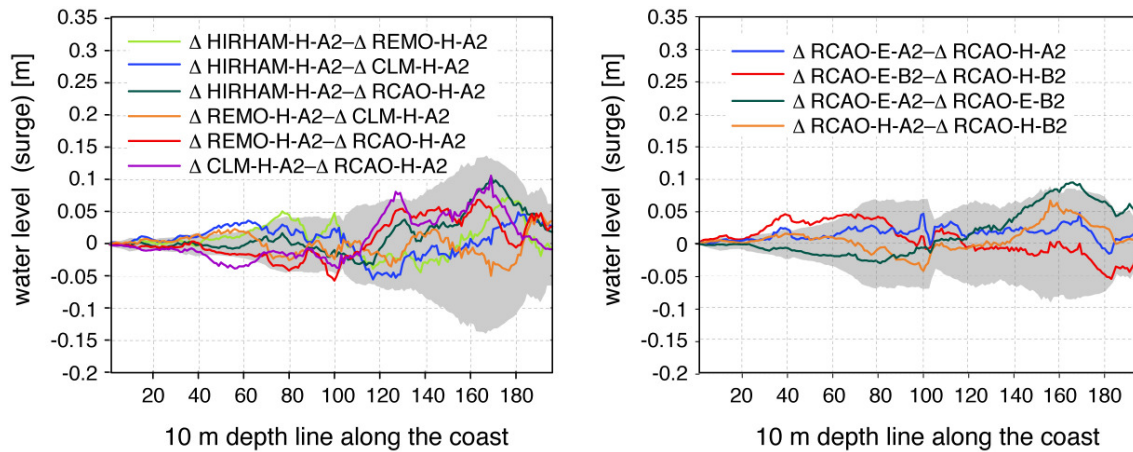
Figure 3.4: Differences (in m) of the climate change surge signal in the 30-year means of the intra-annual 99.5th percentiles.
a) calculated between all combinations of the climate change simulations with different RCMs but the same GCM and same emission scenario (experiment series 1)
b) calculated between all (four) combinations of the climate change simulations with the same RCM but different GCMs and emission scenarios (experiment series 2).
The shading indicates the 95% confidence interval based on t-test statistics. Depicted are grid cells located on the 10-m depth line along the North Sea coast (x-axis; refer to Figure 1 for the numbering of locations).

3.5.2 Localization of storm surge projections for Hamburg

Based on the experiments on the regional scale, a simple approach is presented to esti-mate changes in high water levels at a specific local site. Here, Hamburg St. Pauli, around 100 km inside the Elbe estuary, is used as an example. The link between storm-related water levels at a coastal grid box and high-tide water levels at the specific site takes the form of a nonlinear transfer function and was fitted to the TRIMGEO North Sea hindcast (4.2.1) at a suitable grid box and observations of high-tide water levels taken at the tide gauge Hamburg St Pauli between 1980 and 1990. The particular inter-val from 1980 to 1990 has been chosen because river dredging measures had no signifi-cant impact on the tidal regime in Hamburg (cf. Figure 6.2). Also systematic changes of the difference in surge height in Cuxhaven and St. Pauli could not be found since the 1980s. The transfer function changes at a point x_k, which was determined as 1.7 (m), from a linear function to a quadratic function:

$$f(x) = \begin{cases} f_1(x) = ax + b, x < x_k \\ f_2(x) = cx^2 + dx + e, x \geq x_k \end{cases} \text{ with } f_1(x_k) = f_2(x_k) \text{ and } f_1'(x_k) = f_2'(x_k).$$

This approach has been suggested by *Langenberg et al.* [1999] and also by *Lassen et al.* [2001]. Refer to chapter 6.2.1. for details on the best-fit coefficients in *f*(x), *a*, *b*, *c*, *d* and *e*. The most suitable North Sea grid box, i.e. the one resulting in the best fit, is the coastal cell containing Cuxhaven.

After having estimated this transfer function empirically, the water levels between 2071 and 2100 from all regional experiments at the grid box containing Cuxhaven can then be translated to high-water levels at Hamburg St. Pauli. The resulting differences of the water level between control and scenario simulations are added to the observed high-water level in St Pauli.

In order to be able to make statements on the expected climate change for other time horizons than 2085 (corresponding to the simulation period 2070-2100), a second approximation is applied by interpolating the North Sea water level simulations between the available time horizons 1961-1990 and 2071-2100. In particular, we are interested in the mid-term period around 2030, which is the time horizon of relevance for present planning and adaptation. The interpolation is done proportionally to the expected increase in global mean temperature as provided by IPCC [*Houghton et al.*, 2001]. That means, to establish a projection of the results onto the time horizon 2030, the development of storm-related water level heights are assumed to be proportional to the increase in global mean temperature (see chapter 6.2.2). Since the changes in simulated storm surge heights in A2 and B2 are not significantly different (see 3.5.1) we assume that the mean maximum surge height at the location at the mouth of the Elbe in both scenarios are increased by φ=30% of the rise derived from the various TRIMGEO scenarios for the 2071-2100 time horizon.

The projections provided by the IPCC [*Houghton et al.*, 2001] are also used for the mean sea level rise (*D*), which is added to the change caused by meteorological forcing. For the mid-term time horizon 2030 an increase of 9 cm is used for both scenarios, while the increase reaches 33 cm for A2 and 29 cm for B2 by 2085. The uncertainty of these numbers is given by the IPCC as about ±5 cm and ±20 cm for the different time horizons, which accounts for different global climate models and emission scenarios. If

the possible response of ice-sheets is factored in, the uncertainties rise to about ±10 cm and ±30 cm, respectively [*Houghton et al.*, 2001]. It is assumed that mean sea level rise and changing storm surge height are independent and may simply be added (see also section 2.2.1; *Kauker and Langenberg*, 2001).

To calculate *P*, the expected mean annual maximum high-water level at St Pauli, the statistical transfer function *f*(x) is applied as follows:

$$P = f(\mu_{H,s} + \varphi(t)[M(S) - M(C)]) + D(t) \qquad \text{for t = 2035 and for t = 2085}$$

with $\mu_{H,s}$ = mean annual mean maximum high tide water level as simulated in the hind-cast (selected grid box, Cuxhaven) and with *M* = simulation with specific atmospheric conditions for *S* = scenario and *C* = control run. *D* is the expected mean sea level rise and φ is the fraction of increase of storm-related water level height relative to the total increase at the end of the 21st century derived from global temperature increase as described above.

The storm related change of mean maximum surge level change at the Cuxhaven grid box for the end of the 21st century varies between 42 cm to 61 cm with a mean value, across all models and scenarios, of 50 cm. Using our formula above, we find a mean possible and plausible rise at St. Pauli of 18 cm for 2030 and 63 cm in 2085 (fig. 3.5). The range of minimum and maximum values is 13 cm to 23 cm in 2030 (about ±5 cm) and 48 cm to 82 cm in 2085 (about ±20 cm).
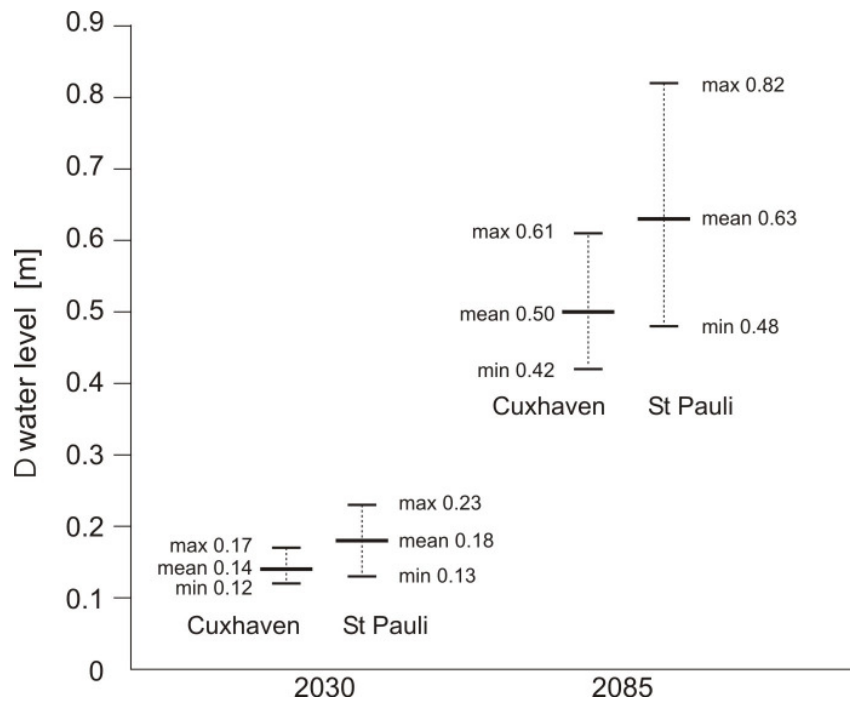
Figure 3.5: Scenarios of changes in storm surge heights including the rise of mean sea level in Cuxhaven and Hamburg St. Pauli in 2030 and 2085. The scenarios are all based on simulations with the TRIMGEO hydrodynamical model, which was forced with winds and air pressure from different regional models and emissions scenarios (Woth, 2005). Since the A2 and B2 scenarios do not significantly differ, the numbers are lumped together in one mean value, across models and scenarios, and in a range given by the minimum and maximum values.

3.6 Minimum range of uncertainty

Estimates of future climate change are affected by a range of uncertainties coming from different sources. In addition to the inherent chaotic nature of the climate system, one source of uncertainty is the unknown development of the global economy, technology and society in general, and thus the evolution of the GHG-relevant emissions as described in section 2.1. Another source is the uncertainty resulting from the use of imperfect models due, e.g., to semi-empirical parameterizations of sub-grid scale processes. In our specific context, the model uncertainties in fact accumulate due to the use of a hierarchy of three model families: global General Circulation Models (GCMs) and regional climate models (RCMs), which are used to model the atmospheric response to the different emission scenarios, and the hydrodynamical model used to simulate the water level response to changing atmospheric conditions. Also the uncertainty due to natural climate variability have to be considered.

Up to now it is not possible to quantify the full range of uncertainties in projections of future storm surge heights. But one useful possibility is to derive a *minimum range of uncertainty* of different components as e.g. *Lowe and Gregory* [2005] have shown for total water level at two locations along the UK coastline. They distinguished between the source of uncertainty from the effect of changes in storminess (coming from GCM and RCM simulations) on surge, the effect of global average sea level rise and the uncertainty in future emissions.

With the limited range of experiments at hand, two contributions to the overall uncertainty in the expected change of surge climate are covered in this thesis: model uncertainty and the uncertainty in future emissions. The uncertainties are analyzed in terms of the differences between 30-year means of the annual 99.5th surge percentiles for the control and future time slice, exemplary for a grid box on the 10-m depth line close to Cuxhaven. Figure 3.6 shows the spread in projected surge changes, separating model uncertainty (left three columns) and emission uncertainty (right two columns).

The first column encompasses all shifts in surge coming from the first series of experiments (same GCM, same emission scenario, but different RCMs). The total range is 4 cm, from an absolute shift between control and future climate projection of 22 cm to a shift of 26 cm. The second column depicts the spread coming from the response of one RCM (RCAO) to the forcings from two different GCMs using the same emission scenario (A2). With a spread of 2 cm, this factor seems to be unimportant in these experiments. Column 3 shows a comparable range, but now for the B2 scenario. Again, the spread of 3 cm is small. Column 4 shows the difference (4 cm) in the percentile shift when using two different emission scenarios, A2 and B2, but the same RCM (RCAO) and the same GCM (ECHAM4/OPYC3). The last column (5 cm spread) is similar to column 4 except that the HadAM3H GCM forcing was used for the two simulations.

Summarizing, the response of the tide surge model in these specific climate scenarios of future storm surge conditions exhibit more similarities than differences between the ensemble members. We can specify a band of the spread in projected surge changes, which has a size of about 15 cm. Contributions of the uncertainty could be distinguished. In this experiment the largest spread in projected surge changes comes from the use of different emission scenarios.
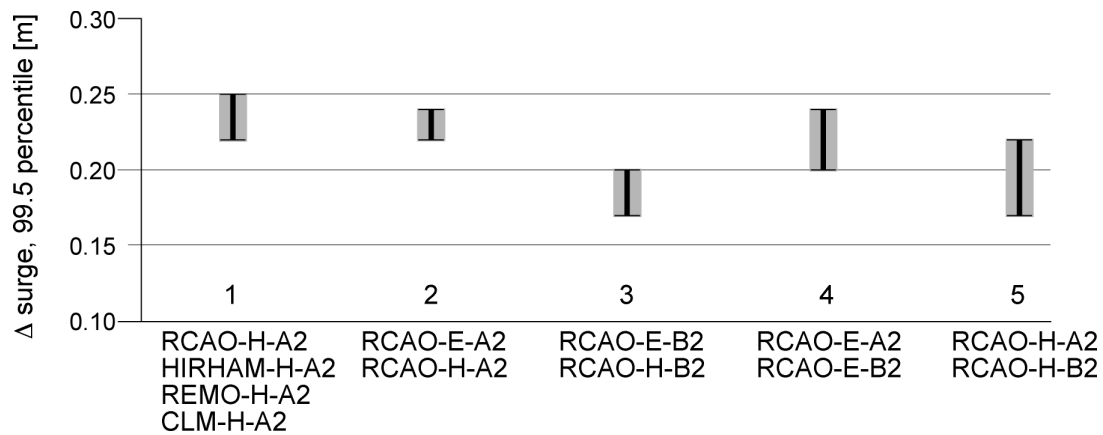
Figure 3.6: minimum range of uncertainty, deduced from the seven future storm surge simulations in the change in 30-year mean of the 99.5[th] percentile. Shown is the spread coming from the use of (**1**) different RCMs (same GCM, SRES A2); (**2**) different GCMs, (same RCM and SRES A2); (**3**) different GCM (same RCM and SRES B2); (**4**) different SRES scenario (same RCM, same GCM); (**5**) different SRES scenario (same RCM, same GCM). Data were derived exemplary for one grid box close to Cuxhaven (No. 154, see figure 3.1).

These results could be due to the similarity of the 'physics' of the GCMs and, of course, by the rather limited experimental design. Certainly, this analysis is valid only for the GCMs, RCMs and emission scenarios used here and can not be easily transferred to a general statement about the magnitude of uncertainty ranges. Thus, this is only a first step to explicitly account for the large uncertainties, which are inherent in such studies dealing with possible future climate change scenarios.

3.7   Conclusions

A state-of-the-art storm surge model was run for present-day control conditions (1961 – 1990) and projected future climate conditions (2071 – 2100) for the North Sea basin. Atmospheric forcings were taken from four different RCMs, which were used to dynamically downscale the 'control climate' and the A2 and B2 SRES scenarios (IPCC) from two driving global models, HadAM3H and ECHAM4/OPYC3. The aim of these climate change experiments was to provide information about possible changes in the characteristics of North Sea storm surge climate. Besides this, a range of minimal uncertainty has been estimated. In addition, the results of these climate change experiments were transferred to a tide gauge not resolved in these North Sea model runs, namely St. Pauli at the river Elbe in Hamburg, Germany. Observed data at St. Pauli were empirically linked to hindcast data at the coastal grid box containing the city of

Cuxhaven. With the help of this transfer function, future conditions were deduced for this locality.

The analysis of changes between control climate and scenarios was based on the inter-annual mean of the 99.5th percentile of half-hourly surge values for the winter months. A climate change signal of increasing surge heights along most of the continental coast emerges for both scenarios, SRES A2 and SRES B2. In most locations, these shifts, relative to the control simulations, are beyond the confidence limit (at the 5% level) characterizing natural variability, with highest values of up to 30 cm for the German Bight. Considering only the differences of these shift among all experiments, it could be shown that neither the use of different RCM as well as different GCM forcings nor the use of different emission scenarios leads to statistically distinguishable results (at the 5% level).

The overall structures of the changes between the scenario and the control simulations are rather similar for all ensemble members. Larger and statistically significant changes are obtained for the continental coast while differences are generally smaller and not significantly different from zero along the UK coast. For the end of this century the IPCC expects a mean sea level rise of about 35-40 cm due to thermal expansion under the emission scenario A2 [*Houghton et al.* 2001]. When adding this additional portion, the simulated shift in storm surge heights rises to a possible increases of about 60 cm to 70 cm in the 99.5th percentile within the German Bight.

Finally changes in mean maximum water levels were deduced from absolute water level heights at the tide gauge St. Pauli. This was done not only for the end of the 21st century but also for a closer time horizon. The estimated increase of mean sea level by IPCC is added to the storm-related change. The calculated increase varies between 13 cm to 23 cm (about +/-5 cm uncertainty from increase in mean sea level) in 2030 and between 48 cm to 82 cm (+/-20 cm uncertainty) in 2085 when considering all seven model simulations.

Chapter 4

Climate change and North Sea storm surge extremes: An ensemble study of storm surge extremes expected in a changed climate projected by four different Regional Climate Models

KATJA WOTH [*]

RALF WEISSE [*]

HANS VON STORCH [*,**]

Institute for Coastal Research, GKSS-Research Centre, Max-Planck-Str. 1, 21502 Geesthacht, Germany

** Department of Meteorology, University Hamburg, Germany*

Abstract

The Coastal Zones are facing the prospect of changing storm surge statistics due to anthropogenic climate change. In the present study we examine these prospects for the North Sea based on numerical modelling. The main tool is the barotropic tide-surge model TRIMGEO (Tidal Residual and Intertidal Mudflat Model) to derive storm surge climate and extremes from atmospheric conditions. The analysis is carried out by using an ensemble of four 30-year atmospheric regional simulations under present-day and possible future-enhanced greenhouse gas conditions. The atmospheric regional simulations were prepared within the EU project PRUDENCE (Prediction of Regional scenarios and Uncertainties for Defining EuropeaN Climate change risks and Effects). The research strategy of PRUDENCE is to compare simulations of different regional models driven by the same global control and climate change simulations. These global

conditions, representative for 1961-1990 and 2071-2100 were prepared by the Hadley Center based on the IPCC A2 SRES scenario.

The results suggest that under future climatic conditions storm surge extremes may increase along the North Sea coast towards the end of this century. Based on a comparison between the results of the different ensemble members as well as on the variability estimated from a high-resolution storm surge reconstruction of the recent decades it is found that this increase is significantly different from zero at the 95% confidence level for most of the North Sea coast. An exception represents the East coast of the UK which is not affected by this increase of storm surge extremes.

4.1 Introduction

In historical times, serious floods have severely impacted coastlines of the North Sea. But also more recent floods in the twentieth century have highlighted the current potential for high-impact damage, threatening human life as well as property. The mechanism leading to coastal floods is well understood. Given the configuration of the coastline and the bathymetry, the severity of the storm surge depends primarily on wind speed, wind direction and duration. The meteorological conditions are affected by the path and the velocity of the depression systems, moving across the North Sea. Mainly three different types of meteorological situations leading potentially to high storm surges at the Southern North sea coast, can be distinguished after *Petersen and Rhode* [1991]: The Jutland-Type, developed over Newfoundland, traveling mostly very fast in easterly direction from England over the North Sea to Jutland. The Scandinavia-Type is a slow-moving depression system, which forms over Greenland and Iceland and travel towards southeast. The track of the third type, the Skagerrak-Type lies between the other two types, traveling mostly from WNW to ESE [*Gönnert et al.* 2001].

When winds push water towards the coast, it tends to accumulate into what is commonly referred to as storm surge. If a particular high surge occurs together with a tidal maximum, both effects accumulate and serious flooding can result, depending on the coastal structure and their protection.

For the North Sea, many studies dealing with dynamical modelling of tide-surges exist. Examples are *Dolata et al.* [1983], *Heaps* [1983], *Flather et al.* [1998], *Kauker* [1998], *Langenberg et al.* [1999], and *Kauker and Langenberg* [2000], among others. They have shown that, provided that the meteorological forcing has sufficient accuracy, storm surges and their statistics can be satisfactorily modelled with hydrodynamic models, especially if the focus is on long-term statistics rather than on single events. Comparing simulations with a 3-dimensional baroclinic model [*Kauker* 1998] and a vertically integrated barotropic model, *Kauker and Langenberg* [2000] found that the latter ones are sufficient for a reasonable description of storm-related water-level variations along the North Sea coast.

Storm surge models have also been used in recent years to assess the potential effects of changing greenhouse gas concentrations on the North Sea storm surge climate. In the WASA project (Waves and Storms in the North Atlantic; *WASA-Group* 1998, *Langenberg et al.* 1999; *Flather and Smith* 1998] the wind and pressure data originated from

two global high-resolution (T106) 5-year simulations, whereas 30-year time slice T106 simulations were used in STOWASUS-2100 project [*Stowasus-Group* 2001]. These results show that under enhanced greenhouse gas conditions, an increase by up to 10% in extreme wind speeds in the North Sea and the Norwegian Sea may take place and can result in an increase in surges extremes of the same magnitude. *Lowe et al*. [2001] were the first, who applied the two-step procedure of a dynamical downscaling of coarse grid general circulation model (GCM) data followed by an integration of a hydrodynamical model. Their results indicate an increase in surge extremes statistically significant along a sizable fraction of the UK coastline under assumed future climate conditions.

Such numerical model integrations have the advantage to generate information at locations and for periods (such as under climate change conditions) without observations. Another advantage of model integrations is the high temporal sampling rate, every hour or even less, while observations are often only available for tidal maxima and minima. To have full access to this advantage, the meteorological forcing data must also be available with high temporal resolution and not just every 12 or 6 hours, as is common in many RCM simulations.

In the present study we follow and extend the way, the previous studies have pursued. Based on high-resolution regional wind and pressure conditions, dynamically downscaled from global Genera Circulation Model GCM output, the present study differs from these previous approaches by using an *ensemble* of regional atmospheric conditions. The ensemble is provided by a series of different RCMs, which are all forced with the same GCM. The wind and air pressure data are provided by the partners of the EU PRUDENCE project (Prediction of Regional scenarios and Uncertainties for Defining EuropeaN Climate change risks and Effects; *Christensen et al*. 2002], for paired 30-year "control" (1961 - 1990) and "climate change" (2071 - 2100) simulations. We use these ensemble members to drive a hydrodynamic tide-surge model at high spatial and temporal resolution. In contrast to previous work this allows us not only assess the response of the storm surge model to a specific RCM but to systematically investigate similarities and differences in the storm surge climate due to the use of different state-of-the-art RCMs, a major goal of the PRUDENCE project.

Our study considers changes in storm surge *extremes* as only strong storm surge events endanger the coastal structure and the biotic and abiotic environment there. By definition, extreme values are rare. Two main methods are mainly used to characterize such extreme events, namely either the analysis of the largest events in a long series, or an extrapolation by fitting shorter data sets to a particular extreme value distribution [e.g.,

Coles 2001]. The various RCM forced simulations provide us with long series of 30 years length, so that we can avoid the "extreme value statistics" extrapolation - as long as we are not asking for large return periods - which is rather sensitive to the choice of the distribution and the fitting procedure. Instead, we are able to provide a phenomenological characterization based on simple characterization of those distributions and underlying properties by means of high percentiles.

The analysis in this study is dealing only with the impact of changing regional wind conditions in the vicinity of the North Sea. In this way, two effects, which we believe to be minor for the *change* of surge statistics, have been neglected. These are the rise in mean sea level and the effect of so-called external surges.

In the context of future mean sea level heights, the IPCC expects a rise due to thermal expansion and the changing volume of glaciers and ice sheets for the end of this century [*Houghton et al*. 2001]. In the A2 SRES scenario, which we use in this study, the rise due to thermal expansion could be about 40 cm, loaded with a large uncertainty [*Houghton et al*. 2001]. For our study, the relevant question is if the storm surge heights are sensitive to changes in mean sea level. This was studied in detail by *Kauker* [1998] and *Lowe et al.* [2001], who found no significant differences in simulations with and without elevated mean sea level. The mean sea level rise essentially adds to the storm surge heights.

External surges are generated under certain weather conditions in the North Atlantic and propagate into the North Sea, pushing additional water masses into the basin. In our set-up, we cannot account for this effect. Instead, we assume that the intensity and frequency of external surges is not significantly altered in the scenario of future conditions. However, this assumption may not be fully justified: Most recent studies indicate a strengthening North Atlantic storm track projected in GCMs for the A2 SRES scenario [e.g., *Fischer-Bruns et al*. 2005], even though some studies envisage other developments [e.g., *Rauthe et al.* 2004]. A strengthening of the storm track would possibly lead to more frequent external surges in a future climate and, thus, the neglected effect of external surges would lead to an underestimation of the change of storm surge extremes.

The present paper is organized as follows: In Sect. 4.2 the hydro-dynamical model and the atmospheric data used to drive the tide-surge model are described and the applied statistical methods are introduced. Results and discussion follow in Sect. 4.3, which is divided into two parts: In Sect. 4.3.1 the control climates of the present-day atmospheric forcing (near surface winds and SLP) and those of the modelled storm surges are ana-

lysed and compared with the climates obtained in hindcasts of corresponding decades. Changes in the atmospheric forcing and subsequently in the storm surge distributions in a perturbed climate described by the A2 SRES scenario are analysed and discussed in Sect. 4.3.2. We conclude in Sect. 4.4.

4.2 Methodology and data

4.2.1 Surge model and model validation

The dynamical downscaling of storm surges is carried out by driving the numerical tide-surge model TRIMGEO (Tidal Residual and Intertidal Mudflat; *Casulli and Catani* 1994], a depth average tide-surge model, using geographical coordinates. This barotropic version of TRIMGEO is based on the shallow water equations with parameterizations for bottom friction and surface stress [*Casulli and Catani* 1994; *Casulli and Stelling* 1998]. The equations are integrated on an Arakawa-C grid using a robust semi-implicit scheme with a time step of 10 min.

The model domain encloses the north-west European continental shelf from 4.25° W to 13.42° E and 48.55° N to 58.75° N with a mesh size of 6' x 10' in latitude and longitude, which corresponds to a grid cell size of about 10×10 km^2. Figure 4.1 shows the TRIMGEO integration area and the bathymetry. The bathymetry was provided by the German Federal Maritime and Hydrographic Agency (BSH) and is similar to the one used in their operational model.
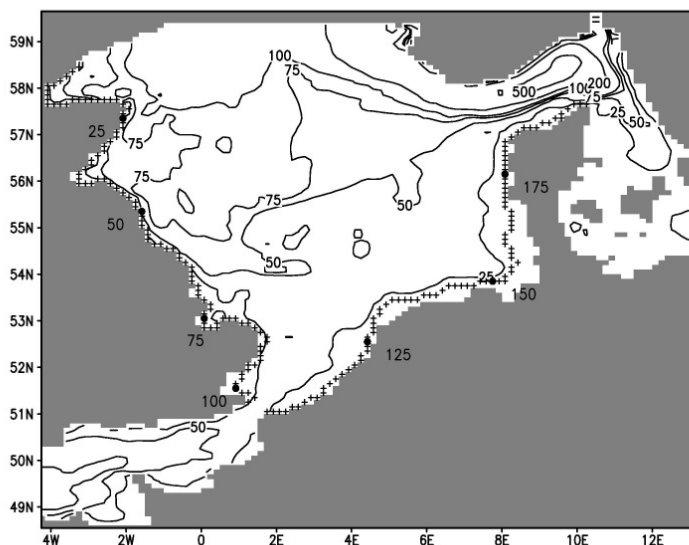

Figure 4.1: Model domain of the tide-surge model TRIMGEO: the bathymetry *(isolines)* and the 196 near coastal grid cells *(crosses)* located on the 10-m bathymetry line along the North Sea coast beginning with 1 in Scotland and ending with 196 in Denmark

48

The model domain has open boundaries in the North, along a line between Wick (UK) and Karmøy (N), and through the English Channel in the West; East of the Danish islands, along a line between the southern tip of Sweden and Rügen, a German Island, the domain is artificially closed, which is acceptable since reflecting waves, coming from that model boundary can hardly affect the North Sea area. A constant water-level and net influx of 0.01498 m^{3}s^{-1} from the Baltic Sea [*Ospar Commission* 2000] are prescribed. Following the operational procedure at BSH constant freshwater influxes from the 33 largest rivers are specified as climatological annual means. For imposing the astronomical tides, sea level anomalies calculated from the amplitudes and phases of 17 partial tides are prescribed along the open boundaries. These amplitudes and phases as well as corrections for each year were adapted also from BSH. For the northern model boundary, long-term observations from buoys were used to derive the tidal components, for the boundary model grid cells in the English Channel, published harmonic composites were adopted [e.g., *Chabert d'Hieres and Provost* 1978]. For comparability, all TRIMGEO model runs are based on the same astronomical tidal coefficients and corrections.

The model was run with a calendar year consisting of 360 days since all RCM simulations simulate years of 360 days – a feature inherited from the driving global – the so-called climate mode. The tides are specified in continuous order so that dates of tidal minima and maxima in terms of real world 365-day calendar no longer fit to the 360-day calendar of the models. This is, however irrelevant, as the simulated weather stream in the RCM simulations cannot be tied to specific hours or days; their timing must be considered random relative to the timing of the tides.

The model is validated by comparing model "hindcast" results of reconstructed water-levels with statistics derived from a local tide gauge and by comparing percentiles along the 10-m depth line with simulations with an operational storm surge prediction model.

This "hindcasts" consist of two steps: first a regional reanalysis of atmospheric conditions was prepared [*Feser et al.* 2001] using the REMO model [*Jacob* 1995] with spectral nudging [SN-REMO; *von Storch et al.* 2000]. The resulting marine wind and air pressure fields were found to be homogeneous and of satisfactory quality [e.g., *Weisse and Feser* 2003; *Sotillo* 2003; *Weisse et al.* 2005]. In a second step, these "analysed" winds and air-pressure field were fed into the tide surge model.

The principle capability of the tide-surge model TRIMGEO to reasonably reconstruct observed regional sea level was recently demonstrated by *Aspelien and Weisse* [2005].

They have shown that sea level heights and surge for the southern North Sea shelf for the period 2000 – 2002 are reasonably reproduced by the present model setup. Thus here we have limited ourselves to some additional validation focusing on the statistics of storm surges as discussed in the present paper. Figure 4.2 shows time series of the annual winter 99th percentile surge (DJF) for Cuxhaven derived from the model hindcast and from the local tide gauge data from 1958 to 2000. The hindcast percentiles fit to the percentiles derived from observations with a correlation coefficient of 0.93 and a root mean square error of 19 cm, which is mainly caused by 2 years in which the model severely underestimates the observed 99th percentile, in particular the very stormy winter 1975/76.
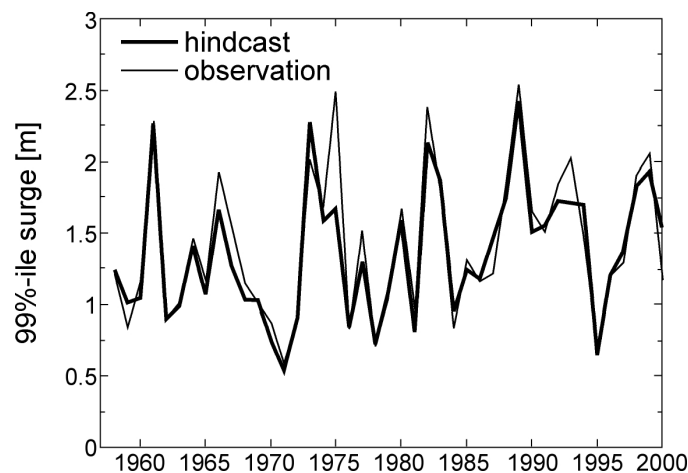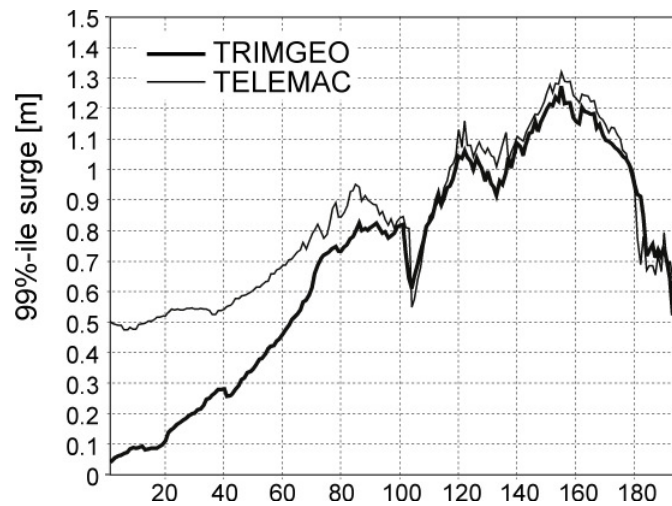

Figure 4.2: Inter-annual mean of the 99th percentile of water-level/surge (DJF) for Cuxhaven for the period 1958 – 2000 (unit: m). Bold line: modelled hindcast (TRIMGEO); thin line: tide-gauge observations. Calculations of percentiles are based on 1 hourly data.

Additionally, we compare the performance of TRIMGEO in simulating extremes in grid boxes along the 10-meter depth line of the model-bathymetry. This is motivated by the fact that our analysis of possible future conditions is focusing on just these gridboxes (see Sect. 4.2.3). However, observation data do not exist for this 10-m depth line. Therefore we compare the TRIMGEO hindcast to a hindcast done with the TELEMAC-2D model of Bundesanstalt für Wasserbau (BAW). TELEMAC-2D is used by BAW for daily operations and is set up with high-resolution refinements along the coast, leading to a spatial resolution of down to 80 m. A TELEMAC-2D hindcast was performed with the same meteorological forcing as described above [*A. Plüss*, personal communication). An additional feature of this simulation is that it assimilates the actual water-level data from Aberdeen. This model has been found to reliably reproduce the observations taken at a number of different tide gauges. An extensive validation has been performed by e.g., *Hervouet and Van Haren* [1996] or *Plüss* [2003], with good results.

Figure 4.3 shows the mean of the annual 99th percentiles (based on 1 hourly data, winter month), derived from both, the TRIMGEO and from the TELEMAC-2D hindcast (1961 to 1990) along the same 10-m depth line. Differences occur along the Eastern coastline of UK. There, the advantage of assimilating Aberdeen-observations into TELEMAC-2D becomes obvious. Along the 10-m line of the continental North Sea coast, TRIMGEO deviates only by less than 10 cm from TELEMAC-2D, likely reflecting the missing effect of the external surges in TRIMGEO. The overall spatial patterns are matching very well.

Figure 4.3: Inter-annual mean of the 99th percentile of water-level/surge (DJF) for the control period 1961 – 1990 (unit: m). Bold line: TRIMGEO; thin line: TELEMAC. Calculations of percentiles are based on 1 hourly data. Depicted are grid cells located along the 10-m depth line along the North Sea coast (for the numbering of locations, refer to Fig. 4.1)

We consider the encouraging performance of the TRIMGEO hindcast as sufficient evidence for allowing TRIMGEO to be considered an adequate tool for studying the implications of possible future climate change on the statistics of storm surges, in particular along the southern and eastern shores of the North Sea.

4.2.2 Atmospheric driving data

This study uses near surface winds and sea level pressure as simulated by four RCMs, namely HIRHAM (High-Resolution regional model, with ECHAM physics) from the Danish Meteorological Institute DMI, RCAO (Rossby Centre regional Atmosphere-Ocean model) from the Swedish Meteorological and Hydrological Institute SMHI, the CLM (Climate version of the "Lokal-Modell", derived from the Limited area Model (LM) of the German Weather Service DWD) of GKSS, and REMO (Regional Model) of the Max-Planck Institute of Meteorology. All simulations were prepared for present-

day (1961-1990) greenhouse gas concentrations and for future conditions (2071-2100) based on the Intergovernmental Panel on Climate Change A2 SRES emission scenario [Houghton et al. 2001].

HIRHAM, REMO and CLM are stand-alone atmosphere models, RCAO [*Döscher et al.* 2002) is a coupled atmosphere-ocean model, which incorporates the Rossby Centers regional atmosphere model RCA [*Rummukainen et al.* 2001; *Jones et al.* 2004] and their ocean model RCO [*Meier et al.* 2003].

Concerning the model dynamics the models have two origins. HIRHAM (an updated version of HIRHAM4 [*Christensen et al.* 1996]) and RCA are both off-springs from the regional weather forecast model HIRLAM (High-Resolution Limited Area Model; [*Machenhauer* 1998; *Källén* 1996]). CLM and REMO [*Jacob et al.* 1995] are climate versions of the weather forecast model developed and used by the DWD. The parameterizations of subgrid-scale processes ("physics") of HIRHAM and REMO are based on the global atmospheric model ECHAM4, developed by *Roeckner et al.* [1996]. The parameterizations from RCAO are mainly taken from HIRLAM. Most of the parameterizations in CLM are taken from the LM, but some, in particular with respect to the soil processes, are improved.

All four RCMs are set up for running on a rotated grid with a mesh size between 0.44 and 0.5°. This mesh size corresponds to about 50 km^2 over the North West European Shelf Sea. All four regional climate models were forced in lateral sponge zones with data prepared by the Hadley Center GCM HadAM3H (high-resolution global atmosphere model) under recent and future climate conditions. Sea ice coverage and sea surface temperature (SST) are the same as used by the HadAM3H model in HIRHAM, CLM and REMO. SST and sea ice coverage for the control run were derived from observations, which were processed by the Met Office Hadley Centre into a data set of monthly fields on a 1-degree latidude longitude grid [*Rayner et al.* 2003]. For the future time-slice SSTs from the coupled HadCM3 (Hadley Centre's Third generation Coupled Ocean-Atmosphere GCM) SRES A2 simulation (2071 – 2100) have been used with a statistical correction obtained from the present-day observed SSTs preserving the observed SST variability. An exception is the RCAO model, which is coupled with the Baltic Sea model so that SST and sea ice coverage are computed directly in interaction of these model modules.

To drive the tide-surge model, 6 hourly, instantaneous values of pressure at mean sea level and the horizontal wind components at 10-m height were extracted from each of

the RCM simulations over the tide-surge model covering domain. These forcing data were interpolated linearly to match with the finer space-time grid of the hydro-dynamical model TRIMGEO.

The usage of 6-hourly is not optimal, but is unavoidable as the RCM output has been stored only once every 6 h. In case of the hindcast with TRIMGEO, hourly SLP and wind analysis prepared by SN-REMO [*Feser et al.* 2001] have been used. Hourly data are undoubtedly much better than 6-hourly data. We found the magnitude of the 99.5th surge percentile increased by about 10% when hourly forcing data are used instead of 6 hourly (not shown). We believe, however, that the effect of a too coarse temporal resolution of the forcing fields will not significantly bias the estimation of the *change* of surge statistics.

4.2.3 Processing results

The object of investigation is not the total water-level at a certain time and location, but wind and pressure-related surge residuals, i.e., the deviations of the overall water-level from the tide. Thus an additional "tidal run" was undertaken, using the same model setup, forced only by water-level variations at the open boundaries representing the global astronomical tidal dynamics. Resulting water-levels of that "tidal run" were subtracted from the water-level obtained in the control and climate change experiments, forced with the same astronomical tidal dynamics. Thus, nonlinear interactions of velocities with the tides are described in the meteorologically forced run. When subtracting the 'tide-only' run, all remaining phenomena are understood as being related to the forces exerted by wind and air pressure, including the interaction with the tides. The state-variables (vertically averaged velocity, water-level) are stored for all "wet" grid points of the model domain every 30 min. The first month of each simulation was discarded to account for potential spin-up effects.

Since most damage is expected in the coastal zone, storm surge residuals were analysed only along the North Sea coastline [*Langenberg et al.* 1999]. To avoid inconsistencies due to near-shore shallow water effects, which are not resolved in TRIMGEO, the analyses based all on a selected line, representing the 10-m depth line in the model bathymetry. This depth line comprises 196 grid cells ranging from the North of Scotland along the southern North Sea coast (Belgium, Netherlands and Germany) to the northeastern top of Denmark near Skagen (Fig. 4.1). As most severe storm surges are generally expected during the winter season, all statistical analyses in this study were carried out only for December, January and February (DJF), so that we get 29

seasons for each of the 30-year-long time-slice experiments, beginning with the first season Dec1961/Jan1962/Feb1962 and ending with the last season Dec1989/Jan1990/Feb1990 for the control runs. For the scenario time-slice the fist season is Dec2071/Jan2072/Feb2072 and the last season is Dec2099/Jan2100/Feb2100.

In our study the principle statistical approach is a straightforward description of extreme climate conditions by high and low percentiles of the distribution.

In that way, we consider the 29-year means of intra-annual percentiles, namely the highest (99th) percentile of wind speed at 10m height and the lowest (1st) percentile for air pressure as characteristic quantities. Since a 90-day DJF season contains $4\times90=360$ intervals of 6-hour length, the 99th percentile is the wind speed, which is exceeded in 1% of 360 cases, i.e., 3 times in a season. Similarly, air pressure is lower than the 1st percentile only during 18 h (3 times).

The comparison of the storm surge residuals in the different experiments is based on the 99.5[th] percentile. In this case, we consider again 90-day winter seasons (DJF) but with 0.5-hourly data, so that per DJF season we have 90×48 cases. To have sufficiently rare events, we use the 99.5[th] percentile, which is exceeded on 22 half hours (approximately 12 h) in each DJF season. We calculate this percentile for each of the 29 seasons and determine the mean value of these 29 percentiles.

We define an extreme event as a period covering one or more half hourly intervals with surge levels reaching or exceeding the 99.5[th] percentile. The average duration and the number of such extreme storm surges are also determined. These temporal characteristics of storm floods are important parameters in the context of coastal protection.

4.3   Results and discussion

4.3.1 Control simulations versus hindcast

Before we assess changes in water-level statistics and in the atmospheric forcing induced by increasing greenhouse gas concentrations in a HadAM3H/RCM world, we want to examine the similarity of the control simulations, which are supposed to be representative for the 1961-1990 period, with the 1961-1990 SN-REMO hindcasts [*Feser et al.* 2001] in terms of atmospheric conditions and surge statistics.

4.3.1.1   Atmospheric forcing

Figure 4.4 shows the statistics of the extremes in deep sea level pressure as well as the extreme near surface wind as obtained in the atmospheric SN-REMO hindcast, described as the 29-long-year mean of the 1st percentile (SLP) and as the 99th percentile (10-m wind speed), respectively. In the hindcast, a gradient of sea level pressure from 970 hPa (North-West) to 982 hPa (South-East) of the North Sea area is found. Wind speeds between 17 and 20 m/s are produced, increasing from South to North.
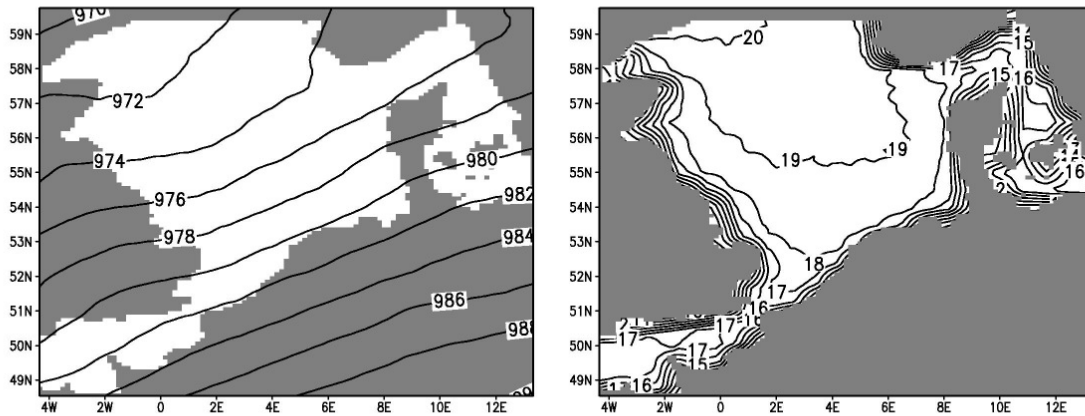
Figure 4.4: Inter-annual mean of the 1st percentile sea level pressure (*left hand side*) and of the 99th percentile 10-m wind speed (*right hand side*) derived from REMO_SN, hindcast, 1996 – 1990. Units: hPa (SLP) and m/s (wind speed). Calculations of percentiles are based on 6 hourly data (DJF)

All four RCM control simulations show an overestimation of the deepest sea level pressures (Fig. 4.5). The largest deviations are found for the HIRHAM and RCAO runs and vary between about 3.5 and 6 hPa. For most of the control simulations, differences increase from West to East. An exception is provided by the CLM control run where the difference pattern is more North-South oriented with smallest differences of about 0.5 hPa occurring in the northern and largest differences of about 4.5 hPa occurring in the southern part of the model domain.
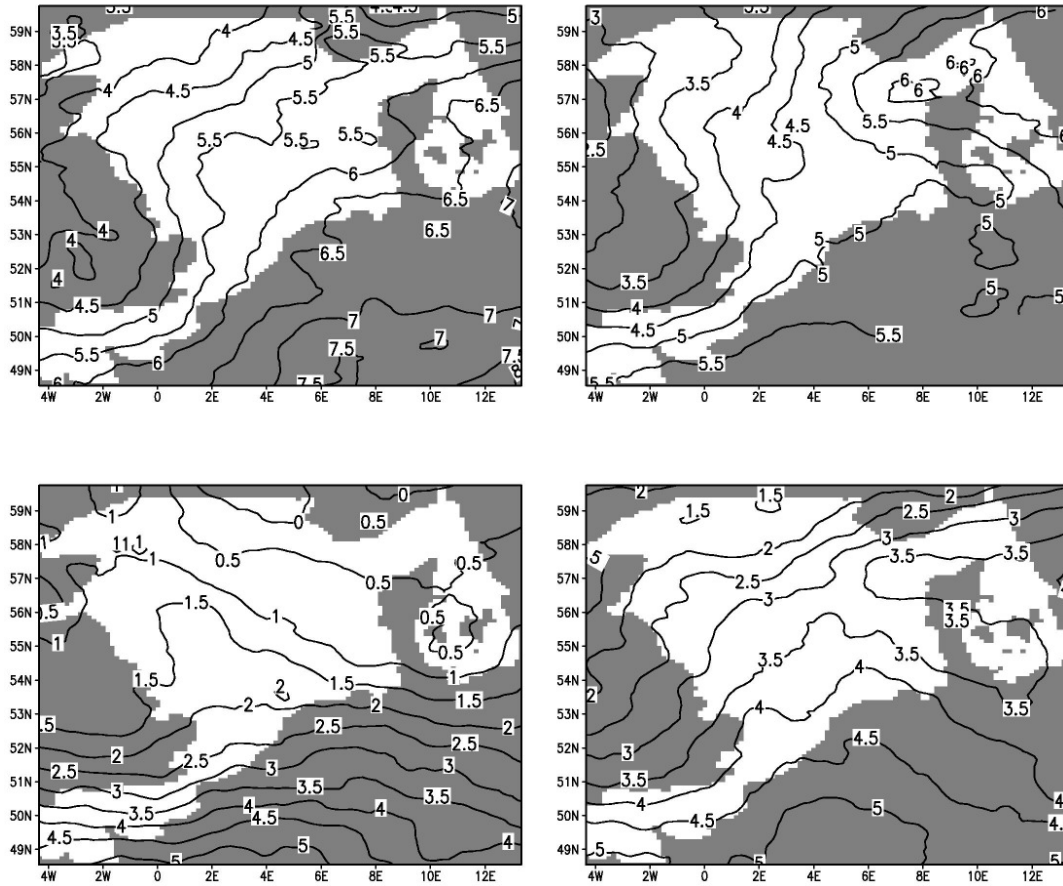
Figure 4.5: Biases of the inter-annual mean of the 1st percentile of sea level pressure in the four considered models relative to REMO_SN hindcast in the control period 1961–1990 (unit: hPa). Upper left: HIRHAM, lower left: CLM, upper right: RCAO and lower right: REMO. Calculations of percentiles are based on 6 hourly data (DJF).

Corresponding to the overestimation of the lowest surface pressures, extreme near-surface wind speeds are underestimated in three of four control simulations compared to the hindcast (Fig. 4.6). Again, the CLM simulation is an exception. Compared to the hindcast, the 99th percentile is about 0.5 m/s higher in the southern and the south-western part of the analysed domain and the differences increase up to about 1.5 m/s in the north-eastern part. The spatial structure of difference in high wind speeds is similar for all other control simulations. While REMO underestimates severe wind speeds slightly by about -0.5 m/s in the Northern and about -1.5 m/s in the Southern North Sea, HIRHAM and RCAO show larger differences in the order of about -2.5 m/s over a large fraction of the North Sea.
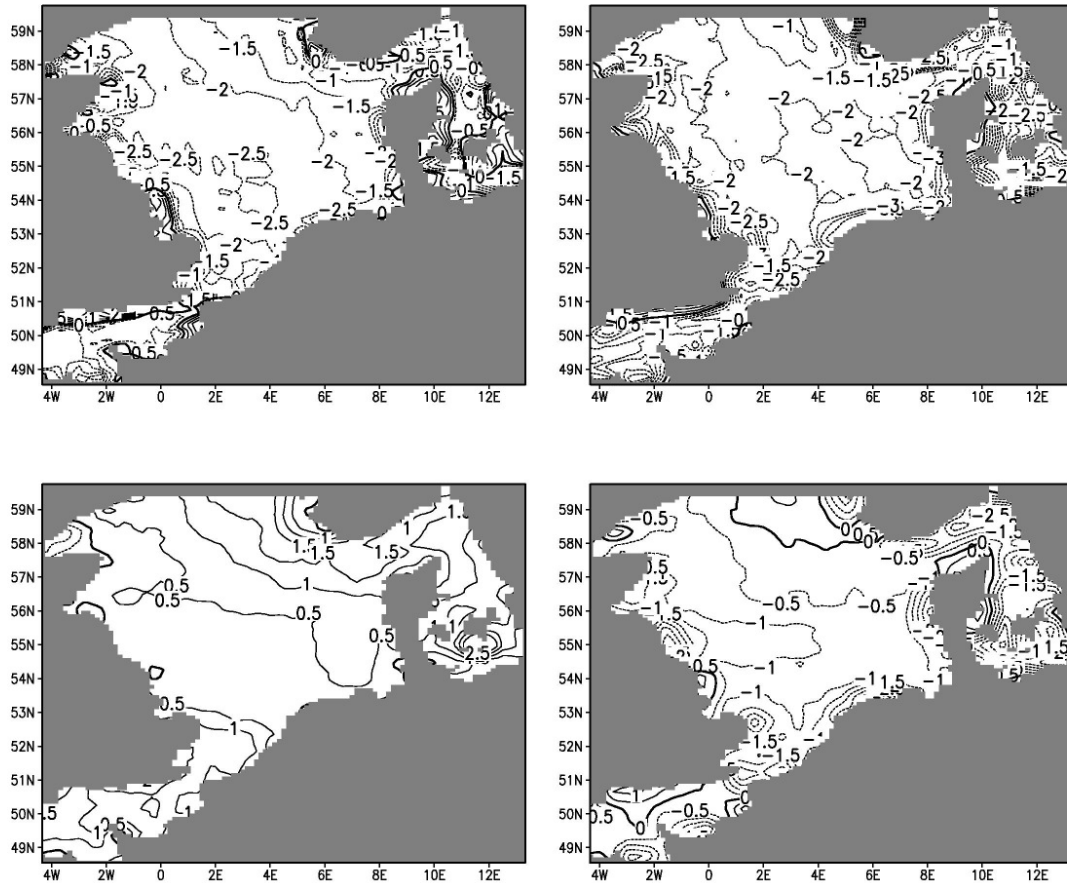
Figure 4.6: Differences in the inter-annual mean of the 99th percentile of 10 m wind speed between the four considered models and the REMO_SN hindcast in the control period 1961–1990 (unit: m/s). Upper left: HIRHAM, lower left: CLM, upper right: RCAO and lower right: REMO. Calculations of percentiles are based on 6 hourly data (DJF)

4.3.1.2 Surge residuals

Storm surge residuals derived from the TRIMGEO runs under control climate conditions and from the hindcast are compared in terms of their 99.5[th] percentiles (Fig. 4.7), Fig. 4.8 show the mean frequencies and the mean durations of extreme events (i.e., episodes when this percentile is exceeded).

In the hindcast simulation, lowest storm surge extremes are generally found along the UK coast (Fig. 4.7). We had seen in Sect. 4.2.1, that TIMGEO underestimates surge levels along most of the UK eastern shore because of tide-only constraints along the northern boundary of the model. Then the 99.5[th] percentiles increase eastward along the 10-m depth line with highest values obtained in the German Bight. Afterwards the height of the most severe surges decreases again. A similar spatial pattern is found for all storm surge control simulations. In correspondence with the differences in extreme wind speeds described above, the absolute value of the 99.5[th] percentile is

underestimated in simulations driven with HIRHAM, RCAO and REMO forcing. Only the CLM wind and pressure fields lead to extreme storm surges of a magnitude comparable to those obtained in the hindcast. In particular, hindcast and CLM forced storm surge residuals reach maxima of up to 1.4 m in the German Bight while HIRHAM and RCAO forcing in this local area only lead to extreme surge heights of about 1m. Extreme surge heights produced with REMO forcing are lying in between with maxima of about 1.2m.
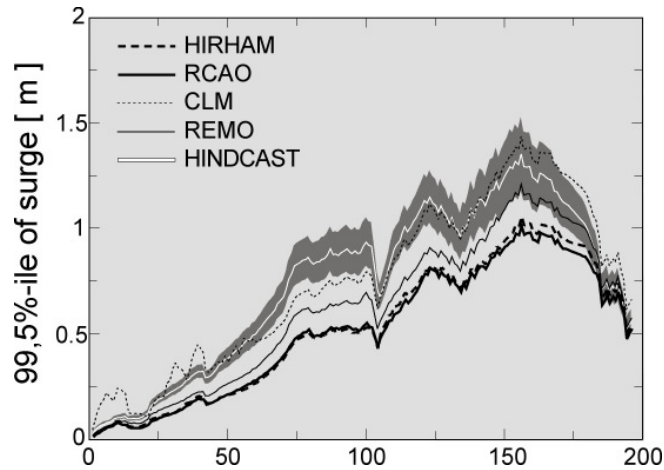

Figure 4.7: Inter-annual mean of the 99.5[th] percentile of water-level / surge (DJF) for the control period 1961 – 1990 (DJF) for all ensemble members and the hindcast. The grey shaded band marks the 95% confidence interval of inter-annual natural variability, inferred from the hindcast. Depicted are grid cells located on the 10-m depth line along the North Sea coast (for the numbering of locations, refer to Fig. 4.1)

Generally in all control storm surge simulations the annual frequency (Fig. 4.8a) of extreme events compare well with the hindcast with a decreasing number of extreme surges from the North of Scotland (six to eight events per year) to the end of the selected 10-m depth line at the top of Denmark (two events per year). Only along the Danish coast the number of such events is slightly underestimated. The mean duration of these events (Fig. 4.8b) is with about 2–5 h relatively short at the Scottish North Sea coast but it increases at the middle and southern English coast up to 7 h in the hindcast. This part is well reproduced in the control climate. Along the continental coast between the English Channel and the German Bight the duration is underestimated. At the North Frisian coast, with the highest 'hindcasted' mean duration of extreme surges (up to about 9 h) and near the Danish coast, with persistence of these events between 6 and 9 h in the mean, the control climate is again in good agreement with the hindcast.
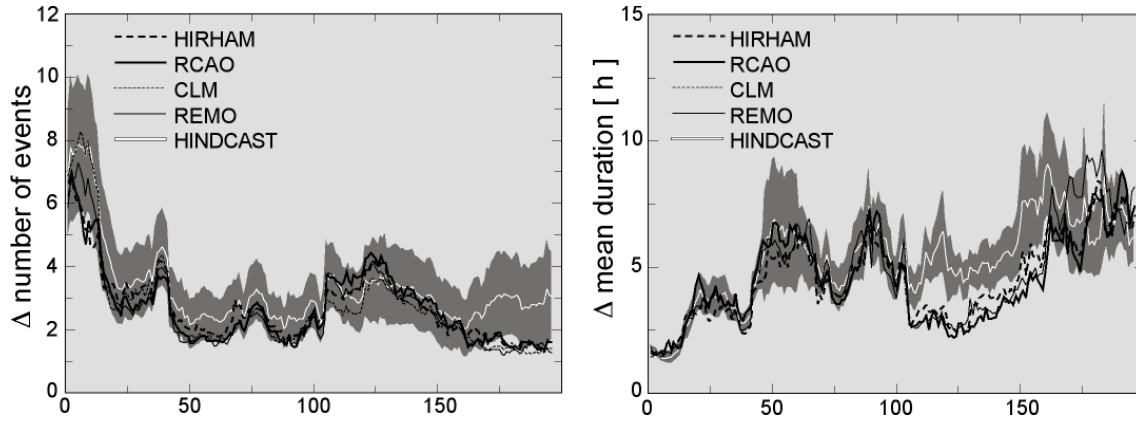
Figure 4.8: Inter-annual mean of number of periods ('events') with percentiles above 99.5 % tile of water-level **(a)** and mean duration of periods with water-levels above 99.5[th] percentile **(b)** for the control period 1961–1990 (DJF) for all four ensemble members and the hindcast. The *grey shaded band* marks the 95% confidence interval of inter-annual natural variability, inferred from the hindcast. Depicted are grid cells located on the 10-m depth line along the North Sea coast (for the numbering of locations, refer to Fig 4.1)

4.3.2   Future climate projections

Because of the deviations between hindcast and control simulations of both, the atmospheric forcing as well as the storm surge residuals, we interpret the differences between scenario and control climate projections as a relative shift of present-day statistics in the projected future. By doing so, we assume that the systematic errors in both the control and the scenario simulations cancel to first order approximation. This assumption is inherent in all climate change studies and represents the best possible option so far.

4.3.2.1   Changes in meteorological forcing, 2071 - 2100

As all RCMs have been driven by the same GCM data, possible reasons for the different response of the storm surge model to atmospheric forcing from the different RCMs may be attributed to differences in the RCM model and experiment design such as for instance different parameterizations of the atmospheric boundary layer.
Possible reasons for the changes in storm surge statistics and their range, found in the different downscaling exercises, are rooted in the different atmospheric RCM formulations (Sect. 4.2.2) used to force the tide-surge model.

Thus, we analysed the different meteorological forcing conditions over the North Sea as changes between the control run and the SRES A2 scenario for SLP and near-surface wind speeds. The latter one is more relevant as a driving condition for storm surges.

Changes in SLP conditions between the CTL time-slice and the A2 scenarios are given by the changes of the 1st percentile level (not shown). All models show a similar pattern simulating a decrease of that percentile. The smallest decrease is simulated in the South West region (around 0.5 hPa), which is getting larger to the North and North Eastern part (from 2 hPa in HIRHAM, and RCAO over 2.5 hPa in REMO, to a decrease of even 4 hPa in CLM).
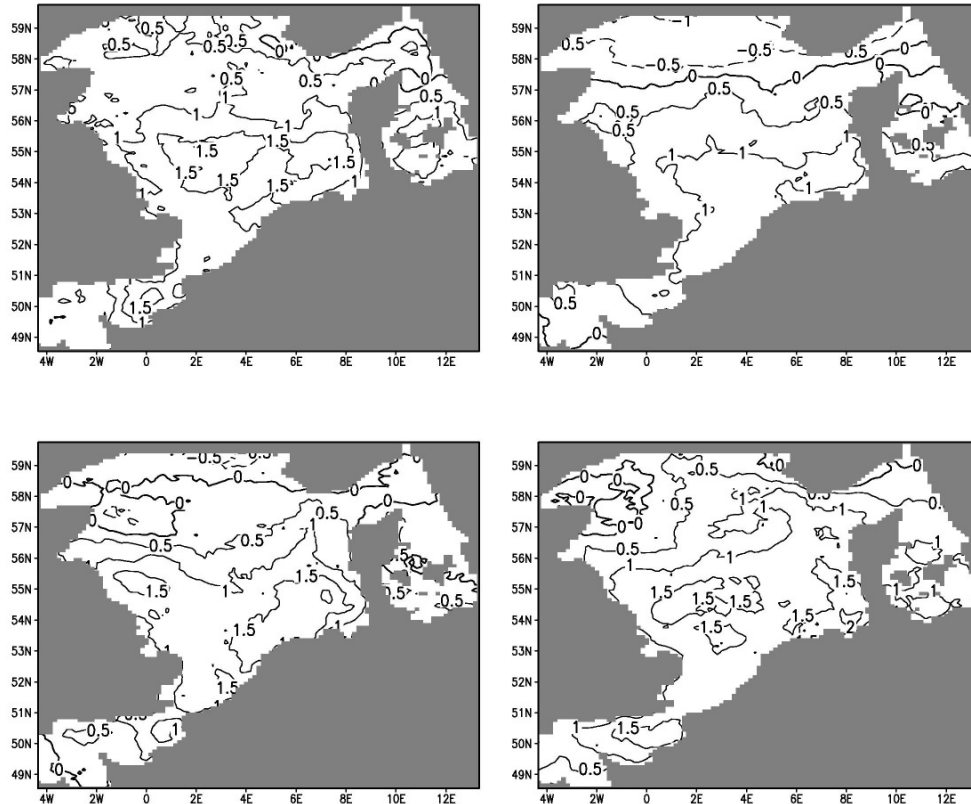

Figure 4.9: Differences "A2 – CTL" in 29-year inter-annual mean of the 99th percentile 10-m wind speed in the four considered models. Calculations of percentiles are based on 6 hourly data (DJF), only for west wind directions. Unit: m/s. Upper left: HIRHAM, lower left: CLM, upper right: RCAO and lower right: REMO

The changes in the 99th percentile in 10-m wind speed are again very similar for each of the four ensemble members, with a very slight increase of up to 1 m/s. The impact of changes in wind speed on storm surge extremes depends on the direction the strong wind is coming from. Thus, the analyses were extended by analysing eight different wind direction sectors, each enclosing 45°. The highest increase in wind speeds in the scenario is found in the sector with westerly wind directions. Figure 4.9 shows the differences in the 99th percentile of 6-hourly sampled 10-m wind speed (westerly sector) for each of the ensemble members. The RCAO wind is increasing by up to 1.4 m/s over

large areas of the North Sea, whereas HIRHAM, REMO and the CLM model show an increase of up to 2 m/s.

4.3.2.2   Changes in surge height extremes, 2071 - 2100

The changes in extreme (99.5th percentile) storm surge statistics obtained from comparing the four IPCC A2 SRES scenario driven simulations and the control runs are shown in Figs. 4.10 and 4.11.

A series of null hypotheses (1)

$$H_o: p_x(CTL\_M) = p_x(A2\_M) \hspace{5cm} (1)$$

is tested to answer the question: is it plausible that the differences merely reflect natural variations and that they are not related to the changing forcing?

Where $p_x(CTL\_M)$ is the mean annual 99.5th percentile, derived in the control run with model M. x represents either the percentile, or the number of events above this percentile or the mean duration of periods with water-level above this percentile. $p_x(A2\_M)$ is the same quantity in the A2 SRES scenario simulation with the model M.

To test these null hypotheses, we determine the 95% confidence interval deduced from a student *t* distribution for the percentiles from the hindcast 1961-1990 and determine for each grid box if the mean difference $p_x(CTL\_M)$ - $p_x(A2\_M)$ lies in the confidence interval or not. In the latter case we reject the null hypothesis (1).

Generally all climate change simulations show a similar spatial pattern:

Changes in the 99.5th percentile surge residual (Fig. 4.10) are minor along the 10-m bathymetry isoline along the UK coast. Here, the model has shown reduced skill in reproducing the observed statistics (Sect. 4.2.1). Eastwards of the West Frisian Islands changes increase up to 30 cm with highest values in the German Bight. In terms of absolute values the RCAO-driven simulations with an increase up to 20 cm show the smallest changes within the ensemble. Along the North Frisian coast changes from all ensemble members are significantly different from zero at the 95% significance level compared to the natural variability obtained from the hindcast.
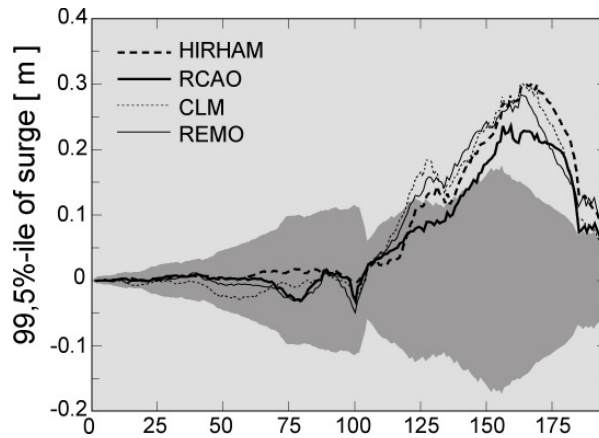
Figure 4.10: Differences "A2 – CTL" in inter-annual mean of the 99.5[th] percentile of water-level/surge (DJF) for all four ensemble members. The 99.5[th] percentile is derived from the control period. The differences are compared to 95% confidence bands reflecting the inter-annual variability in the hindcast. Depicted are grid cells located on the 10-m depth line along the North Sea coast (for the numbering of locations, refer to Fig. 4.1)

Changes in the frequency of extreme events are rather similar in all simulations. Figure 4.11a shows an increase in the number of severe storm surge events along the continental Southern North Sea coast up to about Esbjerg which is significantly different from zero at the 95% confidence level. Here the mean number of severe storm surge events is increased by about two events per year in the period 2071-2100 compared to 1961-1990. This increase corresponds to a relative increase of 50-100%. The duration of severe storm surges (Fig. 4.11b) shows strongest changes along the North Frisian coast with statistically significant changes for all ensemble members of the magnitude of up to 5 h (about 50%), while changes are not significantly different from zero along the West Frisian coast and westwards of it.
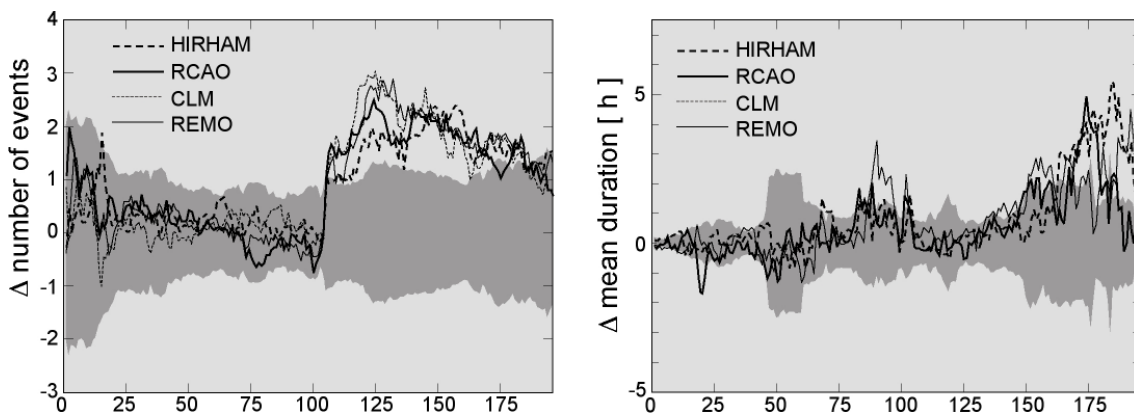

Figure 4.11: Differences "A2 – CTL" in inter-annual mean of number of periods ('events') with water-levels above the 99.5[th] percentile (a) and mean duration of periods with water-levels above the 99.5[th] percentile (b). The 99.5[th] percentiles are derived from the control period. The differences are compared to 95% confidence bands reflecting the inter-annual variability in the hindcast. Depicted are grid cells located on the 10-m depth line along the North Sea (for the numbering of locations, refer to Fig. 4.1)

4.4 Conclusions

A state-of-the-art storm surge model was run for present-day (1961 – 1990) and assumed future climate conditions (2071 – 2100) for the North Sea. Atmospheric forcing was taken from four different state-of-the art regional atmosphere climate models, which dynamically downscale the 'control climate' and the A2 SRES scenario from IPCC. Analysis of changes between control and scenario period of this ensemble are based on a phenomenological characterization of extreme events. Using an ensemble simulation rather than a single one, we are able to detect the signal which is inherent in all storm surge simulations and the range of uncertainty introduced by the use of different RCMs to downscale a given global climate change.

The comparison of the tide-surge model runs forced with control climate conditions with a hindcast using reconstructed atmospheric data gave satisfactory results. On the positive side, the spatial structure of extreme events, with highest storm surges in the German Bight and relatively small values along the UK coast, was found to be in good agreement with reconstructed conditions. However, with the exception of the simulation forced with CLM atmospheric data, the intensity is generally too weak leading to an underestimation of the storm surge 99.5[th] percentile – a finding consistent with *Flather's and Smith's* [1998] results.

The overall structures of the changes between the scenario and the control simulations are rather similar for all ensemble members even though differences in absolute values and statistical significance of the results occur. Larger changes are obtained for the continental coast while differences are generally smaller and not statistically different from zero along the UK coast (where the surge model performs less well). In the western part of the continental coast the increase is primarily a result of more frequent extremes while in the eastern part, from the German Bight up to Denmark, changes in the duration and the intensity of the extremes become more important. Within the German Bight the 99.5[th] storm surge percentile along the 10-m bathymetry line is increased significantly in all scenario simulations by 20–30 cm which corresponds to a rise of around 20% surge heights. In a real world these differences would have different implications for coastal protection. A stand-alone increase in the frequency of extreme events would be less relevant for many coastal facilities, but an increase in duration and magnitude of extreme events could stretch their security limits.

When considering a rise of mean sea level heights due to thermal expansion, the IPCC expects in case of the A2 SRES scenario for the end of this century [*Houghton et al.* 2001] an increase of about 40 cm. (This number may change significantly because of

the changing volume of ice sheets and glaciers.) Since the mean water-levels adds to the storm surge height [*Kauker and Langenberg* 2000], at least as long as the water-level changes are not very large, we have to add this number to our expected increase of extreme surge heights. This results in a possible increases of 60–70 cm in the 99.5th percentile along the 10-m depth line mainly within the German Bight – with a broad range of uncertainty mainly related to the emission scenarios, the unknown behavior of ice sheets and glaciers, and differences in the global climate change simulations.

The difference in modelled surge statistics in the 'control climate', using the four different RCM meteorological forcings, is fully consistent with the analysed high 10-m wind speeds – which is larger in CLM, HIRHAM and REMO than in RCAO. In the future climate scenario all four RCM wind speeds show an increase in the 99th percentile. A maximum increase is found, when this analysis is limited to on westerly directions. This is consistent with the positive trend in surge extremes around the North Sea coast.

The response of the tide-surge model in that specific climate scenario of future storm surge conditions exhibit more similarities than differences between the ensemble members. We can specify a band as a first approximation, wherein the ensemble projections are ranging. This is a first step to explicitly account for the large uncertainties, to be inherent in all studies dealing with possible future climate change scenarios. In this study we only examined the uncertainty related to the use of different RCMs. The use of different emission scenarios and/or global circulation models may have a larger effect on changes of storm surge statistics. Recent studies [e.g., *Leckebusch and Ulbrich* 2004; *Rauthe et al*. 2004] indicate that there might be considerable variability in the response of the extra tropical atmospheric circulation in dependence on the used GCM and in dependence on the chosen greenhouse gas emission scenario. Dealing with such uncertainties will represent a major challenge for climate impact studies in the future.

4.5 References

Aspelien T, and R. Weisse (2005), Assimilation of Sea level Observations for Multi-Decadal Regional Ocean Model Simulations for the North Sea, GKSS report 2005/2

Casulli V, Cattani E (1994) Stability, Accuracy and Efficiency of a Semi-Implicit Method for Three Dimensional Shallow Water Flow. Computers Math. Applic. 27: 99 -112

Casulli V, Stelling GS (1998) Numerical simulation of 3D quasi-hydrostatic, free-surface flows. J. Hydr. Eng. 124: 678 -698

Chabert d'Hieres G, Le Provost C (1978): Atlas des composantes harmoniques de la marée dans la Manche. Les annales hydrographiques, 6, Fascicule 3

Christensen JH, Christensen OB, Lopez P, Van Meijgaard E, and Botzet M (1996) The HIRHAM4 Regional Atmospheric Climate Model. Scientific report. DMI, Copenhagen 96-4: 51

Christensen JH, Carter T, Giorgi F (2002) PRUDENCE employs new methods to assess European climate change. EOS. 83: p. 147

Coles S (2001) An introduction to statistical modeling of extreme values. Springer:Berlin Heidelberg New York

Davies HC (1976) A lateral boundary formulation for multi-level prediction models. Quart. J. R. Meteor. Soc. 102: 405-418

Döscher R, Willén U, Jones C, Rutgersson A, Meier HEM, Hansson U, Graham LP (2002) The development of the coupled regional ocean-atmosphere model RCAO. Boreal Env. Res. 7: 183-192

Dolata LF, Roeckner E, Behr H (1983) Prognostic storm surge simulation with a combined meteorological/oceanographic model. In: Sündermann J, and Lenz W (ed) North Sea Dynamics. Springer: Berlin, Heidelberg New York, pp 266 -278

Feser F, Weisse R, von Storch H (2001) Multidecadel atmosperic modelling for Europe yields multi purpose data. EOS 82: 305 + 310

Fischer-Bruns I, von Storch H, González-Rouco F, Zorita E (2005) Modelling the variability of midlatitude storm activity on decadal to century time scales. Clim Dyn (in press)

Flather R, Smith J (1998) First estimates of changes in extreme storm surge elevation due to doubling CO_2. Global Atmos. Ocean Sys. 6: 193-208

Flather R, Smith J, Richards J, Bell C, Blackman D (1998) Direct estimates of extreme surge elevation from a 40 year numerical model simulation and from observations. Global Atmos. Ocean. Sys. 6: 165-176

Gönnert G, Dube SK, Murty, Siefert T (ed.) (2001) Global Storm Surges. Theory, Observations and Applications. Boyens & Co, Heide. Die Küste 63, 623 p. ISBN 3-8042-1054-6

Heaps NS (1983) Storm surges, 1967 – 1982. Geophys. J. R. astr. Soc. 74: 331-376

Hervouet JM, Van Haren L (1996) TELEMAC2D Version 3.0/Principle Note. Rapport EDF HE-43/94/052/B. Electricité de France, Département Laboratoire National d'Hydraulique, Chatou CEDEX

Houghton JT, Ding Y, Griggs DJ, Noguer M, van der Linden PJ, Dai X, Maskell K, Johnson CA (2001) Climate Change 2001: The Scientific Basis. Cambridge University Press, 881 pp

Jacob D, Podzun R, Claussen M (1995) REMO–-A Model for Climate Research and Weather Prediction. International Workshop on Limited-Area and Variable Resolution Models, Beijing, China, 23 - 27 October, 1995, 273-278

Jones RG, Murphy JM, Noguer M (1995) Simulation of climate change over Europe using a nested regional-climate model I: Assessment of control climate, including sensitivity to location of lateral boundaries. Q. J. R. Meteorol Soc 121: 1413-1449

Jones CG, Willén U, Ullerstig A, Hansson U (2004) The Rossby Centre Regional Atmospheric Climate Model Part I: Model Climatology and Performance for the Present Climate over Europe. Ambio. 33: 4 – 5, 199 -210

Källén E (1996) HIRLAM Documentation Manual, System 2.5. The Swedish Meteorological and Hydrological Institute (Available from SMHI, S-60176 Norrköping, Sweden)

Kauker F (1998) Regionalisation of climate model results for the north sea. PhD Thesis, University of Hamburg.

Kauker F, Langenberg H (2000) Two models for the climate change related development of sea levels in the North Sea. A comparison. Clim Res 15: 61-67

Langenberg H, Pfizenmayer A, von Storch H, Sündermann J (1999) Storm-related sea level variations along the North Sea coast: natural variability and anthropogenic change. Cont Shelf Research 19: 821-842

Leckebusch GC, Ulbrich U (2004) On the relationship between cyclones and extreme windstorm events over Europe under climate change. Glob planet change (In press)

Lowe JA, Gregory JM, Flather RA (2001) Changes in the occurrence of storm surges in the United Kingdom under a future climate scenario using a dynamic storm surge model driven by the Hadley center climate models. Clim Dyn 18: 197-188

Meier HEM, Döscher R, Faxén T (2003) A multiprocessor coupled ice-ocean model for the Baltic Sea: Application to salt inflow. J Geophys Res 108: C8, 3273, doi:10.1029/2000JC000521

Machenhauer B, Windelband M, Botzet M, Hesselbjerg J, Déqué M, Jones GR, Ruti PM, Visconti G (1998) Validation and analysis of regional present-day climate and climate change simulations over Europe. Max-Planck Institute of Meteorology Hamburg, Report No. 275, 87 pp

OSPAR Commision (2000) Quality status report 2000. London

Petersen M, Rohde H (1991) Sturmflut. Die grossen Fluten an den Küsten Schleswig Holsteins und der Elbe. Neumünster

Plüss A (2003) Das Nordseemodell der BAW zur Simulation der Tide in der Deutschen Bucht. Die Küste 67: 83-127

Rauthe M, Hense A, Paeth H (2004) A model intercomparison study of climate change-signals in extratropical circulation. Int. J. Climatol. 24: 643 -662

Rayner NA, Parker DE, Horton EB, Folland CK, Alexander LV, Rowell DP, Kent EC, Kaplan A (2003) Global Analyses of SST, Sea Ice and Night Marine Air Temperature Since the Late Nineteenth Century. J Geophys Res, 108 (D14), 4407, doi:10.1029/2002JD002670

Roeckner E, Arpe K, Bengtsson L, Christoph M, Claussen M, Dümenil L, Esch M, Giorgetta M, Schlese U, Schulzweida U (1996) The atmospheric general circulation model ECHAM-4: Model description and simulation of present-day climate, Report No. 218, 90 pp, Max-Planck-Institut für Meteorologie, MPI, Hamburg

Rummukainen M, Räisänen J, Bringfelt B, Ullerstig A, Omstedt A, Willén U, Hansson U, Jones C (2001) A regional climate model for northern Europe: model description and results from the downscaling of two GCM control simulations. Clim. Dyn. 17: 339-359

Sotillo MG (2003) High resolution multi-decadal atmospheric reanalysis in the Mediterranean Basin. PhD thesis

von Storch H, Langenberg H, Feser F (2000) A spectral nudging technique for dynamical downscaling purposes. Mon. Wea. Rev. 128:3664-3673

STOWASUS-Group (2001) Regional storm, wave and surge scenarios for the 2100 century. Stowasus-final report, DMI. Available from the EU-Commission, DGXII

WASA-Group (1998) Changing waves and storm in the Northern Atlantic? Bulletin of the American Meteorological Society, 79: 741-760

Weisse R and Feser F (2003) Evaluation of a method to reduce uncertainty in wind hindcasts performed with regional atmosphere models. Coast Eng 48: 211-225

Weisse, R., H. von Storch and F. Feser, 2005: Northeast Atlantic and North Sea storminess as simulated by a regional climate model 1958-2001 and comparison with observations. J Clim 18, 465-479

Chapter 5

North Sea storm surge statistics based on projections in a warmer climate: How important are the driving GCM and the chosen emission scenario?

KATJA WOTH

Institute for Coastal Research, GKSS-Research Centre, Max-Planck-Str. 1, 21502 Geesthacht, Germany

Abstract

Climate models, simulating the effect of plausible future emission concentrations (scenarios), describe for the future an increase of high wind speeds over Northwest Europe during winter. With the help of a hydrodynamic model of the North Sea, these atmospheric future conditions are used to project storm surge heights for the Northwest European Shelf Sea. Four different projections are presented, all generated with the same Regional Climate Model, which itself is driven with two different Global Climate Model scenarios both exposed to two different emission scenarios. The analyses are carried out for a 30 year time-slice at the end of the 21st century. All four ensemble members point to a significant increase of storm surge elevations for the continental North Sea coast of between 15 and almost 25 cm. However, the different storm surge projections are not statistically distinguishable from each other but can provide a range of possible evolutions of surge extremes in a warmer climate.

5.1 Introduction

The major geophysical threat for Northwest European coastal areas is related to storm tides, which have the potential to flooding low lying coastal areas. Assuming increasing greenhouse gases in the atmosphere, most state-of-the-art climate models point to an increase in high wind speeds over Northwest Europe at the end of the 21st century [e.g. *WASA group*, 1998; *STOWASUS group*, 2001; *Rauthe et al.*, 2004; *Rockel and Woth,* 2005]. Such an increase in high wind speeds would certainly lead to a change of the storm surge risks for the North Sea coast. These climatic change projections include a large range of uncertainties, coming from different sources.

The EU-PRUDENCE project (**P**rediction of **R**egional scenarios and **U**ncertainties for **D**efining **E**uropea**N** **C**limate change risks and **E**ffects, 2001 - 2004; *Christensen et al.*, 2002) has taken a major step in reducing these uncertainties. By using a range of global and regional climate models, as well as different future emission scenarios, a series of regional climate projections were produced. *Woth et al.*, [2005] evaluated parts of these data with respect to future storm surge statistics along the North Sea coast and found changing storm surge characteristics such as an increase in the amplitude, the frequency and the average duration of such extreme water heights, locally beyond the range of natural variations. The use of the different regional climate models (RCMs), when driven by the same general circulation model (GCM), did not lead to a wide range of different storm surge scenarios.

Other studies as e.g. *Lowe et al.*, [2001]; *Langenberg et al.*, [1999] or *Flather et al.*, [1998] also deal with dynamical modelling of possible evolution of North Sea storm surges in a warmer climate but with some limitations due to e.g. coarser spatial and temporal resolution or shorter time slices of the experiments. All these studies found an increase in local storm surge extremes, although to a different extent, when considering the southern North Sea coast.

Methodologically, the present study follows the approach of *Woth et al.* [2005], dealing with storm surge statistics which focus on high percentiles and extends the analysis. Data are used exclusively from one RCM to force the hydrodynamic storm surge model. This time, the RCM itself was integrated with boundary conditions generated by *two* different GCMs, each exposed to *two* different emissions scenarios, resulting in an ensemble of four climate change projections (*Räisänen et al.*, 2004). The scenarios were characterised in the *IPCC Special Report on Emission Scenarios* (SRES; http://www.grida.no/climate/ipcc/emission). Both chosen scenarios are based on a

heterogeneous world, and focus on local and regional levels. One is focussed on significance self-reliance and preservation of local identities (A2) while the other, B2, is oriented toward more environmental protection and social equity.

This study investigates first if the risk of large storm surges will increase or decrease in future climatic conditions, and second, whether changes estimated using different GCMs and different emission scenarios are distinguishable in a statistical sense.
Neither the influence of an increase in mean sea level, nor the effect of the external part of water mass coming from the Atlantic, the so called 'external surges' are considered. Since the climate change effect is described as the differences between today's climate and possible future climate, it is assumed that the effect due to external surges is unchanged. The effect of mean sea level rise on storm surge heights has been shown to be additive [*Kauker*, 1998; *Lowe et al.*, 2001]. The increase in modelled surge heights was not found to be sensitive to changes in mean sea levels.

The present paper is organized as follows: In section 5.2 the hydro-dynamical model and the atmospheric data used to drive the tide-surge model are described, section 5.3 describes the ensemble experiment and discusses the results.

5.2 Methodology

5.2.1 Tide-surge model

The barotropic TRIMGEO model (Tidal Residual and Intertidal Mudflat) [*Casulli and Catani,* 1994] is used for modelling water levels as the response to 6-hourly North Sea meteorological forcing (pressure at mean sea level and the horizontal wind components at 10 m height) simulated in the different regional climate model scenarios. Surge, defined as the water level minus the astronomical tide, emerges from the interplay of local wind and air pressure, the coastline and the bathymetry. To separate the surge part from the full sea level variations, a tide-only model run was performed without any meteorological forcing and the resulting water heights were subtracted from the climate response simulations.

The model domain covers the North Sea (Fig. 5.1) and is gridded with a mesh size of 6' x 10' in latitude and longitude, which corresponds to a grid cell size of about 10×10 km^2. At the model boundary across the northern North Sea and across the English Channel in the West, boundary conditions in terms of sea level anomalies are given by

17 partial tides. A net influx is prescribed from the Baltic Sea [*OSPAR Commission*, 2000] and from the largest rivers, specified from climatology.
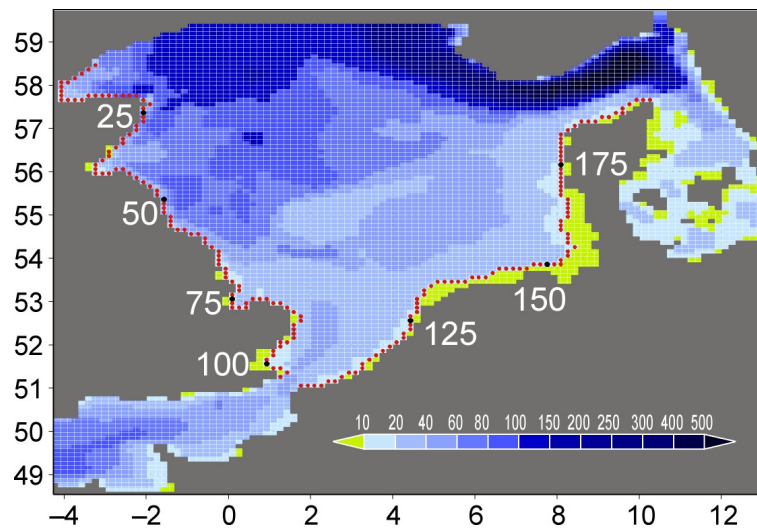

Figure 5.1: Model domain of the tide-surge model TRIMGEO: the bathymetry (isolines) and the 196 near coastal grid cells (red points) located along the 10 m depth line along the North Sea coast beginning with 1 in Scotland and ending with 196 in Denmark.

Aspelien and Weisse [2005] demonstrated the capability of the tide-surge model TRIMGEO of realistically describing surge levels by comparing observed and simulated sea level heights and surges for the southern North Sea for the period 2000 to 2002. Additional validation was done in *Woth et al.* [2005]. A comparison between a model hindcast and observations from a local tide gauge for the annual winter 99th percentile surge at Cuxhaven shows a correlation coefficient of 0.93 and a root mean square error of 19 cm for the period of 1958 to 2000, which is mainly caused by two years in which the model severely underestimates the observed 99th percentile, in particular the very stormy winter 1975/76.

5.2.2 Forcing data and simulations

All atmospheric data to force the tide-surge model in this study, were generated by the regional climate model RCAO [*Döscher et al.*, 2002] from the Swedish Meteorological and Hydrological Institute. RCAO represents a coupled atmosphere-ocean model incorporating the Rossby Center's regional atmosphere model RCA2 [*Jones*, 2001; *Bringfelt et al.*, 2001] and their RCO Baltic Sea model [*Meier et al.*, 1999; *Meier*, 2001]. This RCM was used to regionalize the 'control climate' (1961 – 1990) and the A2 and B2 SRES scenarios (2071 – 2100) from both the Hadley Center General Circulation model

HadAM3H (high-resolution global atmosphere model) [*Hudson and Jones*, 2002; *Hulme et al.*, 2002], and the ECHAM4/OPYC3 GCM [*Roeckner et al.*, 1999]. These six datasets were used to run the hydrodynamic model and produced the following ensemble of tide-surge runs: RE_CTL, RE_A2, RE_B2 and RH_CTL, RH_A2, RH_B2, where *R* stands for RCAO, *E* for ECHAM4/OPYC3 and *H* for HadAM3H. *CTL* stands for control conditions, *A2* and *B2* for the chosen emission scenario.

5.3 Results

The following statistical analyses consider the inter-annual means of the seasonal December, January and February 99th percentile surge derived from computed half hourly values of surge elevation. The 99th percentile is exceeded on average 43 times (ca. 21/22 h) in one winter season, corresponding to 2 – 4 height surge events with a mean duration of 5 to 10 hours, depending on their local occurrence. Results are shown for the 10 meter depth line along the North Sea coast (red points in Figure 5.1).

To assess the changes in surge heights, Figure 5.2 shows the long-year mean annual 99th percentile for both control runs, RE_CTL and RH_CTL. Systematically larger values occur in the control run (up to 15 cm) forced with ECHAM4/OPYC3 boundary conditions compared to those performed with HadAM3H data. In the German Bight the 99th percentile reaches almost 1 m (RE_CTL) and 85 cm (RH_CTL), respectively. However, the spatial pattern along the coastline is very similar in both model integrations.
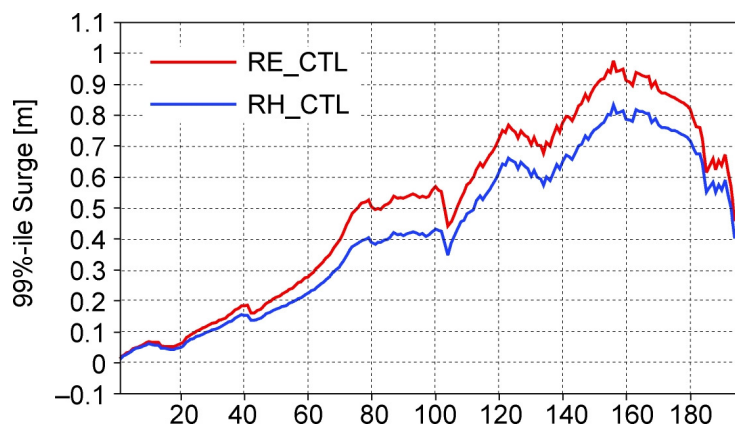

Figure 5.2: Long term mean of the annual 99th percentile of water level / surge (DJF) for the control period 1961 – 1990 (DJF) for both control runs: RE_CTL (red) and RH_CTL (blue). Shown are values for the grid cells located along the 10 m depth line along the North Sea coast (for the numbering of locations, refer to Figure 5.1).

Figure 5.3 shows the changes in this percentile, calculated for all four climate change simulations relative to their control climate. Both A2 projections show an increase, locally limited, up to 22 cm and 18 cm, respectively. Both B2- projections show a similar spatial pattern but with a smaller increase of up to 15 cm in the German Bight.
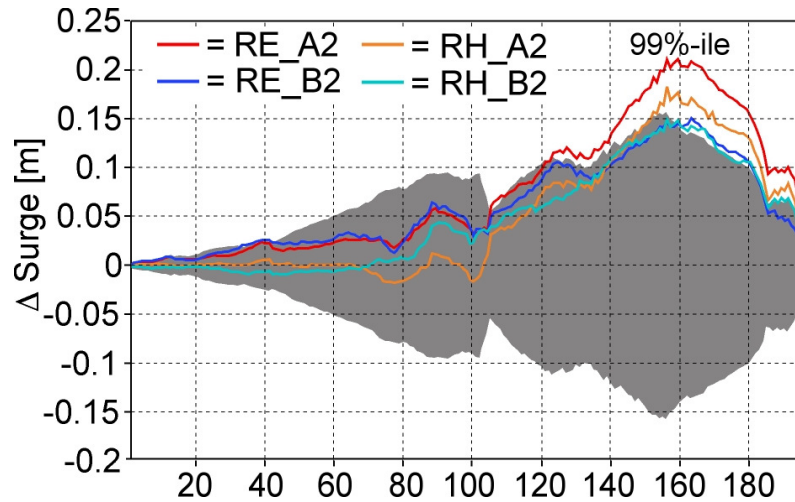

Figure 5.3 : Differences "A2 – CTL" in long term mean of the annual 99th percentile of water level / surge (DJF) for all four ensemble members. The shading indicates the 95% confidence interval based on t-test statistics(see text). Depicted are grid cells located on the 10 m depth line along the North Sea coast (for the numbering of locations, refer to Figure 1).

As a first part of this study, differences of the 99th percentile between the control- and scenario-runs are examined to determine if they could merely reflect natural variability or if the climate change projections differ significantly from the control climate conditions. We test the null hypothesis:

$$H_o: p_{99}(CTL\_M_x) = p_{99}(Sc_y\_M_x) \tag{1}$$

where $p_{99}(CTL\_M_x)$ is the mean annual 99 percentile, derived in the control run with model M_x, for x =RE and RH. $p_{99}(Sc_y\_M_x)$ is the same quantity in a scenario Sc_y, for y = A2 and B2. The 95% confidence interval - depicted as grey band in Figure 5.3 - is derived from the student t distribution (critical values), using the standard deviation of the inter-annual 99th percentile surge residual derived from the hindcast simulation described in *Woth et al.*, 2005. The period of the hindcast analyzed was that of the present control climate, 1961-1990. This was undertaken as a result of, and to accommodate, the higher standard deviation found in the hindcast compared to the projections used in this study. The locations where the null hypothesis (1) is rejected are those grid cells not lying inside the confidence interval (figure 5.3).

Most parts of the continental coast show significant changes between future and today's condition in RE_A2–simulation. For RH_A2 and both B2 forced simulations, the number of grid cells showing significant changes decreases and are locally limited on the German Bight and the Danish coast.

With the rejection of the null hypothesis (1) and thus the acceptance of at least a local limited change - a second question arises, namely: Are the climate change signals, resulting from differences between climate scenario and control conditions, *among* the four future surge scenarios statistically distinguishable? Two null hypotheses are tested:

H_o: $\Delta p_{99}(A2, M_x) = \Delta p_{99}(B2, M_x)$ for M_x = RE and RH   (2)

and

H_o: $\Delta p_{99}(Sc_y, RE) = \Delta p_{99}(Sc_y, RH)$ for Sc_y = A2 and B2   (3)

where ($\Delta p99$) is the difference of each climate change projection relative to today's climate in the mean 99th percentile. Thus, for both null-hypotheses two test-statistics are possible:

$\Delta p_{99}(A2, RE) - \Delta p_{99}(B2, RE)$ and $\Delta p_{99}(A2, RH) - \Delta p_{99}(B2, RH)$: in order to test H_o (2);

$\Delta p_{99}(A2, RE) - \Delta p_{99}(A2, RH)$ and $\Delta p_{99}(B2, RE) - \Delta p_{99}(B2, RH)$: in order to test H_o (3).

Accordingly, the changes in different emission scenarios, given a global forcing, are considered in (2), and the changes obtained with different GCMs, given an emission scenario, in (3). This time, the null hypothesis is tested with an ordinary 2-sided t-test, assuming the same variance in all model simulations. Figure 5.4 shows the result. Grid points at which the null hypothesis is rejected with a risk of 5% are outside the grey band, which represents the 95% range of differences consistent with the null hypothesis.
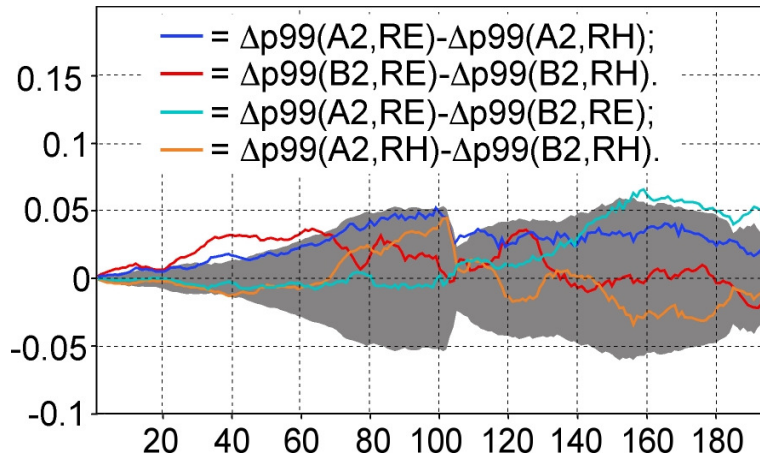
Fig 5.4: Differences in the shift of each climate change projection relative to today's climate in the mean 99th percentile (Δp99) calculated between all four combinations of future simulations. Unit: [m]. The shading indicates the 95% confidence interval based on t-test statistics (see text). Depicted are grid cells located on the 10 m depth line along the North Sea coast (for the numbering of locations, refer to Figure 5.1).

When considering the continental coast, for which hypothesis (1) was rejected, only two future surge experiments can be discriminated statistically, namely the scenario runs A2 and B2 with ECHAM4/OPYC3 forcing (null hypothesis 2) for which differences lie outside the confidence interval locally limited along the Danish North Sea coast. The null hypothesis (3) dealing with different global forcings is rejected only for A2 at a few grid points located at the French Channel coast – but the rate of rejection is not multiply significant. Differences between GCMs using the same scenarios are distinguishable along parts of the coast of United Kingdom for B2, but without any climate change signal (hypothesis (1)).

5.4 Conclusions

A state-of-the-art storm surge model was run for present day control conditions (1961 – 1990) and assumed future climate conditions (2071 – 2100) for the North Sea basin. Atmospheric forcing was taken from the Rossby Centre RCM, which has dynamically downscaled the 'control climate' and the A2 and the B2 SRES scenarios (IPCC) from two driving global models HadAM3Hand ECHAM4/OPYC3.

Analysis of changes between control climate and scenarios are based on the inter-annual mean of the 99th percentile of half hourly surge values for winter months. A climate change signal of increasing surge heights along most of the continental coast emerges for both scenarios, SRES A2 and SRES B2 as well as for both GCM forcings. In most locations these shifts, relative to the control simulations, are beyond the confidence

limit characterizing natural variability, with highest values for the German Bight up to 21 cm. The spread of the 99th percentile in the ensemble is found to be less then 10 cm, approximately 10 to 15 %.

Woth et al. [2005] found that the use of different RCMs subjected to the same driving GCM forcing did not lead to distinguishable results. In this study a further question was addressed: whether a different GCM forcing or a different specification of future atmospheric emissions leads to more or larger uncertainties (differences) in the results simulated with the impact model.

Concerning the 99th percentile of the surge residual, which is an important parameter for coastal protection, a clear statistical distinction was not possible between the four tide-surge climate change projections. Only the two SRES emission scenarios A2 and B2 driven with ECHAM4/OPYC3 forcing are locally distinguishable. The other experiments are not distinguishable statistically: neither the HadAM3H projection, forced with two different SRES emission scenarios, nor both projections, driven with two different GCM forcings.

The results could be influenced by the similarity of the 'physics' of these GCMs and the rather limited experimental design. However this study confirms and extends results of earlier studies (see introduction), which underline the robustness and the importance of these findings for the research field of coastal protection under climatic change conditions.

Acknowledgements

5.5 References

Aspelien, T. and R. Weisse (2005), Assimilation of Sea level Observations for Multi-Decadal Regional Ocean Model Simulations for the North Sea, GKSS report 2005/2. Available from: http://dvsun3.gkss.de/BERICHTE/GKSS_Berichte_2005/GKSS_2005_2.pdf

Bringfelt, B., J. Räisänen, S. Gollvik, G. Lindström, L.P. Graham and A. Ullerstig (2001), The land surface treatment for the Rossby centre Regional Atmospheric Climate Model – version 2 (RCA2), *SMHI Reports Meteorology and Climatology*, *98*, pp40.

Casulli, V. and E. Cattani (1994), Stability, Accuracy and Efficiency of a Semi-Implicit Method for Three Dimensional Shallow Water Flow, *Computers Math. Applic.*, *27*, 99 – 112.

Christensen J.H., T. Carter and F. Giorgi (2002), PRUDENCE employs new methods to assess European climate change, *EOS*, *83*, p. 147.

Döscher R, U. Willén, C. Jones, A. Rutgersson, H.E.M. Meier, U. Hansson and LP. Graham (2002), The development of the coupled regional ocean-atmosphere model RCAO. *Boreal Env. Res*. 7: 183 – 192

Flather R. and J. Smith (1998), First estimates of changes in extreme storm surge elevation due to doubling CO_2. *Global Atmos. Ocean Sys.*, *6*, 193 – 208

Hudson DA and R.G. Jones (2002), Simulations of present-day and future climate over southern Africa using HadAM3H, Hadley Centre Technical Note, No. 38, Met Office, Exeter, UK

Hulme M, G.J. Jenkins, X. Lu, J.R Turpenny, T.D. Mitchell, R.G. Jones, J. Lowe, J.M. Murphy, D. Hassell, P. Boorman, R. Macdonald and S. Hill (2002), Climate-Change Scenarios for the United Kingdom: The UKCIP02 Scientific Report. Tyndall Centre for Climate Change Research, School of Environmental Sciences, University of East Anglia, Norwich, UK, 120pp

Jones C. (2001), A brief description of RCA2 (Rossby Centre Atmosphere Model Version 2). SWECLIM Newsletter 11: 9-14 (available from SMHI, S-60176 Norrköping, Sweden)
.

Kauker F. (1998), Regionalisation of climate model results for the north sea. PhD Thesis University of Hamburg. GKSS Report 99/E/6 (GKSS Research Center, Max Planck Strasse 1, 21502 Geesthacht, Germany.

Langenberg H, A. Pfizenmayer A, H. von Storch and J. Sündermann (1999), Storm-related sea level variations along the North Sea coast: natural variability and anthropogenic change. *Cont. Shelf. Research.*, *19*, 821 – 842

Lowe J.A., J.M. Gregory and R.A. Flather (2001), Changes in the occurrence of storm surges in the United Kingdom under a future climate scenario using a dynamic storm surge model driven by the Hadley center climate models, *Clim. Dyn., 18*: 197 – 188.

Meier H.E.M. (2001), On the parameterization of mixing in 3D Baltic Sea models, *J. Geophys. Res*., *106*: 30,997 – 31,016

Meier H.E.M., R. Döscher, A.C. Coward, J. Nycander and K. Döös (1999), RCO – Rossby Centre regional Ocean climate model: model description (version 1.0) and first results from the hindcast period 1992/1993. SMHI Reports Oceanography 26, 102 pp (available from SMHI, S-60176 Norrköping, Sweden).

OSPAR Commission. 2000. Quality status report 2000. London

Räisänen J., U. Hansson, A. Ullerstig, R. Döscher, L.P. Graham, C. Jones, H.E.M. Meier, P. Samuelsson and U. Willén (2004), European climate in the late twenty-first century: regional simulations with two driving global models and two forcing scenarios. *Clim. Dyn*., *22*, 13 – 31 ,doi 10.1007/s00382-003-0365-x.

Rauthe M., A. Hense and H. Paeth (2004), A model intercomparison study of climate-change signals in extratropical circulation, *Int. J. Climatol*., 24, 643-662.

Rockel B. and K. Woth (2005), Future changes in near surface wind speed extremes over Europe from an ensemble of RCM simulations, submitted to *Clim. Res*.

Roeckner E., L. Bengtsson, J. Feichter, J. Lelieveld and H. Rodhe (1999), Transient climate change simulations with a coupled atmosphere-ocean GCM including the tropospheric sulphur cycle. *J. Clim*., *12*, 3004 – 3032.

Rummukainen M, J. Räisänen, B. Bringfelt, A. Ullerstig, A. Omstedt, U. Willén, U. Hansson and C. Jones (2001), A regional climate model for northern Europe: model description and results from the downscaling of two GCM control simulations. Clim. Dyn., 17, 339 – 359.

STOWASUS-Group (2001), Regional storm, wave and surge scenarios for the 2100 century, Stowasus-final report, DMI. Available from the EU-Commission, DGXII.

WASA-Group (1998), Changing waves and storm in the Northern Atlantic? Bulletin of the American Meteorological Society, 79: 741 – 760.

Woth K, R. Weisse and H. von Storch (2005), Climate change and North Sea storm surge extremes: An ensemble study of storm surge extremes expected in a changed climate projected by four different Regional Climate Models. Ocean Dyn. 56, 1 – 15, doi:10.1007/s10236-005-0024-3

Chapter 6

Localization of global climate change:
Storm surge scenarios for Hamburg in 2030 and 2085

IRIS GROSSMANN[1], KATJA WOTH[1] AND HANS VON STORCH[1,2]

[1]*Institute for Coastal Research, GKSS Research Center, Geesthacht*

[2]*Meteorological Institute, University of Hamburg, Hamburg*

Abstract

A local scenario for future storm surge heights for the tide gauge of Hamburg, St. Pauli is constructed on the basis of a regional scenario prepared with a hydrodynamical model of the North Sea. Two different emission scenarios, A2 and B2 (characterized in the IPCC Special Report on Emission Scenarios, SRES), which were projected onto European climate conditions by different global and regional climate models, are considered. Increases of the annual maximum water levels in St. Pauli of about 20 cm appear possible and plausible for the time horizon of 2030. In 2085, the mean scenario for St. Pauli amounts to an increase of 63 cm. These calculations employ an increase of the mean sea level of 9 cm (2035) and of 29 and 33 cm (2085), respectively. These values are uncertain, in particular for the time horizon 2085, not only because of the employed emission scenarios but also because of a series of downscaling steps, which describe the cascade of processes from increased emissions to local changes. When using different scenarios and models, we find uncertainties of up to +-20 cm in 2030 and +-50 cm in 2085. These numbers also account for the uncertainty in mean sea level rise and the unknown response of land-ice in a warmer climate.

6.1 Introduction

Since both, the disastrous flood of 1962 and the well-managed 1976 storm surge, flood protection in the city of Hamburg and the area downstream between Hamburg and the Elbe mouth has been constantly adapted to changes in high water levels. Such changes may be due to river construction measures [*Freie und Hansestadt Hamburg*, 2005; *Arbeitsgemeinschaft für die Reinhaltung der Elbe*, 1984; *Siefert et al.*, 1988] or to changes in the global and regional climate [*Freie und Hansestadt Hamburg*, 2005].

Figure 6.1 shows, among others, the temporal development of the depth of the river Elbe and of the mean high tide (red curve) in the Port of Hamburg since 1950. The river was repeatedly deepened; the first time in the late 1950s when the shipping channel was deepened to 11 m. At the same time, the mean high tide in St. Pauli rose by 10 cm. A depth of 13.50 m was achieved in the mid 1970s; then the mean high tide had increased by about 40 cm since 1950. The tidal change displayed in the figure is due to coastal protection measures and modifications of the tributaries, and to the deepening of the shipping channel [*Gönnert, pers. comm.*]. This measure also had an effect on the heights of severe storm surges – estimates are 45 cm caused by measures of coastal defense and 15 cm by deepening the shipping channel [*Haake*, 2004: 27].
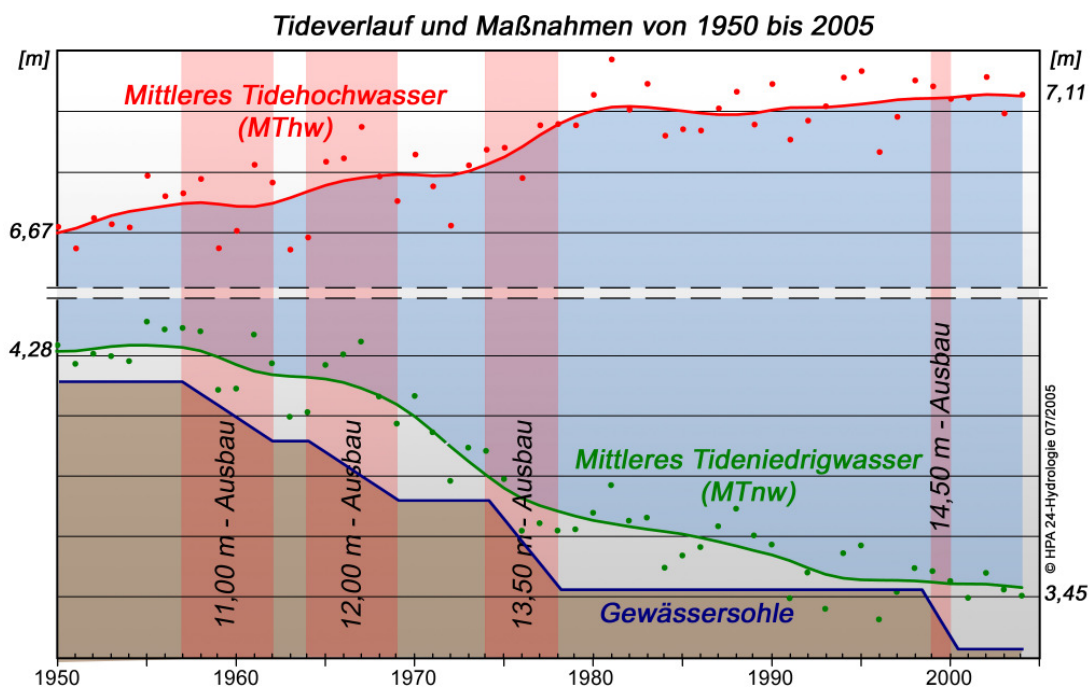

Figure 6.1: Mean depth of the shipping channel, mean low water (MTnw, green line) and mean high water (MThw, red line) at Hamburg St. Pauli 1950-2004. The mean low water is not stable during the interval of interest (1980-1990) but the mean high water is stable. The horizontal lines delineate 20 cm differences. Courtesy to Hamburg Port Authority, Hydrology.

Since the 1980s the mean high tide has remained relatively constant. Another indication that the hydrodynamical regime of the Elbe estuary has not changed significantly since the 1980s is provided by Figure 6.2 – the difference of storm surge heights in St. Pauli and in Cuxhaven has remained stationary since about 1980. That shows that the influence of human impact on the Elbe River on storm surges has stabilized since the 1980s.
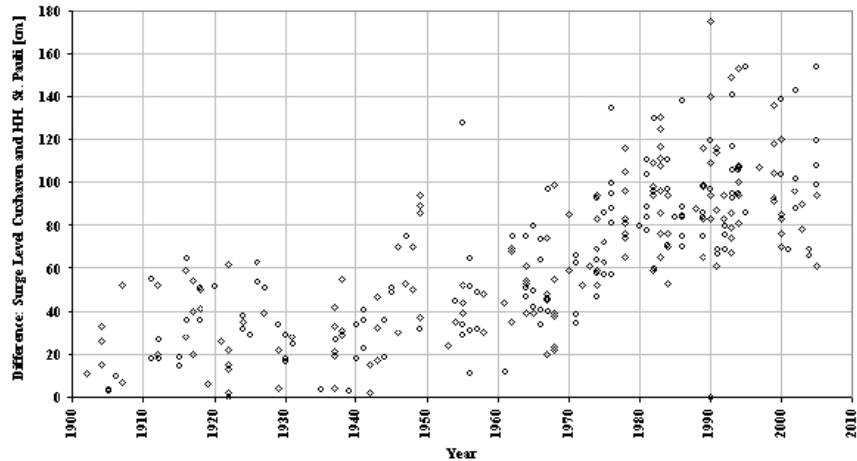

Figure 6.2: Storm surge differences between St Pauli and Cuxhaven (in cm). Due to dredging of the shipping channel and coastal defense measures the difference has grown during the 1950s, 60s and 70s, but since about 1980s conditions are stationary. Courtesy to Hamburg Port Authority, Hydrology.

In the present study, the influence of the possible future climate change on water levels at high tide in Hamburg St. Pauli is investigated. This possible future climate change is described by "scenarios" of future climate change. These scenarios present possible, consistent, plausible but not necessarily probable futures [e.g., *Schwartz*, 1991]. They have been prepared by first envisaging emissions of climatically relevant substances into the atmosphere, and by then simulating the effect of these emissions on the climate system with numerical models.

Towards this end, results from "A2" and "B2"-scenarios [*Houghton et al.*, 2001] of storm surge levels at the North Sea coast between 2071 and 2100 are projected for Hamburg St. Pauli for the time horizons 2030 and 2085. These scenarios are part of a series of scenarios which have been considered in the EU project PRUDENCE [*Christensen et al.*, 2002]. They are all derived from global climate change simulations with either the General Circulation Model HadAM3H of the Hadley Center or the Max-Planck Institute for Meteorology model ECHAM4/OPYC3. The two emission scenarios A2 and B2 envisage an increase of atmospheric greenhouse gas concentrations at the end of the 21st century which correspond to more than a tripling of pre-industrial levels (A2) and more than a doubling (B2). A2 is a relatively pessimistic scenario, whereas B2

expects considerably lower emissions (see also http://www.grida.no/climate/ipcc/emission).

A series of North Sea storm surge scenarios [*Woth et al.*, 2005] is constructed in two steps. First, the HadAM3H global atmospheric scenarios given on a 300×400 km² grid are dynamically downscaled to a 50 km grid covering Northern Europe. Then the barotropic hydrodynamic model TRIMGEO of the North Sea is exposed to the downscaled wind and air pressure fields. TRIMGEO simulates water levels and currents on a grid of about 10×10 km² [e.g., *Aspelien and Weisse*, 2005] for decades of years. When future conditions are simulated then the expected rise in mean sea level is not considered. Instead, following *Kauker and Langenberg* [2000] and *Lowe et al.* [2001], we assume that surge heights are unaffected by the mean sea level, at least in the North Sea itself. Therefore, we consider changes in mean sea level height and surge heights as independent developments. This may not be so in the Elbe estuary, i.e., for the St. Pauli tide gauge, but is expected to provide an upper boundary for changes in the high water levels.

The dynamical downscaling is achieved with four different regional models [*Woth et al.*, 2005] – but the eventual storm surge scenarios depend only weakly on the regional climate model used. Figure 6.3 shows one of these scenarios, which was obtained by running the TRIMGEO model with winds simulated with the regional climate model RCAO of the Rossby Center in Norrköping, Sweden. RCAO [*Döscher et al.*, 2002] is a coupled atmosphere-ocean model, which incorporates the Rossby Centers regional atmosphere model RCA [*Rummukainen et al.*, 2001] and their ocean model RCO [*Meier et al.*, 2003].

The downscaling cascade described above leads to an estimate of the expected changes from 1961-90 to the time horizon 2071-2100 given the emission scenario A2 or B2. It is not possible to use the simulation for the 2071-2100 directly as a possible future for this time. This is because of the systematic errors in the simulations – when simulating the 1961-90 time horizon, the simulated high water levels are underestimated, which originates mainly from the global climate change simulation. Therefore it is common in climate research to consider only the change, assuming that the relatively small systematic errors cancel out.
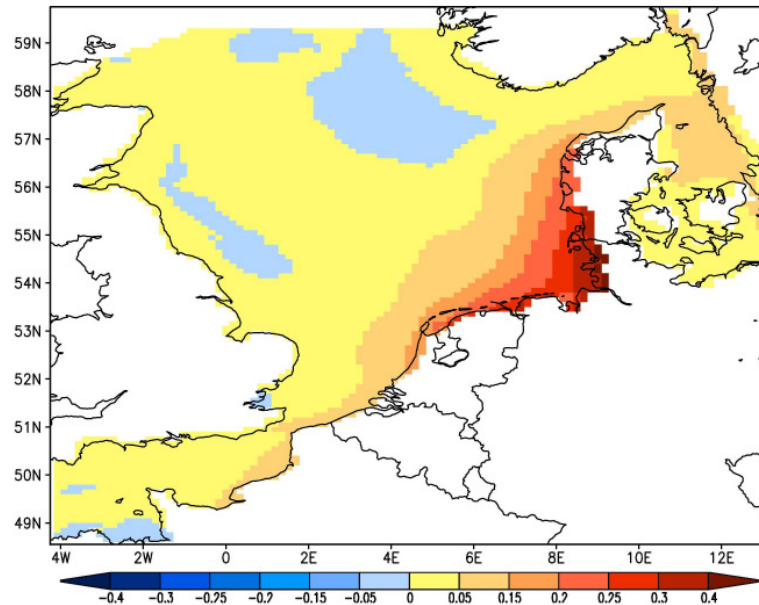
Figure 6.3: A2-changes of the 30 year winter mean of the annual maximum of storm surge heights [m] projected for 2071-2100, as simulated by TRIMGEO as response to RCAO winds.

An interesting detail is the similarity between A2 and B2 changes in surge height [*Woth*, 2005]. The differences between A2 and B2 surge height changes are statistically not significant, and numerically small. Therefore, we do not distinguish between the two scenarios.

As a result of the downscaling cascade, scenarios of possible and plausible storm surge height changes in grid boxes covering the North Sea are available. We relate changes in boxes in the mouth of the river Elbe to the water level in St. Pauli located some 140 km upstream of the Elbe estuary in Hamburg. One of the boxes, which later emerges as the best suited box, contains the tide gauge of Cuxhaven. Case studies have shown that in a storm surge situation the water levels grow from the deeper North Sea to the German Bight and to the shoreline gauges [*Lassen et al.*, 2001], so that differences between the grid box values and the local values in Cuxhaven have to be expected. In fact, the simulated surge levels in the box compare well with the observed surge heights [*Woth et al.*, 2005], but the tidal signal is too strong in the simulations.

In the following we present a simple statistical method to derive estimates for the site St. Pauli in Hamburg for the foreseeable future of 2030, and for the more remote time of 2085 from the North Sea storm surge changes simulated for grid boxes in the Elbe mouth.

6.2 Methodology

We need to introduce two empirically based approximations:

- A link relating water levels at coastal grid boxes near the Elbe mouth simulated by the TRIMGEO model with the water level at St. Pauli in the port of Hamburg. This approach has been suggested by *Langenberg et al*. [1999]. See also *Lassen et al*. [2001].

- An estimation of the situation at the midterm 2030 from the two available time horizons 1961-90 and 2071-2100. For the horizon 2085 no such approximation is needed, because this is simulated directly by the hydrodynamical model.

6.2.1 Linking North Sea surge levels and St. Pauli surge levels

A statistical function is derived which describes common variations of water levels at the coastal grid box and in Hamburg St. Pauli. The function allows estimating the water level in Hamburg St. Pauli given the water level in the coastal box.

For this purpose, data on high tide water levels in Hamburg St. Pauli between 1980 and 1990 is used. This particular interval has been chosen because river deepening measures which might influence water levels have not been carried out during this time (Figure 6.1). Also, future dredging of the shipping channel in the Elbe river is not expected to go along with further significant changes of the hydrodynamic regime [*Heinzelmann and Heyer*, 2004]. The St. Pauli-data are related to the high tide water levels in a grid box of a "hindcast" run [*Woth et al*., 2005] during the same time period. This hindcast run was made with the TRIMGEO model, forced with high-resolution "analyzed" wind and air pressure. "Analyzed" means a best guess of the synoptic situation derived from observations [*Feser et al*., 2001].

When the exercise is repeated for the period 1990-2000 a virtually identical empirical model is found to be the best fit (not shown).

High tide water levels for 3 different grid boxes located at the coast close to the Elbe mouth and for 2 grid boxes located on the 10m bathymetry-line close to the Elbe mouth are considered. A preliminary comparison of the two data sets on the basis of scatter diagrams suggested that a curve, which changes at a point x_k from a linear function to a quadratic function, would provide a good fit (Figure 6.4). Thus, $f(x)$ is a linear function $f_1(x)$ for $x < x_k$ and a quadratic function $f_2(x)$ for $x \geq x_k$:

$$f(x) = \begin{cases} f_1(x) = ax + b, x < x_k \\ f_2(x) = cx^2 + dx + e, x \geq x_k \end{cases} \text{ with } f_1(x_k) = f_2(x_k) \text{ and } f_1'(x_k) = f_2'(x_k).$$
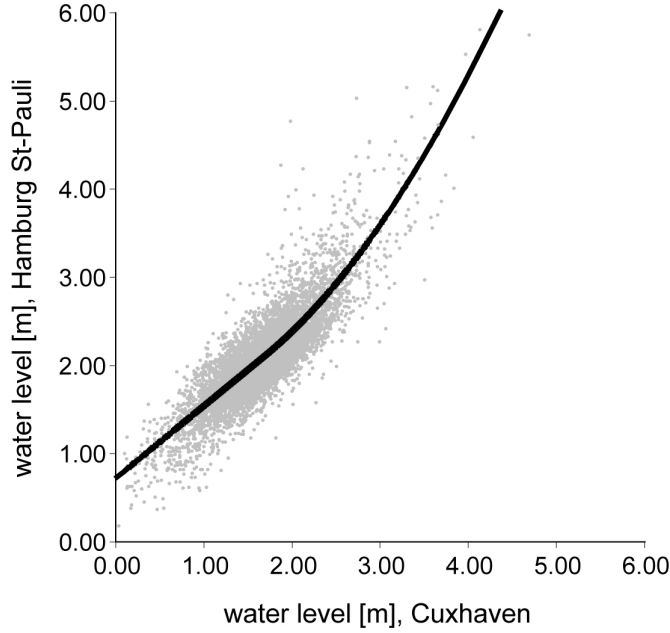

Figure 6.4: : Linear-quadratic fit for high water levels at Hamburg St. Pauli (vertical axis) and at the coastal grid box 53.8°N / 8.8°E (Cuxhaven; horizontal axis). Units: m.

We want to describe the change in storm surge heights in terms of the multiyear mean of annual maxima. Therefore, we add the constraint $f_2(\mu_{H,s}) = \mu_{SP}$. Here $\mu_{O,SP} = 4.56$ m represents the multiyear annual maximum in observations O at St. Pauli recorded between 1980 and 1990 and $\mu_{H,s}$ the multiyear annual maximum at the grid box s close to the Elbe mouth of the hindcast H.

We determine the coefficients $a, b, c, d, e, \lambda_1, \lambda_2, \lambda_3$ which minimize for the site s and given x_k the error

$$\varepsilon(s, x_k) = \sum_{i=1}^{k-1}(f_1(x_i) - y_i)^2 + \sum_{i=k}^{n}(f_2(x_i) - y_i)^2$$
$$+ \lambda_1 \gamma_1 (f_1(x_k) - f_2(x_k)) + \lambda_2 \gamma_2 (f_1'(x_k) - f_2'(x_k)) + \lambda_3 \gamma_3 (f_2(\mu_{H,s}) - \mu_{O,SP}) = \min!$$

The last three terms, featuring the Lagrangian multipliers $\lambda_1, \lambda_2, \lambda_3$, have been introduced to enforce the constraints mentioned above. The numbers γ_i are weights given to the constraints. In our case, we have $\gamma_1 = 500, \gamma_2 = 1$ and $\gamma_3 = 1$. Thus, maximum weight is given to the continuity of the fit. Minimum weight is given to the equivalence

of the multiyear annual maximum heights at St. Pauli and at the grid box at the mouth of the Elbe, and to the continuity of the derivative of the fit. We calculate the error $\varepsilon(s, x_k)$ for a range of possible x_k values and for a total of five coastal grid boxes.

The smallest value for $\varepsilon(s, x_k)$ is reached for the coastal grid box s centered at 53.8°N 8.8°E and for x_k =1.714. This grid box contains Cuxhaven. The optimal constants are a = 0.8197, b = 0.6882, c = 0.2428 , d = -0.0128, and e = 1.402. Figure 6.4 shows the linear/quadratic fit for this set of parameters and the scatter cloud of pairs of high tide values at St. Pauli and at the selected grid box containing Cuxhaven. The constraints of continuity of the function and its derivative is satisfactorily fulfilled, also the condition is met that the simulated mean maximum $\mu_{H,s}$=3.63 m at s is mapped on the observed mean maximum of $\mu_{O,SP}$ = 4.56 m at St. Pauli.

For low high water levels, say 2 m, the observed St Pauli heights is about 30 cm higher than the simulated Cuxhaven heights, for 3 m the difference is on average 50 cm, but for 4 m the difference is about 1.20 m, which is similar to the observed differences between the two tide gauges.

The root mean square error of the fit, i.e.,

$$\sqrt{\frac{1}{k-1}\sum_{i=1}^{k-1}(f_1(x_i)-y_i)^2 + \frac{1}{n-k+1}\sum_{i=k}^{n}(f_2(x_i)-y_i)^2} \; ,$$

amounts to 37 cm for the selected optimal set of parameters.

6.2.2 Temporal interpolation

As outlined in the introduction, the simulations provide at this time only a projection of the expected change from the "control" period 1961-90 to 2071-2100, given scenario A2 or B2 and the global HadAM3H simulation.

To establish a projection of the results onto the time horizon 2030, we assume a development of storm surge heights parallel to the increase of temperature in the global scenario [*Houghton et al.*, 2001]. The expected increase in A2 from 1990 to 2030 is 0.7 K which is about 20% of the increase from the interval 1961-1990 to the interval 2071-2100 (3.25 K). For the B2 scenario the temperature rise after 2030 is slower than in A2. The B2 temperature increase of 0.9 K from 1990 to 2030 is about 40% of the increase from the interval 1961-1990 to the interval 2071-2100 (2.45 K). As already mentioned

the changes in simulated storm surge heights in A2 and B2 are not significantly differ-ent [*Woth*, 2005] even though the temperature changes are markedly different. There-fore we assume that the mean maximum surge height at the location at the mouth of the Elbe in both, the A2 and B2 scenarios are increased by φ =30% of the rise derived from the various TRIMGEO scenarios for the 2071-2100 time horizon.

For the mean sea level rise *D*, which we add to the meteorologically caused change, we use the projections provided by the IPCC [*Houghton et al.*, 2001] for 2030, and for 2085, namely for A2 9 cm and 33 cm, and for B2 9 cm and 29cm. The uncertainty of these numbers is given by the IPCC to be about ±5 cm and ±20 cm, which accounts for different global climate models and emission scenarios. If the possible response of land-ice is factored in, the uncertainties rise to about ±10 cm and ±30 cm [*Houghton et al.*, 2001]. We assume that mean sea level rise and changing storm surge height are inde-pendent and may simply be added. This assumption may not be fully fulfilled in the case of an estuary like the Elbe but is expected to provide upper bounds of plausible changes.

6.3 Results

We consider the multiyear means of the annual maximum *M*, specifically for the hind-cast simulation $H_{1961-90}$, the "control" simulation $C_{1961-90}$ and the A2/B2 Scenarios $S_{2071-2100}$. In the following we drop the indices. We begin with using the control and the A2-scenario-simulation generated with the RCAO/HadAM3H winds and air pressure (see above). The heights obtained with this model are somewhat in the middle of the range of changes obtained with the different regional climate models. This range is later used to estimate a range of uncertainty.

The RCAO/HadAM3H projected mean annual maximum high tide water level P at St. Pauli is estimated as

$$P = f(\mu_{H,s} + \varphi[M(S) - M(C)]) + D$$

The difference of the mean annual maximum high tide at the Cuxhaven coastal grid box *s* = (53.8°N 8.8°E) in the Scenario S=A2 and Control-Run C, M(S)-M(C), amounts to 0.21 m. The present mean annual maximum $\mu_{H,s}$ is 3.63 m. The expected global mean sea level rise in 2030 is D = 0.09 m. For the Cuxhaven grid box, the increase would be 0.09 m plus 30% of 21 cm, i.e., about 0.15 cm. For the projected mean annual maxi-

mum high tide at St. Pauli in 2030 we have P = NN + 4.73 m, which represents an increase of 0.17 m. If the mean sea level would not simply add, the increase would be smaller, namely 0.08m.

For the time horizon 2085 the expected increase in mean sea level is 0.33 m, so that the total increase in Cuxhaven would be 0.54 m. For St. Pauli, the mean annual maximum is expected to be P = NN + 5.25m, which is 0.69 m higher than the present $\mu_{SP} = 4.56$ m.

As pointed out in the introduction, more surge scenarios for the Cuxhaven grid box have been produced [*Woth et al.*, 2005, *Woth*, 2005) mostly for the A2 but also for the B2 IPCC scenario. These scenarios have been obtained with different regional and global models. The mean and range of the expected changes in storm surge heights for St. Pauli for 2030 and 2085 are depicted in Figure 6.5 (for details, see figure caption).
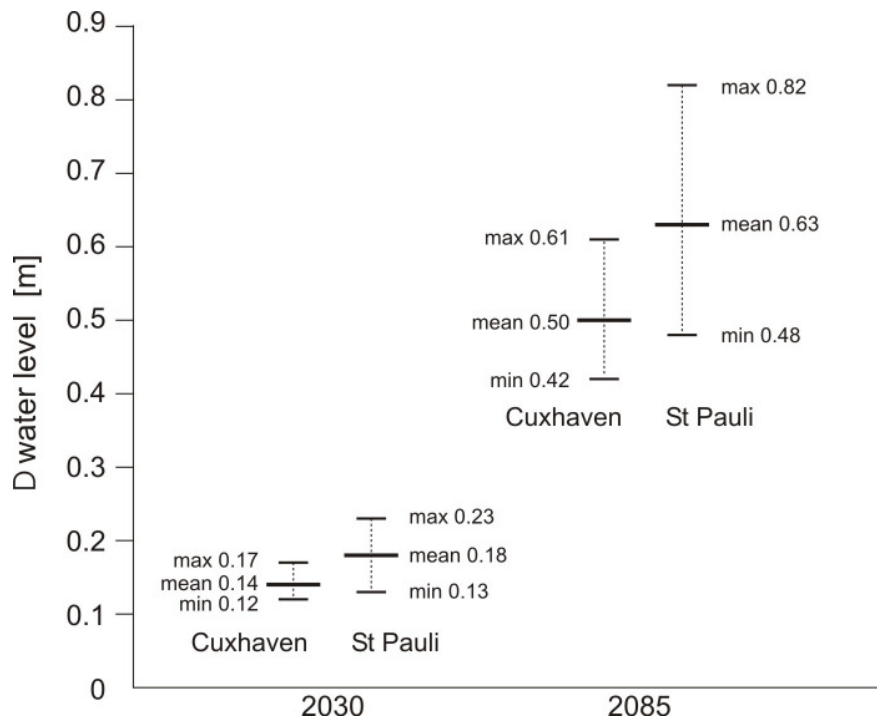

Figure 6.5: Scenarios of changes in storm surge heights including the rise of mean sea level in Cuxhaven and Hamburg St. Pauli in 2030 and 2085. The scenarios are all based on simulations with the TRIMGEO hydrodynamical model, which was forced with winds and air pressure from different regional models and emissions scenarios [*Woth*, 2005]. Since the A2 and B2 scenarios do not significantly differ, the numbers are lumped together in one mean value, across models and scenarios, and in a range given by the minimum and maximum values.

The storm related change of mean maximum surge level change at the Cuxhaven grid box for the end of the 21st century varies between 42 cm to 61 cm with a mean value, across all models and scenarios, of 50 cm. Using our formula above, we find a mean possible and plausible rise at St. Pauli of 18 cm for 2030 and 63 cm in 2085. The range

of minimum and maximum values is 13 cm to 23 cm in 2030 (about ±5 cm) and 48 cm to 82 cm in 2085 (about ±20 cm).

If we factor in the uncertainty of mean sea level rise, then these ranges widen to ±10 cm in 2030 and to ±40 cm in 2085 when only the model and scenario uncertainty is accounted for. If the unknown response of land-ice is added, the numbers increase to ±20 cm and ±50 cm, respectively.

6.4   Discussion and caveats

We have presented a simple approach to estimate changes in extreme water levels at the tide gauge of Hamburg St. Pauli. This method relates scenarios for North Sea near-coastal conditions to the highly location-specific conditions far inside the Elbe estuary. This link takes the form of a transfer function, which maps coastal high water levels simulated in a hindcast with a hydrodynamical model, on observations taken at the tide gauge. This transfer function is valid only for the specific hydrodynamical model TRIMGEO, which has been employed in the hindcast and in the scenario simulations. The transfer function is also only valid for a morphodynamical configuration of the Elbe estuary, which is close to the present one.

The resulting values suffer from significant uncertainty, not only because of the employed emission scenarios but also because of a series of downscaling steps, which describe the cascade of processes linking increased emissions and local climate change impact.

In a further step, we have examined the projected increases in storm surge heights in a series of A2 and B2 scenarios. The A2 scenarios range from 9 cm to 28 cm and the B2 scenarios from 15 cm to 19 cm. Different combinations of global and regional climate models were employed. The uncertainty amounts to ±20 cm in 2030 and to ±50 cm in 2085.

Scenarios are not meant to be forecasts but storylines which allows decisions makers to assess which threats may develop in which time, which countermeasures should be considered and possibly prepared [*Schwartz*, 1991]. The scenarios all point to higher storm surge heights both in Cuxhaven and subsequent in Hamburg St. Pauli. Until 2030 the possible increases seem less dramatic and to be manageable within presently available tools and strategies. For the later time horizon 2085, however, the possible and

plausible changes may require not only much more costly but possibly different adaptations measures.

Altogether these results show that Hamburg's safety level of NN + 7.30 m has been well chosen in view of present and possible future surge risks. The highest storm surge in Cuxhaven and Hamburg was in February, 1976 with NN + 6.45 m in Hamburg St. Pauli. Adding 0.20 m in 2035, the storm surge level would be about 6.65 m. This number is well below the safety level in Hamburg (NN + 7.30 m) even if the uncertainty of ±0.20m is taken into account. Also for 2085, our estimate of 6.45 + 0.63 m = 7.08 is below that critical value, but the uncertainty at that time is rather large (± 0.5 m). However, because of the time lag until then for the foreseeable future it is sufficient to carefully monitor the future development and to implement no-regret measures to reduce the risk of the already today unabatedly dangerous storm surges in the Elbe estuary. Hopefully, the worst scenarios for 2085 can be avoided by efficient reductions of greenhouse gas emissions into the atmosphere.

6.5 References

Arbeitsgemeinschaft für die Reinhaltung der Elbe, 1984: Gewässerökologische Studie der Elbe. Arbeitsgemeinschaft für die Reinhaltung der Elbe, Hamburg.

Aspelien, T. and R. Weisse, 2005: Assimilation of Sea level Observations for Multi-Decadal Regional Ocean Model Simulations for the North Sea, GKSS report 2005/2

Christensen, J.H., T. Carter, F. Giorgi, 2002: PRUDENCE employs new methods to assess european climate change, EOS, Vol. 83, p. 147.

Döscher R, Willén U, Jones C, Rutgersson A, Meier HEM, Hansson U, Graham LP, 2002: The development of the coupled regional ocean-atmosphere model RCAO. Boreal Env. Res. 7: 183 – 192

Feser, F., R. Weisse and H. von Storch, 2001: Multidecadal atmospheric modelling for Europe yields multi-purpose data. EOS 82, 305+310

Freie und Hansestadt Hamburg, Behörde für Stadtentwicklung und Umwelt, 2005: Hochwasserschutz in Hamburg: Stand des Bauprogramms. Amt für Bau und Betrieb, Hamburg.

Haake, P., 2004: Coastal Protection in Hamburg. In: Jahrbuch der Hafenbautechnischen Gesellschaft, p. 24:29.

Heinzelmann, C., Heyer, H, 2004: Überprüfung der Hochwasserneutralität eines weiteren Ausbaus der Seehafenzufahrten nach Hamburg und Bremerhaven, in , Gönnert, G., Grassel, H., Kunz, D., Probst, B., von Storch, H. and Sündermann, J. , 2004. Klimaänderung und Küstenschutz , proceedings of workshop 29th-30th November 2004.

Houghton, J.T., Y. Ding, D.J. Griggs, M. Noguer, P. J. van der Linden and D. Xiaosu (Eds.), 2001. Climate Change 2001: The Scientific Basis. Contribution of Working Group I to the Third Assessment Report of the Intergovernmental Panel on Climate Change (IPCC). Cambridge University Press, UK.

Kauker, F, and H. Langenberg, 2000: Two models for the climate change related development of sea levels in the North Sea. A comparison. Clim. Res. 15: 61 – 67

Lowe J.A., J.M. Gregory, and R.A. Flather, 2001: Changes in the occurrence of storm surges in the United Kingdom under a future climate scenario using a dynamic storm surge model driven by the Hadley center climate models. Clim Dyn. 18: 197 – 188

Langenberg, H., A. Pfizenmayer, H. von Storch and J. Sündermann, 1999: Storm related sea level variations along the North Sea coast: natural variability and anthropogenic change.- Cont. Shelf Res. 19: 821-842

Lassen, H., W. Siefert and G. Gönnert, 2001. Windstauentwicklung in dem Tiefwasserbereich der Südöstlichen Nordsee bei Sturmflutwetterlage. Die Küste 64.

Meier HEM, Döscher R, Faxén T (2003) A multiprocessor coupled ice-ocean model for the Baltic Sea: Application to salt inflow. J. Geophys. Res. 108: C8, 3273, doi:10.1029/2000JC000521

Rummukainen M, Räisänen J, Bringfelt B, Ullerstig A, Omstedt A, Willén U, Hansson U, Jones C (2001) A regional climate model for northern Europe: model description and results from the downscaling of two GCM control simulations. Clim. Dyn. 17: 339-359

Schwartz, P., 1991: The art of the long view. John Wiley & Sons, 272 pp

Siefert, W. Havnoe, K., 1988. Einfluss von Baumassnahmen in und an der Tideelbe auf die Höhen hoher Sturmfluten, Die Küste 47

Woth K, Weisse R, H. von Storch (2005) Climate change and North Sea storm surge extremes: An ensemble study of storm surge extremes expected in a changed climate projected by four different Regional Climate Models. Ocean Dyn 56: 1-15, doi:10.1007/s10236-005-0024-3

Woth K (2005) Projections of North Sea storm surge extremes in a warmer climate: How important are the RCM driving GCM and the chosen emission scenario? Geophys Res Lett: 32, L22708, doi:10.1029/2005GL023762

CHAPTER 7

Outlook

In calculating the security standards for coastal protection constructions, engineers have to consider a time horizon of up to 100 years (i.e. flood barrages). In 2001, the state Government of Schleswig-Holstein, which has a 1190 km coastline, adopted a new master plan 'Integrated coastal defense Management in Schleswig-Holstein' (MI, Schleswig-Holstein, 2001). For the first time, this plan takes into account the EU principles on the Integrated Coastal Zone Management in (ICZM) (Hofstede, 2004) and thus possible greenhouse gas emission-induced changes in storms and storm floods. In consensus with regional and local experts, one of the inferences of this study is: Until 2030, the possible increases in local storm surges seem less dramatic and to be manageable with presently available tools and strategies. But for the later time horizon 2085, the possible and plausible changes may require new coastal security standards not only much more costly but possibly using different adaptations measures. This underlines the importance of carefully observing the development of storm floods in the future, and being proactive in light of potential changes.

Thus, such scientific studies, assumed to be sufficiently accurate, can be seen – besides other scientific aspects – as a service to regional or local decision makers and public authorities. The consequence of the recent response from experts and public to the results contained in this thesis, strongly suggest the necessity for continued study. Future research has the potential to enhance localized information pertain to possible changes of storm surge heights under increasing emissions, not only for one local tide gauge but also for larger coastal areas. As has been demonstrated, localization can be carried out from a coarser model output to a local tide gauge (example St. Pauli), a systematic downscaling will be undertaken for all coastal model grid boxes. By applying this method, the whole ensemble of the projected climate change scenarios of this thesis can be transferred to high-resolution data of about 50×50 m sectors.

In a larger context, today and in the coming years, one of the main interests in climate change studies is to describe and to quantify the inherent uncertainty resulting from inexact input fields and forcings, as well as parameter settings of the models as has been

discussed in this work. For this sake, multiple ensemble studies are under way now in present projects and under preparation in future project plans. Continuing from PRUDENCE, significant effort is being employed to address known knowledge gaps, in the project ENSEMBLES [*Hewitt*, 2005; *Hewitt and Griggs*, 2004; *Stainforth et al.* 2005; http://ensembles-eu.org] where more than 70 partner institutions are integrated in the process of producing and analyzing future climate change scenarios. The improvement to the PRUDENCE project, in which this thesis was embedded, is on the one hand a larger number of model ensemble members, considering a huge number of GCMs, RCMs and emission scenarios, but also a higher spatial and temporal resolution of these simulations. Some of the simulations are not restricted to a 'time-slice' mode (i.e. 30 years) but are integrated for more than hundred model years in so-called transient model simulations, avoiding an interruption between today's and future climate simulation.

Another interesting project with the aim of quantifying the uncertainty in climate change studies is the climate*prediction*.net project [*Allen*, 1999; *Stainforth et al.* 2005]. The idea of this project was to involve as many as possible private persons and institutions, who 'borrow' their computational resources to process climate simulations. Methodologies and technical tools were developed which allow them to download and run a PC version of a GCM with specific initializations on their personal computers or PC clusters, storing and reporting key variables and fields back to the project data server.

In both projects a huge number of simulations are and will be performed and can then be analyzed with respect to e.g. extreme events such as storms, floods or droughts with the help of further downscaling steps. Doing so, an assessment of future occurrence probabilities of extreme weather events on regional and on local scales might be possible in the future.

Bibliography

Alexandersson H, Schmith T, Iden K, Tuomenvirta H (1998) Long-term trend variations of the storm climate over NW Europe. The Global Atmos. Oc. System 6: 97-120

Alexandersson H, Tuomenvirta H, Schmidth T, Iden K (2000) Trends of storms in NW Europe derived from an update pressure data set. Climate Res 14: 71-73

Arbeitsgemeinschaft für die Reinhaltung der Elbe (1984) Gewässerökologische Studie der Elbe. Arbeitsgemeinschaft für die Reinhaltung der Elbe, Hamburg

Aspelien T, and Weisse R (2005) Assimilation of Sea level Observations for Multi-Decadal Regional Ocean Model Simulations for the North Sea, GKSS Report 2005/2

Backhaus JO (1983) On seasonal circulation patterns in the North Sea. In: North Sea Dynamics, ed. Sündermann J, Lenz W, Springer Verlag, Berlin, Heidelberg

Bärring L and von Storch H (2004) Northern European Storminess since about 1800. Geophys Res Lett 31: L20202, doi:10.1029/2004GL020441

Bringfelt B, Räisänen J, Gollvik S, Lindström G, Graham LP and Ullerstig A (2001) The land surface treatment for the Rossby centre Regional Atmospheric Climate Model – version 2 (RCA2), SMHI Reports Meteorology and Climatology, 98, pp40

Cabanes C, Cazenave A, Le Provost C (2001) sea level rise during the past 40 years determined from satellite and in situ observations. Science 294: 840-842

Casulli V and Cattani E (1994) Stability, Accuracy and Efficiency of a Semi-Implicit Method for Three Dimensional Shallow Water Flow. Computers Math. Applic. 27: 99-112

Casulli V and Stelling GS (1998) Numerical simulation of 3D quasi-hydrostatic, free-surface flows. J. Hydr. Eng. 124: 678-698

Chabert d'Hieres G and Le Provost C (1978): Atlas des composantes harmoniques de la marée dans la Manche. Les annales hydrographiques, 6, Fascicule 3

Christensen JH, Christensen OB, Lopez P, Van Meijgaard E, and Botzet M (1996) The HIRHAM4 Regional Atmospheric Climate Model. Scientific Report 96-4: 51 pp., DMI, Copenhagen

Christensen JH, Carter T, Giorgi F (2002) PRUDENCE employs new methods to assess European climate change. EOS. 83: p. 147

Coles S (2001) An introduction to statistical modeling of extreme values. Springer: London Berlin Heidelberg

Davies HC (1976) A lateral boundary formulation for multi-level prediction models. Quart. J. R. Meteor. Soc. 102: 405-418

Döscher R, Willén U, Jones C, Rutgersson A, Meier HEM, Hansson U, Graham LP (2002) The development of the coupled regional ocean-atmosphere model RCAO. Boreal Env. Res. 7: 183-192

Dolata LF, Roeckner E, Behr H (1983) Prognostic storm surge simulation with a combined meteorological/oceanographic model. In: J. Sündermann and W. Lenz: North Sea Dynamics. Springer: Berlin, Heidelberg: 266-278

Doms G, Förstner J, Heise E, Herzog HJ, Raschendorfer M, Schrodin R, Reinhardt T, Vogel G (2005) A description of the Nonhydrostatic Regional Model LM, Part II: Physical parameterization, Deutscher Wetterdienst, P. O Box 100465, 63004 Offenbach, Germany (http://cosmo-model.cscs.ch)

Feser F, Weisse R, von Storch H (2001) Multidecadel atmosperic modelling for Europe yields multi purpose data. EOS 82: 305 + 310

Fischer-Bruns I, von Storch H, González-Rouco F, Zorita E (2005) Modelling the variability of midlatitude storm activity on decadal to century time scales. Clim. Dyn. 25: 461-476, DOI 10.1007/s00382-005-0036-1

Flather R, Smith J (1998) First estimates of changes in extreme storm surge elevation due to doubling CO_2. Global Atmos. Ocean Sys. 6: 193-208

Flather R, Smith J, Richards J, Bell C, Blackman D (1998) Direct estimates of extreme surge elevation from a 40 year numerical model simulation and from observations. Global Atmos. Ocean. Sys. 6: 165-176

Freie und Hansestadt Hamburg, Behörde für Stadtentwicklung und Umwelt (2005) Hochwasserschutz in Hamburg: Stand des Bauprogramms. Amt für Bau und Betrieb, Hamburg.

Giorgi F, and Mearns LO (1991) Approaches to the simulation of regional climate change: A review. Rev. Geophys. 29, 191-216

Godet M (1987) Scenarios and strategic management. Butterworth Scientific Ltd

Gönnert G (2003) Sturmfluten und Windstau in der Deutschen Bucht. Charakter, Veränderungen und Maximalwerte im 20. Jahrhundert. In: Die Küste 67185-365

Gönnert G, Dube SK, Murty, Siefert T (eds) (2001) Global Storm Surges. Theory, Observations and Applications. Heide: Boyens & Co. Die Küste 63. 623 p. ISBN 3-8042-1054-6

Grossmann I, K. Woth, H. von Storch (2005): Localization of global climate change: Storm surge scenarios for Hamburg in 2030 and 2085. Submitted

Grotch SL, MacCracken MC (1991) The use of general circulation models to predict regional climate change. J Clim 4, 286-303

Haake P (2004) Coastal Protection in Hamburg. In: Jahrbuch der Hafenbautechnischen Gesellschaft, p. 24-29

Heaps NS (1967) Storm surges. Oceanography and Marine Biology – an Annual Review, 5,11-47

Heaps NS (1983) Storm surges, 1967 – 1982. Geophys. J. R. astr. Soc. 74: 331-376

Heinzelmann C and Heyer H (2004) Überprüfung der Hochwasserneutralität eines weiteren Ausbaus der Seehafenzufahrten nach Hamburg und Bremerhaven, in: Gönnert G., Grassel H, Kunz D, Probst B, von Storch, H and Sündermann J. (2004) Klimaänderung und Küstenschutz , proceedings of workshop 29th-30th November 2004

Hensen W (1966) Bericht der Arbeitsgruppe Sturmfluten im Küstenausschuss Nord- und Ostsee. In: Die Küste 14, 1: 63-70

Hervouet JM and Van Haren L (1996) TELEMAC2D Version 3.0 / Principle Note. Rapport EDF HE-43/94/052/B. Electricité de France, Département Laboratoire National d'Hydraulique, Chatou CEDEX

Hewitt CD (2005) ENSEMBLES – providing ensemble-based predictions of climate changes and their impacts. Parliament Magazine, 11. July 2005, 57

Hewitt CD and Griggs DJ (2004) Ensemble-based prediction of climate changes and their impacts. EOS: 85, 566

Hofstede J (2004) A new coastal defense master plan for Schleswig-Holstein. In: Schernewski, G. & T. Dolch (Hrsg.): Geographie der Meere und Küsten. Coastline Reports 1

Hofstede J (2005) COMRISK Common Strategies to Reduce the Risk of Storm Floods in Coastal Lowlands: an Introduction. In: Die Küste 70, Special Edition: COMRISK, 1-7

Houghton JT, BA Callender, SK Varney (eds.) (1992) Climate Change 1992. The Supplementary Report to the IPCC Scientific Assessment. Cambridge. University Press.

Houghton JT, GJ Jenkins, JJ Ephraums (eds.) (1990) Climate Change. The IPCC Scientific Assessment. Cambridge: University Press.

Houghton JT, Meira Filho LG, Bruce J, Hoesung Lee, Callander BA, Haites E, Harris N, Maskell K (eds.) (1995) Climate Change 1994. Radiative Forcing of Climate Change and An Evaluation of the IPCC IS92 Emission scenarios. Cambridge. University Press.

Houghton JT, Ding Y, Griggs DJ, Noguer M, van der Linden PJ, Dai X, Maskell K, Johnson CA (2001) Climate Change 2001: The Scientific Basis. Contribution of Working Group I to the Third Assessment Report of the Intergovernmental Panel on Climate Change (IPCC). Cambridge University Press, UK.

Hudson DA and Jones RG (2002) Simulations of present-day and future climate over southern Africa using HadAM3H, Hadley Centre Technical Note, No. 38, Met Office, Exeter, UK

Hulme M, Jenkins GJ, Lu X, Turpenny JR, Mitchell TD, Jones RG, Lowe J, Murphy JM, Hassell D, Boorman P, Macdonald R and Hill S (2002) Climate-Change Scenarios for the United Kingdom: The UKCIP02 Scientific Report. Tyndall Centre for Climate Change Research, School of Environmental Sciences, University of East Anglia, Norwich, UK, 120pp

Jacob D, Podzun R, Claussen M (1995) REMO - A Model for Climate Research and Weather Prediction. International Workshop on Limited-Area and Variable Resolution Models, Beijing, China, October 23 – 27, 1995, 273-278

Jelesnianki CP (1978) Storm surges. In: Geophysical predictions. Washington D.C., National Academy of Sciences, pp 185-192

Jones C (2001) A brief description of RCA2 (Rossby Centre Atmosphere Model Version 2). SWECLIM Newsletter 11: 9-14 (available from SMHI, S-60176 Norrköping, Sweden)

Jones RG, Murphy JM, Noguer M (1995) Simulation of climate change over Europe using a nested regional-climate model I: Assessment of control climate, including sensitivity to location of lateral boundaries. Q. J. R. Meteorol. Soc. 121: 1413 – 1449

Jones CG, Willén U, Ullerstig A, Hansson U (2004) The Rossby Centre Regional Atmospheric Climate Model Part I: Model Climatology and Performance for the Present Climate over Europe. Ambio. 33: 4 -5, 199-210

Kaas E, Li TS, Smith T (1998) northeast Atlantic winter storminess 1875-1995 re-analysed. Clim Dyn 14: 529-536

Källén E (1996) HIRLAM Documentation Manual, System 2.5. The Swedish Meteorological and Hydrological Institute (Available from SMHI, S-60176 Norrköping, Sweden)

Kalnay E, Kanamitsu M, Kistler R, Collins W, Deaven D, Gandin M, Iredell M, Saha S, White G, Woolen J, Zhu Y, Chelliah M, Ebisuzaki W, Higgins W, Janowiak J, Mo KC, Ropelewski C, Wang J, Leetmaa A, Reynolds R, Jenne R, Joseph D (1996) The NCEP/NCAR reanalysis project. Bull. Amer. Meteor. Soc., 77, 437-471

Karl TR, RG Quayle and Groisman PY (1993) Detecting climate variations and change: New challenges for observing and data management systems. J. Climate 6, 1481-1494

Kauker F (1998) Regionalisation of climate model results for the north sea. PhD Thesis University of Hamburg. GKSS Report 99/E/6 (GKSS Research Center, Max Planck Strasse 1, 21502 Geesthacht, Germany

Kauker F, and Langenberg H (2000) Two models for the climate change related development of sea levels in the North Sea. A comparison. Clim. Res. 15: 61-67

Kauker F, and von Storch H (2000) Statistics of synoptic circulation weather in the North Sea as derived from a multi-annual OGCM simulation. J. Phys. Ocean. 30: 3039-3049

Koopmann G (1962) Wasserstandserhöhungen in der Deutschen Bucht infolge von Schwingungen und Schwallerscheinungen und deren Bedeutung bei der Sturmflut vom 16.-17. Februar 1962. In: Deutsche Hydrographische Zeitschrift 15-5. 181-198

Langenberg H, Pfizenmayer A, von Storch H, Sündermann J (1999) Storm-related sea level variations along the North Sea coast: natural variability and anthropogenic change. Cont Shelf Research. 19: 821-842

Lassen H, Siefert W, Gönnert G (2001) Windstauentwicklung in dem Tiefwasserbereich der Südöstlichen Nordsee bei Sturmflutwetterlage. Die Küste 64.

Leckebusch GC and Ulbrich U (2004) On the relationship between cyclones and extreme windstorm events over Europe under climate change. Global and planetary change: 44, 181-193

Lowe JA, Gregory JM, Flather RA (2001) Changes in the occurrence of storm surges in the United Kingdom under a future climate scenario using a dynamic storm surge model driven by the Hadley Center Climate models. Clim Dyn. 18: 197-188

Lowe JA, Gregory JM (2005) The effects of climate change on storm surges around the United Kingdom. Phil. Trans. R. Soc. A 363: 1313 – 1328. DOI: 10.1098/rsta.2005.1570

Machenhauer B, Windelband M, Botzet M, Hesselbjerg J, Déqué M, Jones GR, Ruti PM, Visconti G (1998) Validation and analysis of regional present-day climate and climate change simulations over Europe. Max-Planck Institute of Meteorology Hamburg, Report No. 275, 87 pp

Meier HEM, Döscher R, Faxén T (2003) A multiprocessor coupled ice-ocean model for the Baltic Sea: Application to salt inflow. J. Geophys. Res. 108: C8, 3273, doi:10.1029/2000JC000521

Nakicenovic (ed.) (2000) IPCC special report on emission scenarios. Cambridge, UK: Cambridge University press

Niemeyer, HD, Kaiser R (1999) Meeresspiegelanstieg. In: Nationalparkverwaltung Niedersächsisches Wattenmeer und Umweltbundesamt (ed.) Umweltatlas Wattenmeer, Band 2, Ulmer Verlag.

Ogilvy JA (2002) Creating better futures. Scenario planning as a tool for a better tomorrow. Oxford University Press

OSPAR Commision (2000) Quality status report II: Greater North Sea. London

Otto L, Zimmerman JTF, Furnes GK, Mork M, Saetre R, Becker R (1990) Review of the Physical Oceanography of the North Sea. Netherlands Journal of Sea Research 26 (2-4): 161-238

Petersen M and Rohde H (1991) Sturmflut. Die großen Fluten an den Küsten Schleswig Holsteins und der Elbe. Neumünster.

Pfizenmayer A (1997) Zusammenhang zwischen der niederfrequenten Variabilität in der großräumigen atmosphärischen Zirkulation und den Extremwasserständen an der Nordseeküste. Diplomarbeit Institut für Geographie Universität Stuttgart

Pielke RA (1991) A recommended specific definition of "resolution". Bull. Amer. Met. Soc. 72: 1914

Plüß A (2004) Das Nordseemodell der BAW zur Simulation der Tide in der Deutschen Bucht. Die Küste 67: 83-127

Pugh DT (1987) Tides, surges and Mean-Sea-Level. A handbook for Engineers and Scientists. John Wiley and Sons, pp. 472

Räisänen J, Hansson U, Ullerstig A, Döscher R, Graham LP, Jones C, Meier HEM, Samuelsson P and Willén U (2004) European climate in the late twenty-first century: regional simulations with two driving global models and two forcing scenarios. Clim Dyn: 22, 13 – 31, doi 10.1007/s00382-003-0365-x

Rauthe M, Hense A, Paeth H (2004) A model intercomparison study of climate change-signals in extratropical circulation. Int J Climatol 24: 643-662

Rayner NA, Parker DE, Horton EB, Folland CK, Alexander LV, Rowell DP, Kent EC, Kaplan A (2003) Global Analyses of SST, Sea Ice and Night Marine Air Temperature Since the Late Nineteenth Century. Journal of Geophysical Research, 108 (D14), 4407, doi:10.1029/2002JD002670

Rockel B, and Woth K (2005) Near surface wind speed extremes over Europe and their future changes from an ensemble of RCM simulations. Accepted for publication in Climate change, PRUDENCE Special Issue.

Roeckner E, Arpe K, Bengtsson L, Christoph M, Claussen M, Dümenil L, Esch M, Giorgetta M, Schlese U, Schulzweida U (1996) The atmospheric general circulation model ECHAM-4: Model description and simulation of present-day climate, Report No. 218, 90 pp., Max-Planck-Institut für Meteorologie, MPI, Hamburg

Roeckner E, Bengtsson L, Feichter J, Lelieveld J and Rodhe H (1999) Transient climate change simulations with a coupled atmosphere-ocean GCM including the tropospheric sulphur cycle. J Clim: 12, 3004 – 3032.

Ronde, JG de and Vogel, JA (1989) Kustverdedigingna 1990. Technisch Rapport 6: Zeespiegelrijzing. Rijkswaterstaat, The Hague.

Rummukainen M, Räisänen J, Bringfelt B, Ullerstig A, Omstedt A, Willén U, Hansson U, Jones C (2001) A regional climate model for northern Europe: model description and results from the downscaling of two GCM control simulations. Clim. Dyn. 17: 339-359

Schmitz HP, Habicht D, Volkert H (1988) Barotropic numerical experiments on external surge generation at the edge of the north western European shelf. Gerlands Beitr. Geophysik (97) 5: 422-437

Schwartz P (1991) The art of the long view. John Wiley & Sons, 272 pp

Siefert W, Havnoe K (1988) Einfluss von Baumassnahmen in und an der Tideelbe auf die Höhen hoher
        Sturmfluten. Die Küste 47.

Sotillo MG (2003) High resolution multi-decadal atmospheric reanalysis in the Mediterranean Basin. PhD thesis

Steinforth DA, Aina T, Christensen C, Collins M, Faull N, Frame JA, Kettleborough JA, Knight S, Martin A,
        Murphy JM, Piani C, Sexton D, Smith LA, Spicer RA, Thorpe AJ, Allen MR (2005) Uncertainty in
        predictions of the climate response to rising levels of greenhouse gases. Nature, 433: 403-406

von Storch H (1995) Inconsistencies at the interface of climate impact studies and global climate research.
        Meteorol. Zeitschrift 4 NF: 72-80

von Storch H (2005) Veränderliches Küstenklima – die vergangenen und zukünftigen 100 Jahre. In M. Fansa
        (ed): Kulturlandschaft Marsch: Natur, Geschichte und Gegenwart, Isensee-Verlag, Oldenburg, 229-245

von Storch H (2006) Klimaänderungsszenarien. In: Gebhardt H, R Glaser, U Radtke, P Reuber (ed.): Lehrbuch
         Geographie Spektrum Verlag, Heidelberg (in press)

von Storch H and Zwiers F (1999) Statistical analysis in climate research, Cambridge University press

Müller P, and von Storch H (2004) Computer Modelling in Atmospheric and Oceanic Sciences Building
        Knowledge. Springer Verlag Berlin - Heidelberg - New York, 304pp, ISN 1437-028X

von Storch H, Langenberg H, Feser F (2000) A spectral nudging technique for dynamical downscaling purposes.
        Mon. Wea. Rev. 128: 3664 -3673

STOWASUS-Group (2001) Regional storm, wave and surge scenarios for the 2100 century. Stowasus-final report,
        DMI. Available from the EU-Commission, DGXII

Sündermann J, Beddig S, Radach G, Schlünzen H (2001) Die Nordsee – Gefährdung und Forschungsbedarf. Zentrum
        für Meeres- und Küstenforschung, Hamburg

Wakelin S, Woodworth P, Flather R, Williams J (2003) Sea-level dependence on the NAO over the NW
        European Continental Shelf. Geophys Res Lett 30: 1403, doi:10.1029/2003GL017041

WASA-Group (1998) Changing waves and storm in the Northern Atlantic? Bulletin of the American
        Meteorological Society, 79: 741-760

Weisse R and Feser F (2003) Evaluation of a method to reduce uncertainty in wind hindcasts performed with
        regional atmosphere models. Coastal Engineering, 48: 211-225

Weisse R, Plüß A (2005) Storm related Sea level Variations along the North Sea Coast as Simulated by a High
        resolution Model 1958-2002. Ocean Dyn. 56: 16-25

Weisse R, H. von Storch and F. Feser (2005) Northeast Atlantic and North Sea storminess as simulated by a regional climate model 1958-2001 and comparison with observations. J. Climate, 18: 465-479

Woth K, Weisse R, H. von Storch (2005) Climate change and North Sea storm surge extremes: An ensemble study of storm surge extremes expected in a changed climate projected by four different Regional Climate Models. Ocean Dyn, 56.1: 1-15, doi:10.1007/s10236-005-0024-3

Woth K (2005) Projections of North Sea storm surge extremes in a warmer climate: How important are the RCM driving GCM and the chosen emission scenario? Geophys Res Lett: 32, L22708, doi:10.1029/2005GL023762

Acknowledgments